PSZ 19:16 (Pind. 1/07)

UNIVERSITI TEKNOLOGI MALAYSIA

DECLARATION OF THESIS / UNDERGRADUATE PROJECT PAPER AND COPYRIGHT

Author's full name : MOHD ALSHAFIQ BIN TAMBI CHIK

Date of birth : 12 JUNE 1989

Title : OPTIMIZATION OF OTEC AND LOW TEMPERATURE THERMAL DESALINATION PLANT FOR ELECTRICITY AND FRESHWATER PRODUCTION IN MALAYSIA

Academic Session : 2016/2017 - 2

I declare that this thesis is classified as :

[ ]	**CONFIDENTIAL**	(Contains confidential information under the Official Secret Act 1972)*
[ ]	**RESTRICTED**	(Contains restricted information as specified by the organization where research was done)*
[/]	**OPEN ACCESS**	I agree that my thesis to be published as online open access (full text)

I acknowledged that Universiti Teknologi Malaysia reserves the right as follows:

1. The thesis is the property of Universiti Teknologi Malaysia.
2. The Library of Universiti Teknologi Malaysia has the right to make copies for the purpose of research only.
3. The Library has the right to make copies of the thesis for academic exchange.

Certified by :

SIGNATURE	**SIGNATURE OF SUPERVISOR**
890612-05-5465	
(NEW IC NO. /PASSPORT NO.)	**NAME OF SUPERVISOR**
Date :	Date :

NOTES : * If the thesis is CONFIDENTAL or RESTRICTED, please attach with the letter from the organization with period and reasons for confidentiality or restriction.

"I hereby declare that I have read this thesis and in my opinion this thesis is sufficient in terms of scope and quality for the award of the degree of Master of Philosophy"

Signature	:	....
Name of Supervisor	:	DR NOR’AZIZI BIN OTHMAN
Date	:	....

BAHAGIAN A – Pengesahan Kerjasama*

Adalah disahkan bahawa projek penyelidikan tesis ini telah dilaksanakan melalui kerjasama antara ________________________ dengan ________________________

Disahkan oleh:

Tandatangan : .... Tarikh : ....

Nama : ....

Jawatan : ....
(Cop rasmi)

* *Jika penyediaan tesis/projek melibatkan kerjasama.*

BAHAGIAN B – Untuk Kegunaan Pejabat Sekolah Pengajian Siswazah

Tesis ini telah diperiksa dan diakui oleh:

Nama dan Alamat Pemeriksa Luar : ____

____

Nama dan Alamat Pemeriksa Dalam : ____

____

Nama Penyelia lain (jika ada) : ____

____

Disahkan oleh Timbalan Pendaftar di Sekolah Pengajian Siswazah:

Tandatangan : --- Tarikh : -----------

Nama : ----------------------

OPTIMIZATION OF OTEC AND LOW TEMPERATURE THERMAL DESALINATION PLANT FOR ELECTRICITY AND FRESHWATER PRODUCTION IN MALAYSIA

MOHD ALSHAFIQ BIN TAMBI CHIK

A thesis submitted in fulfilment of the
requirements for the award of the degree of
Master of Philosophy

Malaysia-Japan International Institute of Technology
Universiti Teknologi Malaysia

MAY 2017

I declare that this thesis entitled "*Optimization of OTEC and Low Temperature Thermal Desalination Plant for Electricity and Freshwater Production In Malaysia*" is the result of my own research except as cited in the references. The thesis has not been accepted for any degree and is not concurrently submitted in candidature of any other degree.

Signature	:	....
Name	:	MOHD ALSHAFIQ BIN TAMBI CHIK
Date	:	………………………………………

To my beloved parents, wife and family.

ACKNOWLEDGEMENT

First and foremost, my sincerest gratitude to my Almighty, the most gracious and merciful with His blessing until I accomplished my research work

My first gratitude sincerely goes to my parents. I have received support from my beloved mother whose encourage me to complete this research. To my late father, I’m sure that you would do the same thing if you are still alive. My gratitude also goes to my beloved wife. Her support, encouragement, patience and unwavering love were undeniably.

I wish to express my deep sense of gratitude to all the lecturers for the valuable guidance and providing necessary facilities to make this project successfully.

Last but not least, I humbly extend my gratitude to all persons who helped me to achieve my dream.

ABSTRACT

Sources of electricity in Malaysia depend highly on fuel, natural gas, and coal which can give a negative impacts to the environtment such as air pollution. The desalination plant as brackish water consumes high electricity to produce freshwater as associated with heating, cooling, water treatment and separation process. OTEC plant is a green renewable energy method to generate electricity. This study used a desalination method without pre-heating the incoming water called OTEC-LTTD plant. In this method, the water vapor is produced when the hot water is transferred into a de-pressurized chamber below the saturation pressure corresponding to the water temperature. The steam will then condensed on the surface of the condenser through the supplied cold water. This method is called "Low Temperature Thermal Desalination". For the purpose of this study, the simulation on OTEC plant, desalination plant (LTTD) and integrated OTEC-LTTD plant were carried out under the tropical temperature and topographic information found in Malaysia. The input parameters will be optimized to identify the optimum operating parameters that provide low-grade energy to produce freshwater. The results reveal that the specific power consumption needed to produce freshwater from OTEC-LTTD plant is lower than others types of desalination plant. From the proposed simulation, it is found that the net power of 804 kW and freshwater rate of 16.49 kg/s (59.36 t/h) can be produced at warm seawater temperature and cold seawater temperature of 26 °C and 4 °C respectively. The energy that is required to produce 59.36 t/h freshwater by using the most energy-efficient desalination process would be 207 kW and this is by using RO method. At the highest temperature of this simulation which was 30 °C, the freshwater capacity produced was 11.57 kg/s, equivalent to 1000 ton/day of freshwater. From a thermodynamic point of view, the results from combining the sustainable energy with desalination technology had provided useful knowledge for human kind.

ABSTRAK

Sumber tenaga elektrik di Malaysia adalah sangat bergantung kepada bahan api, gas asli dan arang batu yang memberi kesan negatif kepada persekitaran seperti pencemaran udara. Loji penyahgaraman seperti air payau menggunakan tenaga elektrik yang tinggi untuk menghasilkan air tawar seperti untuk proses pemanasan, penyejukan, rawatan air dan pengasingan. Loji OTEC menggunakan sumber tenaga hijau untuk menjana tenaga elektrik. Kajian ini menggunakan kaedah penyahgaraman tanpa memanaskan air yang masuk dikenali sebagai loji OTEC-LTTD. Dalam kaedah ini, wap terhasil apabila air panas dipindahkan ke dalam ruang di bawah tekanan tepu sepadan dengan suhu air. Kemudian stim akan memeluap pada permukaan pemeluwap melalui air sejuk yang dibekalkan. Kaedah ini dikenali sebagai " Penyahgaraman Haba Suhu Rendah". Bagi tujuan kajian ini, simulasi ke atas loji OTEC, loji penyahgaraman (LTTD) dan loji OTEC-LTTD bersepadu telah dijalankan di bawah suhu tropika dan maklumat topografi yang terdapat di Malaysia. Parameter input akan dioptimumkan untuk mengenalpasti parameter optimum yang memberikan tenaga gred rendah untuk menghasilkan air tawar. Keputusan menunjukkan bahawa penggunaan kuasa khusus untuk mengeluarkan air tawar daripada loji OTEC-LTTD adalah lebih rendah daripada jenis loji penyahgaraman lain. Daripada simulasi yang dicadangkan, tenaga bersih 804 kW dan kadar air 16.49 kg/s (59.36 t/j) boleh dihasilkan pada suhu air laut panas dan suhu air laut sejuk masing-masing pada 26 °C dan 4 °C. Tenaga yang diperlukan untuk menghasilkan 59.36 t/j air tawar dengan menggunakan proses penyahgaraman yang paling efektif adalah 207 kW dan ini adalah dengan menggunakan kaedah RO. Pada suhu tertinggi dalam simulasi ini iaitu 30 °C , kapasiti air tawar yang diperolehi adalah 11.57 kg/s, bersamaan dengan 1000 tan/hari air tawar terhasil. Dari sudut termodinamik, hasil daripada gabungan tenaga boleh diperbaharui dengan teknologi penyahgaraman telah memberikan ilmu pengetahuan yang berguna kepada manusia.

TABLE OF CONTENTS

LIST OF TABLES

LIST OF FIGURES

LIST OF ABBREVIATIONS

BPR	-	Boiling Point Rise
COP	-	Coefficient of Performance
CSIRO	-	Commonwealth Scientific and Industrial Reseach Organisation
DCC	-	Direct Contact Condenser
ED	-	Electrodialysis
GHG	-	Greenhouse Gases
GSW	-	Gibbs Seawater
GWP	-	Global Warming Potential
IAPSO	-	International Association Physical Science of the Ocean
IDE	-	Integrated Development Environment
LTTD	-	Low Thermal Temperature Difference
MED	-	Multi-Effect Distillation
MLD	-	Million Litre Per Day
MSF	-	Multi-Stage Flash
ODP	-	Ozon Depletion Potential
ORC	-	Organic Rankine Cycle
OTEC	-	Ocean Thermal Energy Conversion
PHE	-	Plate Heat Exchanger

RO	-	Reverse Osmosis
SCOR	-	Supply chain Operations Reference
SEE-VC	-	Single Effect Evaporation Coupled With Vapor Compression
STHE	-	Shell and Tube Heat Exchanger
WEC	-	Wave Energy Converter

SEE-VC - Single Effect Evaporation Coupled With Vapor Compression
STHE - Shell and Tube Heat Exchanger
WEC - Wave Energy Converter

LIST OF SYMBOLS

Q	-	Useful heat gain
m	-	Fluid mass flow rate
C_p	-	Specific heat of fluid
η	-	Efficiency
m	-	Mass flow rate
T	-	Temperature
U	-	Overall heat transfer coefficient
A	-	Area
UA	-	Thermal conductance
h	-	Enthalpy
s	-	Entropy
ΔH	-	Head difference
ΔT_{lm}	-	Log mean temperature difference
L	-	Pipe Length
W	-	Work
WP	-	Pumping power
v	-	Velocity
ϵ	-	Surface roughness
D	-	Diameter

σ	-	Clearance
f	-	Friction
μ	-	Viscosity
P	-	Pressure
ρ	-	Density
g	-	Gravitational acceleration
ΔT_{lm} -	-	Log Mean Temperature Difference
ΔH	-	Head difference
Re	-	Reynold number
R	-	Gas constant
K_a	-	Specific heat ratio

Subscript :

Atm	-	Atmospheric
cs	-	Cold seawater
ws	-	Warm seawater
sat	-	Saturation temperature
dc	-	Desalination condenser
dw	-	Desalinated water / freshwater
th	-	Thermal
wf	-	Working fluid
vp	-	Vacuum
eq	-	Equivalent

Den	-	Density difference in seawater
fric	-	Friction loss
fc	-	Flash chamber
i	-	Inlet
o	-	Outlet
E	-	Evaporator
C	-	Condenser
T-G	-	Turbine generator
T	-	Turbine
G	-	Generator
net	-	Net
tot	-	Total

LIST OF APPENDICES

CHAPTER 1

INTRODUCTION

1.1 Background of the Study

Freshwater is used by the energy sector along the complete supply chain from extraction and conversion of raw material through to generation of power. Energy and water are valuable resources that underpin human prosperity and are, to a large extent, interdependent. This chapter addresses water for energy in the context of the energy scenarios. It provides information on future water requirements for energy production and identifies the particular water resource risks associated with our energy scenarios.

1.1.1 Electricity Demand

With the high consumption of electricity these days, it makes electricity as one of the global demand. The use of electricity in home appliances, industrial, all domestic and non-domestics causing the electricity to become so vital. Figure 1.1 shows the electricity consumption per capita in Malaysia whereby its population is used as a benchmark for identifying how much electricity consumption is needed. In 2013 electricity consumption per capita in Malaysia is 4511.97 kWh and it has been increasing rapidly from 1990 to 2013. This rapid increase in electricity consumption over the years is due to economic and population growth.

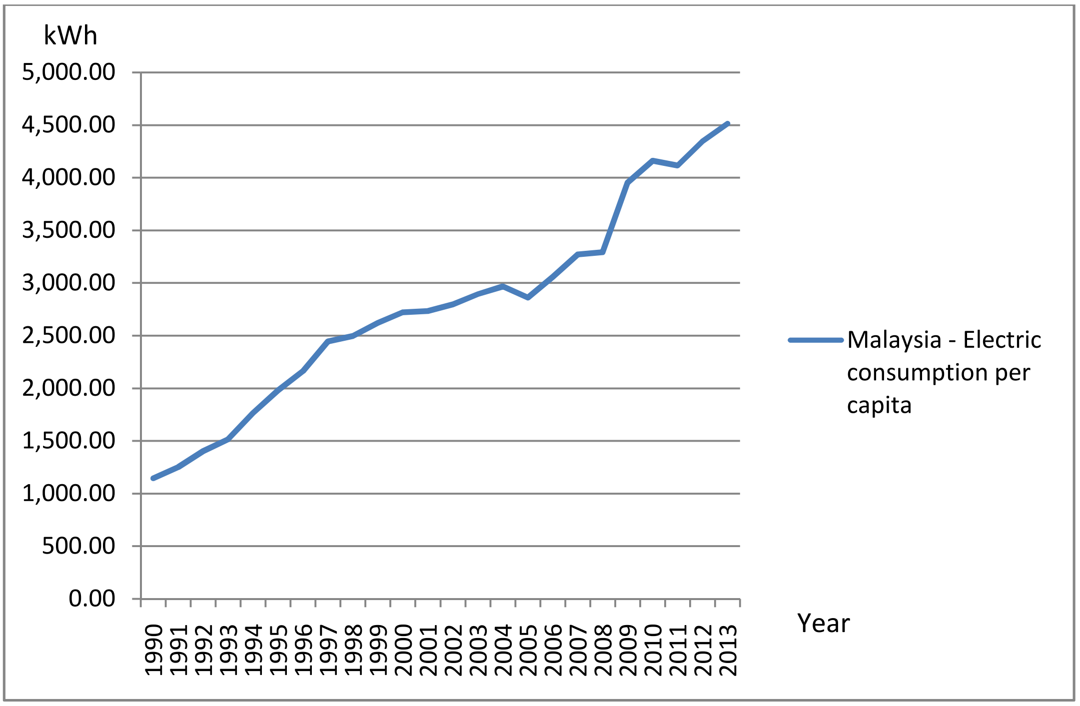

Figure 1.1 Electric Consumption Per Capita (Saboori and Sulaiman, 2013)

Figure 1.2 shows the relationship between electric power consumption and total electricity generation by year. This shows that as the population increases every year it has affected the demand for electricity. According to an article written by Ali Imran Mohd Noor (2012) of Bernama, the electricity consumption per household in Malaysia is 251 kWh per month which means that one household can release 171.68 kg of carbon dioxide per month. As such, electricity produced from fossil fuel, oil, coal and gas released many gases into the air thereby contributing a negative impact on the environment such as the climate change and global warming. These problems make many parties strive to reduce the problem by implementing the green technology.

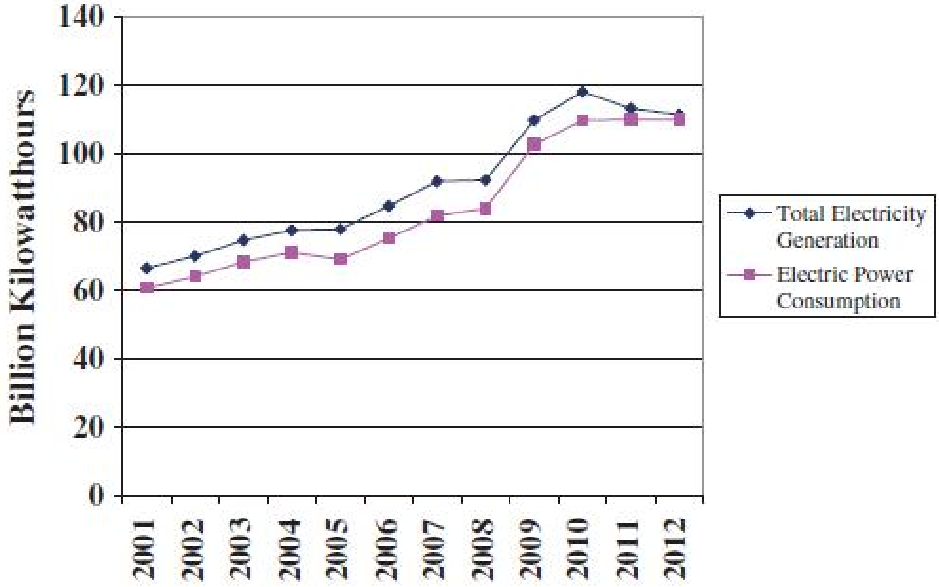

Figure 1.2 Power generation and electricity consumption in Malaysia (Hosseini and Abdul Wahid, 2014)

The alternative power generation from renewable energy sources such as ocean thermal and solar can help to protect the earth from being destroyed. Figure 1.3 shows the solar panel and the wind energy for power generation that has been applied in Malaysia.

Figure 1.3 Solar panel and wind turbine plant for power generation (Darus et al., 2008)

1.1.2 Freshwater Demand

The water desalination technology is one of the most important and commercialized technology available nowadays. In the present situation, the world is facing shortage of available freshwater resources from rivers and groundwater which are presently limited. For the incoming years, more freshwater will be needed to support the increase in population rates, expansion of industrial activities and for agriculture purpose. All living creatures and many economic activities will depend on water and it's impossible to live without it. Today, many countries are meeting their freshwater demands by depending on desalination technologies such as in the Middle East countries (eg: Kuwait, Saudi Arabia, and the United Arab Emirates) where the seawater desalination is important and dependable freshwater resources (Mistry et al., 2013, Lee et al., 2013). Nowadays, seawater is a huge source for freshwater through seawater desalination technologies. Figure 1.4 shows the global water distribution where it indicates that seawater is a major water reservoir of which 97% of the global water distribution is covered by the ocean. The available groundwater or freshwater for the earth's total water supply account less than 0.7% which is very limited resources (Kim et al., 2013). The distribution of freshwater that needs to support the world water demand is relatively small and depleted as the years go by. An abundant of seawater is beneficial to support the ecosystem by converting into freshwater.

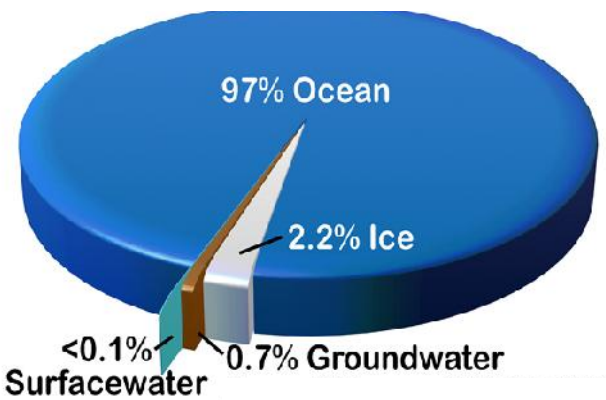

Figure 1.4 The World Global Water Distribution (Cosgrove and Rijsberman, 2014)

In future, the increase in population, agriculture, and all industry will contribute to the water scarcity (Cosgrove and Rijsberman, 2014), as shown in Figure 1.5. Therefore, any approach or method that should be taken must be able to meet the freshwater demand.

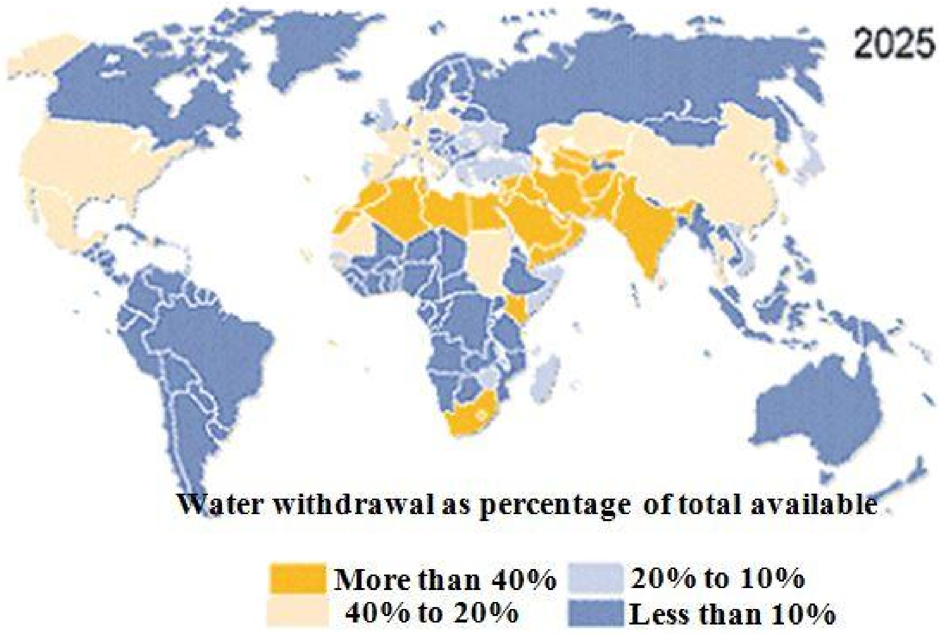

Figure 1.5 Projected Water Scarcity in 2025 (Hoekstra, 2014)

Desalination process is the prosess of separating saline seawater into two streams. The first stream is the freshwater which contais a low concentration of dissolved salts and the other one is a concentrated brine stream. Numerous seawater desalination technologies have been growing, for example membrane separation, thermal distillation, freezing and electrodialysis. There are two types of seawater desalination process which is thermal desalination and membrane separation. The multi-stage flash (MSF) and multi-effect distillation (MED) are the sort of thermal distillation while the reverse osmosis is the kind of membrane separation. The flash evaporation under vacuum process is a distinguishing future of desalination technologies. This process involves heat mass transfer process which the evaporator and condenser operate in partial vacuum ranging from 1 percent to 3 percent of atmospheric pressure (Kulkarni and Joshi, 2016).

All technologies pose a practical concern and technical limitation that must be addressed (Elimelech and Phillip, 2011, Ghaffour et al., 2013). Ocean Thermal Energy Conversion (OTEC) is the technology that utilises the seawater as a energy carrier by harnessing the temperature difference between the sun-warmed surface of the tropical oceans and the cold deep seawater to generate electricity indirectly (Khan et al., 2017). The open cycle OTEC has the same concept as a low-temperature thermal desalination process. Both systems uses vacuum pumps to create a low-pressure, a low-temperature environment in which water evaporates even at a temperature gradient of 8 °C between two volumes of water. A hybrid cycle is a coupled technology that combines both the closed and open cycle systems. An example of a hybrid cycle is OTEC-desalination or OTEC-desalination-hydrogen. Instead of generating electricity, the condenser in open and a hybrid cycle is used to generate desalinated water which suitable for human consumption, agriculture, refrigeration, hydrogen and etc (Huang et al., 2003). Hence, by integrated both technologies, we are able to produce electricity, freshwater and byproducts simultaneously.

The study was conducted to review the advanced seawater desalination technology based on the distillation system (under vacuum process). The flash boiling concept has been applied in this process. In the flash evaporation process is when the liquid is preheated and is then subjected to a pressure below its vapor pressure causing boiling or flashing to occur. The vapors flash off the warm liquid and the salts exit with the remaining water. The investigation is aimed at utilizing different outlet temperature in an evaporator and condenser so as to produce freshwater using a low-temperature thermal desalination process. The input parameters will be optimized to identify the optimum operating parameters that provide low-grade energy to produce freshwater. The sources for generating electricity can bring environmental pollution and the process of getting freshwater would consume much electricity. Therefore, a green renewable energy like OTEC is seen to be the promising solution to maintain the environmental benign and sustainability.

1.2 Problem Statement

Water is essential to human being because all living creatures are dependent on it. The lack of freshwater will cause huge sanitation issues, safe drinking supply, poor hygiene, slow industrial development and many more issues. From the issues of GHG emissions and water scarcity, the awareness of these problems would be important for everybody on the planet (Nair et al., 2014). The need of freshwater is rising rapidly every year due to population growth and other uses. Furthermore, the source of freshwater is less than 0.7 percent which is relatively critical to support the rapidly increasing in population over the years. Thus, using desalination by converting the seawater into freshwater is needed as the source is freely available to use. In order to produce freshwater, high energy consumption is needed and pre-treatment process is needed for stand-alone and conventional desalination plant. For electricity, the sources of energy is mainly obtained from fossil fuel, oil and coals which have released undeniable gases into the air, which is not only harmful but cause pollution to the environment. Like freshwater, the demand for electricity is also increasing through the years. Currently, Malaysia is largely dependent on fuels and coal as its primary electricity generation. Therefore, it is important that it move towards generating electricity by using clean and renewable energy in order to support the electricity demand. One of the solutions is to develop an integrated OTEC cycle like OTEC-desalination technology that can generate fresh water and electricity with zero emission of carbon dioxide gas. Many research and studies have been conducted on OTEC and desalination like their cost effectiveness, efficiencies, design, new techniques and the hybrid system. A low vacuum distillation consists of flash evaporation is a distinguishing feature of open cycle OTEC (Vega, 2013). The simulation model of an integrated OTEC has been studied by Syo Nakamura. A desalination plant was constructed in order to solve the energy and water problems. At the same time, several reviews on simulation results have been conducted for individual OTEC and desalination system under the same condition (Nakamura et al., 2009). A simulation study of OTEC-LTTD plant will be conducted to investigate the optimum parameter for the operating condition. The study will then be followed by varying the inlet seawater temperature and mass flow rate of the evaporator and condenser. The performance of the system was evaluated by varying system parameters based on Malaysia topographic condition to yield electricity and freshwater. The results will show the feasibility of OTEC- LTTD to be constructed in Malaysia.

1.3 Site Potential of OTEC and Desalination Plant in Malaysia

Currently, there is not any global map showing Malaysia as having a potential area for generating ocean thermal energy. However in 2008, a marine team that has done a survey in the South China Sea confirmed that Malaysia has a great potential to exploit electricity by using OTEC technology. This potential area is located in the North-Borneo trough or known as Sabah trough as shown in Figure 1.6.

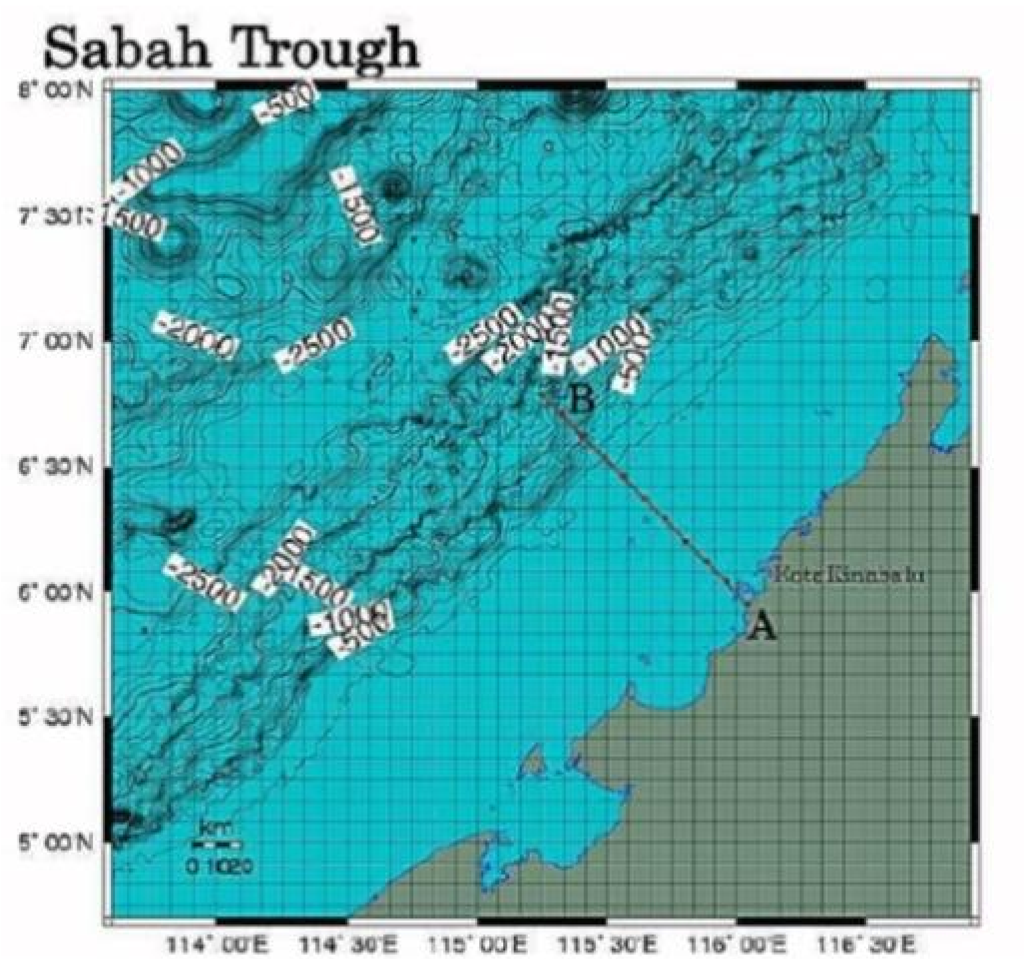

Figure 1.6 Sabah Trough

Figure 1.7 shows the temperature vs. depth at the Sabah trough where the average surface temperature is 28 ^{o}C and located 1200 m at the bottom of the sea is 3 ^{o}C. According to the popular literature, any area with such a temperature differential of over 20 ^{o}C has the potential generating not only renewable energy but also freshwater. Malaysia is a country with equator season year-round. The mean sea temperature around the Malaysia calculated more than 26 ^{o}C up to 31 ^{o}C. Unfortunately, the depth of the ocean in Malaysia does not exceed the basic requirement for OTEC implementation, which is the temperature differential at least 20 ^{o}C. However, only at Sabah trough the cold deep seawater temperature is around 4-3 ^{o}C range from 1.0 km to 1.2 km depth.

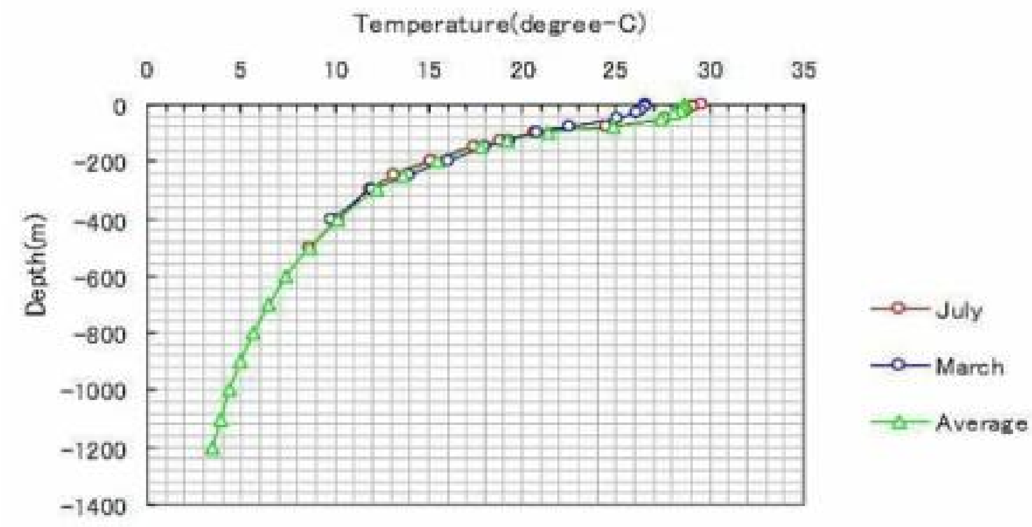

Figure 1.7 The graph temperature vs depth of Sabah Trough.

Figure 1.8 shows that the distribution of the average surface seawater temperature at Sabah trough, range from 26 -30 ^{o}C. The temperature difference *ΔT*, of warm seawater and cold seawater is more than 20 ^{o}C. The plant can be designed according to the warm seawater temperature of 26 ˚C and 6 – 4 ˚C of cold seawater on 760 - 1000 m depth from the surface water level. The information for thermal temperature, topographic and site potential of OTEC plant were referring to Abu Bakar Jaafar (2013).

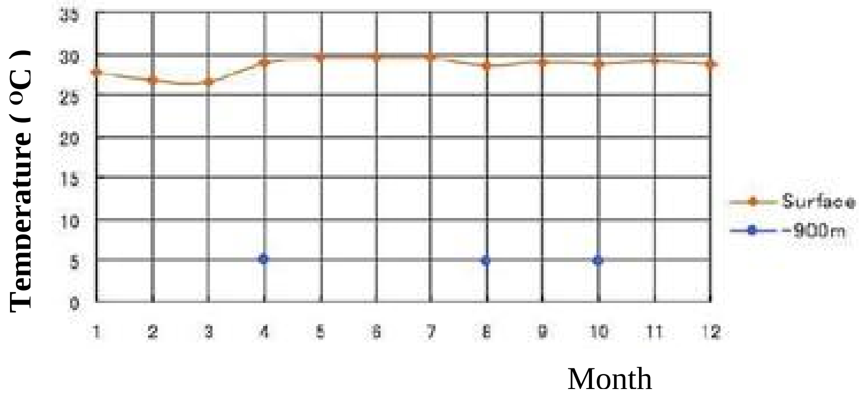

Figure 1.8 The graph of average surface seawater temperature at Sabah Trough

1.4 Objective of the Study

The main objective of this project is to optimize the desalination plant for an integrated OTEC desalination plant under the Malaysian tropical condition. The study aims to use a numerical and simulation study to investigate the OTEC and LTTD system performance. The focus of the research is to evaluate the optimum operating condition based on electricity generation and desalinate freshwater production. Apart from that, a simulation of experimental data by suitable model will be of interest in this research. The study will propose the 1 MW OTEC plant combined with LTTD plant that will boost the OTEC plant through freshwater production. This study will show a comparison in terms of specific energy consumption to produce desalinated freshwater, between integrated OTEC desalination plant and other desalination technology.

1.5 Scope of the Study

The scope of this study will be covered as follows:

i. Literature review on desalination technologies and another desalination concept.

ii. Develop a simulation on LTTD plant to study the input parameters effect.

iii. Develop a simulation on OTEC-LTTD plant.

iv. Generate data based on Malaysia tropical temperature condition and temperature data.

v. Identify optimum operating condition design.

1.6 Significance of the Study

An OTEC-LTTD plant is a combination of closed and open cycle OTEC where typically closed cycle is for electricity generation while open cycle is for freshwater production. However, there is a larger pressure different when the working fluid inside the closed cycle passes through the open cycle. This situation will create either a single stage or two-stage flash evaporation. The power consumption required to generate freshwater in OTEC-LTTD plant is much lower than a stand-alone desalination plant because its power is only required for vacuum pump (Panchal and Bell, 1987). Although there has been numerous research conducted on the performance and characteristics of flash desalination in terms of cost and design, but still lacking in reliable data based on the best condition parameter for ocean flash desalination system. Furthermore, the modeling and simulation study are preferable in identifying the design parameter and controller design before proceeding to the real plant (Upadhyay and Sharma, 2014). The optimization technique will be conducted in order to analyze the performance based on existing OTEC and integrated OTEC-LTTD system. In this study, selecting the best performance in giving the maximum electricity generation and freshwater production rate will be discussed. Besides, there are several parameters that are significant to the study that will be configured. Therefore, the results obtained from this study can provide the necessary information to be used as a guideline for the future implementation of OTEC-LTTD plant in Malaysia.

CHAPTER 2

LITERATURE REVIEW

2.1 OTEC Working Principle

Ocean Thermal Energy Conversion is one of the methods in green technology that use seawater as a solar agent. The concept of temperature difference between surface seawater and cold deep seawater is applied to generate electricity. From the previous research, the difference in temperature of at least 20 ˚C where the cold seawater is taken from the specific depths of the ocean is necessary to sustain and maintain the performance of the OTEC system (Bregman et al., 1995). This causes the available seawater as the main source to generate electricity. Seawater absorbs most of the heat transferred by sunlight and it redistribute by mixing effect induced by the surface current. The temperature of seawater is relatively uniform up to a depth of 100 m. In OTEC cycle, the range of the tropical temperature is around 26 ˚C – 30 ˚C (Tierney et al., 2015) and is enough to vaporize the working fluid such as Ammonia and Freon in the evaporator. These working fluids are commonly used because of the low boiling point at the vapor state. Figure 2.1 shows the general arrangement of OTEC cycle. Firstly, the ammonia that has been vaporized in the evaporator will expand and spin the turbine coupled with a generator to produce electricity. The cold seawater is used to condense the ammonia vapor into a liquid state. Then, the working fluid is pumped back into the system to be reused and the loop is continued.

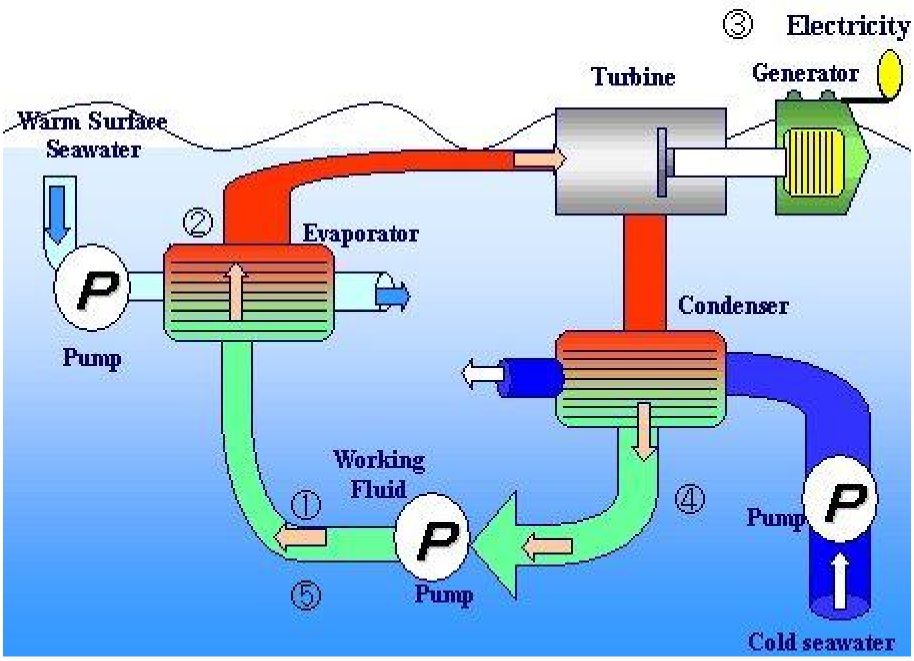

Figure 2.1 OTEC cycle

2.2 LTTD Working Principle

Low Thermal Temperature Distillation (LTTD) is the technology that makes use of flash evaporation and vacuum concept. Flash or partial evaporation is the boiling of a liquid that occurs when a saturated liquid encountering sudden reduction of its pressure which generates vapor and non-evaporating liquid. The warm seawater will undergo a process of "flash evaporation" or the rapid boiling after entering the flash evaporator chamber. The vapor generated in the flash chamber is then cooled and condensed by the deep cold seawater in the condenser. The freshwater that are obtained from the condensation process occur in the condenser.

The steps of flash desalination system are described in Figure 2.2. The process is similar to the open cycle OTEC where the working fluid vapor expands through a low-pressure turbine to generate power before being condensed back to water using cold water piped up from the depth of the ocean. Therefore, vacuum desalination is one of alternative technology that converts saline water to freshwater.

Besides, by decreasing the pressure in the flash chamber rather than heating the seawater to the boiling point, it will be an advantage in term of energy consumption (Chung et al., 2012). In a LTTD plant, a vacuum pump is needed to create a low pressure in condenser and evaporator.

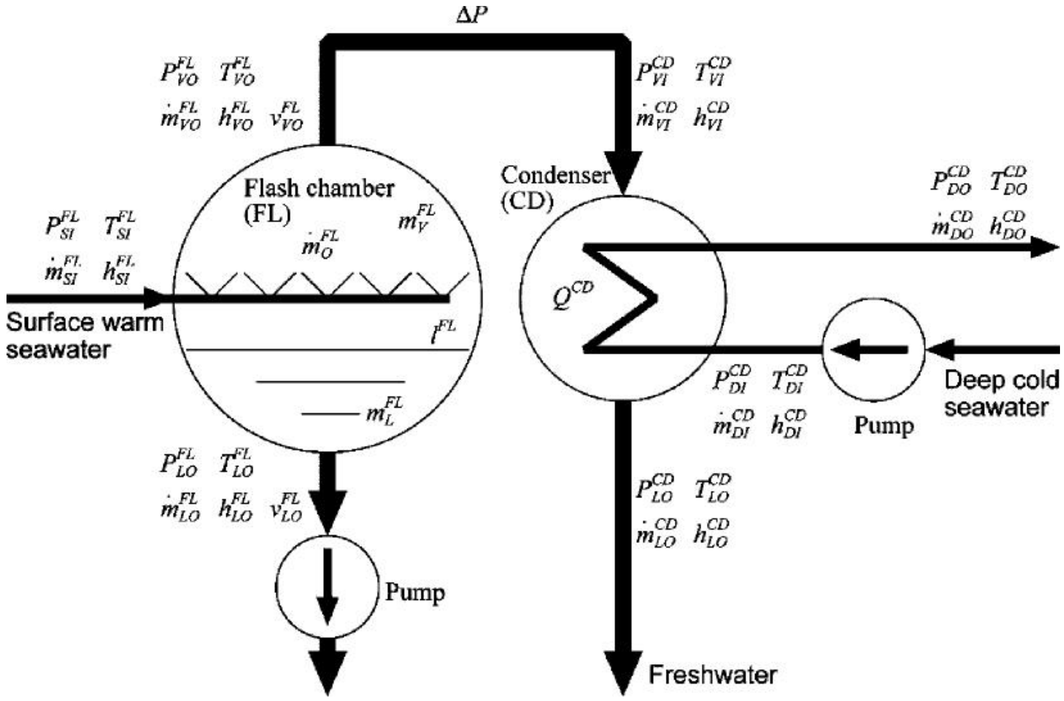

Figure 2.2 Spray flash desalination system schematic diagram (Goto et al., 2008)

2.3 Ocean Energy Power Generation

Generally, renewable energy can be defined as the energy that comes from resources which are naturally replenished such as ocean and geothermal heat. However, not all renewable energy is green and zero CO_2 emission. Power generation from ocean energy sources is a green renewable energy and can be produced from two sources, ocean energy which is thermal energy from the sun heat and mechanical energy from the tides and waves (Ellabban et al., 2014). The thermal energy source is fairly constant while tidal and waves are the intermittent source of energy. The source of mechanical energy is free but it is not available in 24 hours a day throughout the year like in OTEC technology.

2.3.1 Wave Energy

Winds drive and transport the energy that is naturally generated by the wave. The potential kinetic energy available in wave energy is the reasons why wave energy is so competitive in line with other resources. Nowadays, there are many parties have started to explore wave energy and come out with different technologies, methods and machine for generating electricity. The typical machine used to generate electricity is called as the Wave-Energy-Converter (WEC). Here, every machine is applying the same concept to capture the wave kinetic energy. Figure 2.3 shows the principles of generating electricity by exploiting wave kinetic energy stored in the wave.

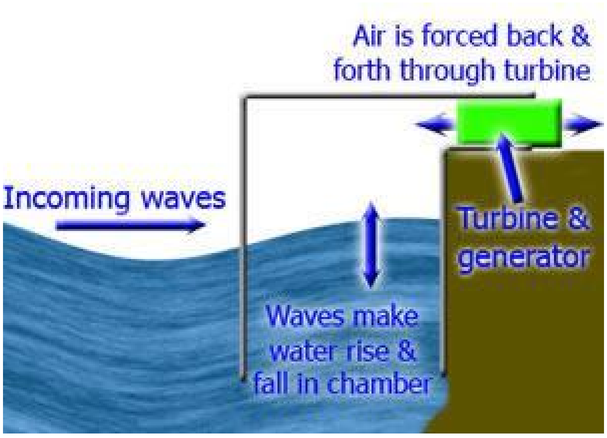

Figure 2.3 Principle of wave energy (López et al., 2013)

The Agucadoura wave farm is the first wave farm with the capacity of 2.25 MW in the world as shown in Figure 2.4. However, it was shut down two months after its official opening due to the financial (Drew et al., 2009) and technical problems of the wave machines (Vosough, 2011). However, until now most of the wave energy projects remain in the pilot study because of the difficulty to deal with the wavelength. Some areas have unreliable wave behavior and it becomes unpredictable to forecast accurate wave power. Therefore, wave energy cannot be trusted as a reliable energy source.

Figure 2.4 Pelamis machine bursting through a wave (Dalton et al., 2010)

2.3.2 Tidal Energy

The tide is created by the gravitational effect of the sun and the moon on the earth causing cyclical movement of the seas. Generally, the tidal range is on vertical differences in high tide and low tide. Tidal energy converts the energy of tides into electricity but it is predictable. Tidal energy will be a competitive energy resource in the near future and its working principle is shown in Figure 2.5.

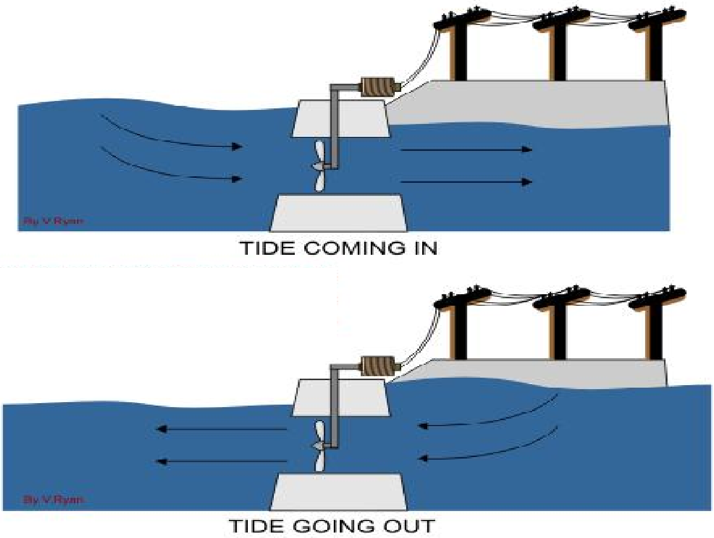

Figure 2.5 Principle of tidal energy. (Khan et al., 2017)

2.3.3 Thermal Energy

OTEC is a form of thermal energy and unlike mechanical energy, its source is free, abundant and continually being restored as long as the sun shines and natural current exist. The main input source of OTEC is warm and cold seawater. Furthermore, the heat stored in the surface ocean is available all day and that makes OTEC a stable energy power supply. Other ocean energy does not have a stable input supply because both methods are dependent on wind and the rise and fall of ocean tides. The first evaluation on OTEC technology was done in the 80's mainly on technical feasibility rather than economical. However, due to technical improvement and changes in social situations over the years, this technology once again has attracted interest from various parties. Recently, due to awareness of global warming, higher electricity cost to secure energy, commercialization of OTEC has seen to be economically viable especially on a tropical island. Figure 2.6 shows the largest operating plants namely the Sihwa Tidal Plant and Jiang Xia Power Plant. The actual electricity generation counted less than half of the installed capacity for the turbine power. This is due to the unstable supply of the input energy for the plant. This makes OTEC Power Plant more competitive to produce electricity continuously.

Figure 2.6 Tidal Energy Power Plants. (Cho and Park, 2014, Zhou et al., 2016)

Figure 2.7 (a) shows the first 15 kW Mini-OTEC plant that has been developed since 1979 in Keahole Point, Hawaii. This plant was built at the Natural Energy Laboratory of Hawaii Authority (NELHA) to demonstrate the concept. Recently, with the maturity and advancement of technology, Makai Ocean Engineering has completed its operation of 105 kW OTEC power plant to produce electricity as shown in Figure 2.7 (b). In Figure 2.7 (c), it shows the OTEC desalination plant by NIOT, India that produced 1000 t/d of freshwater production. This plant has been developed since 1979 and still in operation until now. Figure 2.7 (d) shows the operating OTEC plant in Japan which is located on Kumijema Island, Okinawa. This plant started its operation in April 2013 and research is conducted by Saga University, Japan. The latest news is the first OTEC in India project coming up in Karavatti, Lakshadweep with 200 kW capacity to power a desalination plant (ANI, 2016).

(a) (b)

(c) (d)

Figure 2.7 OTEC Energy Power Plant (a) 15 kW closed cycle Mini-OTEC plant, Hawaii (Owens and Trimble, 1981) (b) 105 kW OTEC plant, Hawaii (c) OTEC desalination plant, India (Ravindran and Abraham, 2002) (d) OTEC plant, Okinawa Japan (Yamada et al., 2009)

2.4 Global Potential of Ocean Energy

The power generation from ocean energy has a lot of potential, however until now the technology is not yet commercialized. The global potential of electricity generation by ocean energy is promising though not yet marketed because its generation technologies are not widely demonstrated and the plants are not well developed. A number of researches have been conducted by many parties because they have seen the potential of OTEC as power generating system. The ocean energy has seen to be a future green power generation technology since there are many existing proposed power generation plant. As shown in Figure 2.8, the OTEC technology has a big potential since the source input is available in 24 hours per day. OTEC technology is capable to extract 3-11 Terawatt-years from available 23000 Terawatt-years of energy per year which make an OTEC is the highest renewable energy to produce electricity over the years.

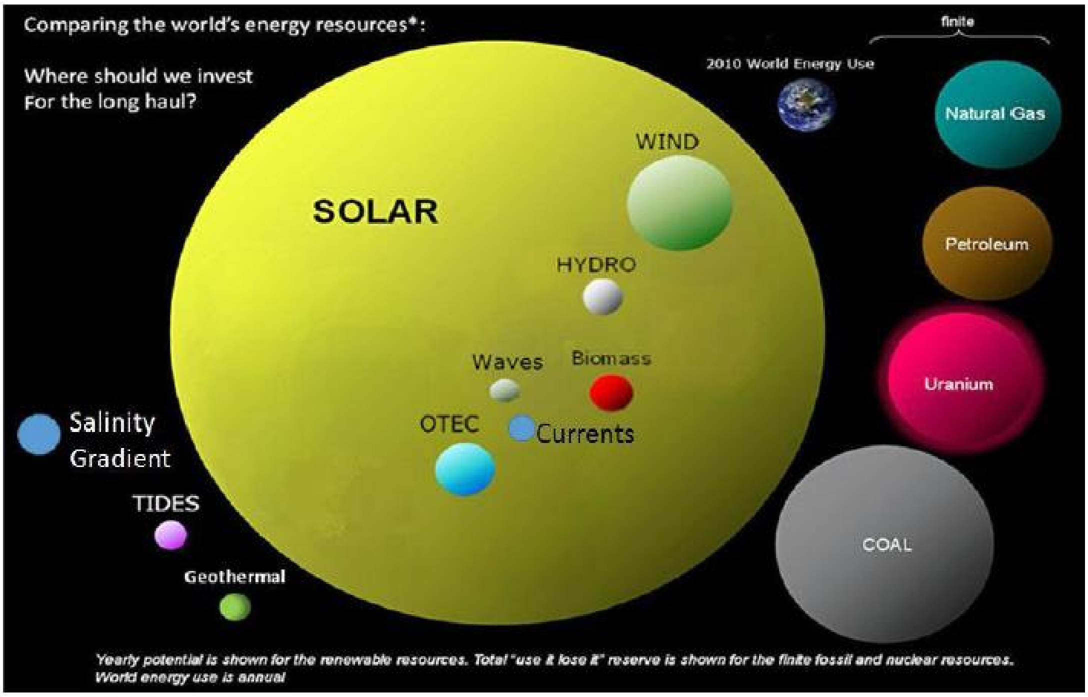

Figure 2.8 Sources of power generation (Abu Bakar Jaafar, 2016)

2.5 Seawater Desalination

This sub-chapter will cover existing methods used for seawater desalination technologies and the previous research of low vacuum desalination. There are numerous advanced technologies that have been developed for seawater desalination plants. Many aspects such as geological aspect, design and energy consumption have to take into consideration in order to build up a decent plant. Desalination technology is very popular in the arid region such of Arabia and North African region. Although, the 'Water Rich' regions are available but the water quality is low due to the contamination, thus people have to rely on desalination technology to get freshwater. Humans do need water for circulation, respiration, and converting food to energy.

After oxygen, water is the body's 2nd most important needs. Simply said, humans need water to survive. This means that desalination technology is very important to generate safe water supply and indirectly contributes significant effort to global sustainability. Generally, all the desalination methods have the same concepts and basic principle. The main objective of the desalination process is to separate the contained brackish or salty water. The brine is disposed off as waste from the desalination processed. All desalination process needs the energy to convert saline water to freshwater as shown in Figure 2.9. Different type of desalination needs different capacity and energy consumption. A lot of technologies have been developed for desalination every year and it will continue be better for future technologies on the basis of thermal distillation, membrane separation, freezing and electrodialysis (Ellabban et al., 2014).

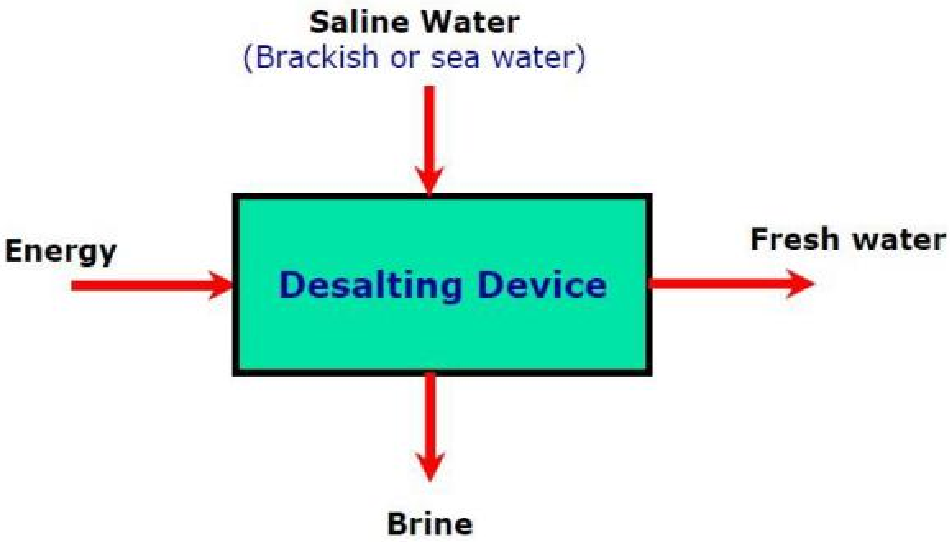

Figure 2.9 Desalination principles (Banat, 2007)

Multi-stage flash (MSF) and multi-effect distillation (MED) are the types of thermal desalination used frequently. This desalination process was described as the process of heating the water solution and collecting the portable water yield when the vapor cools and condensation occur (Gude, 2015). Reverse osmosis is the process that uses a semi permeable membrane to remove larger particles from drinking water. Normally, reverse osmosis is always being selected to undergo the desalination process due to low specific energy consumption (Miller et al., 2015). Figure 2.10 shows the commercial desalination process available nowadays.

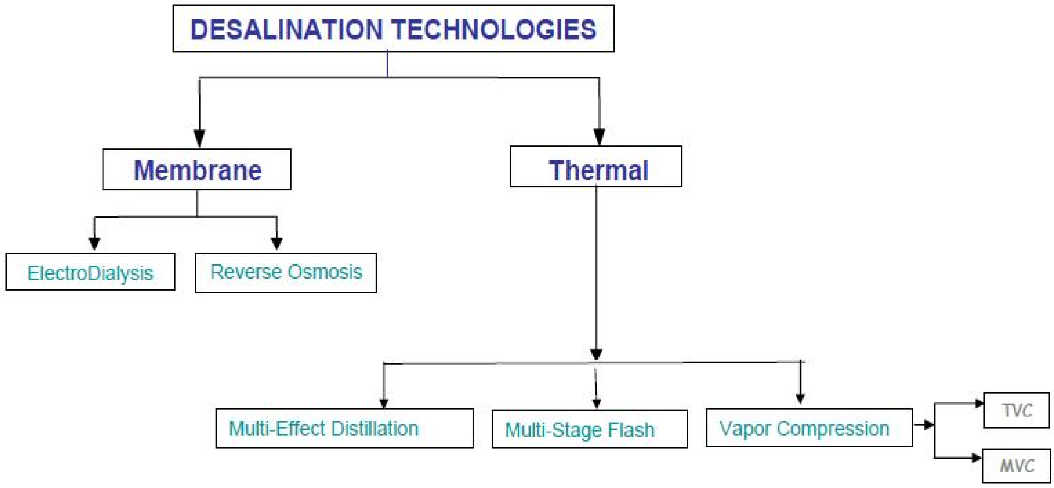

Figure 2.10 Desalination technologies (Ghaffour et al., 2014)

2.6 Thermal and Membrane Desalination Process

In thermal desalination process, the freshwater will be separated from saline or brackish water by using the phase-change concept. It occurs within two ways either by evaporating (i.e. using flash evaporation) the saline water and condensing the steam generates by evaporation processed or the other way is by producing fresh ice crystal by freezing the water and go to the separation process, then melting the ice crystal. The process applying this concept is MSF, MED, single effect evaporation coupled with vapor compression (SEE-VC) and a solar drive method distillation.

In MSF process, the feed water is being heated at the certain temperature and enter into a depressurize evaporator to flash into steam. It can be worked by using a single stage or various stages, where the following stage must have a lower pressure than previous stages. The MSF can be divided into heating section, heat recovery and heat rejection section as in Figure 2.11.

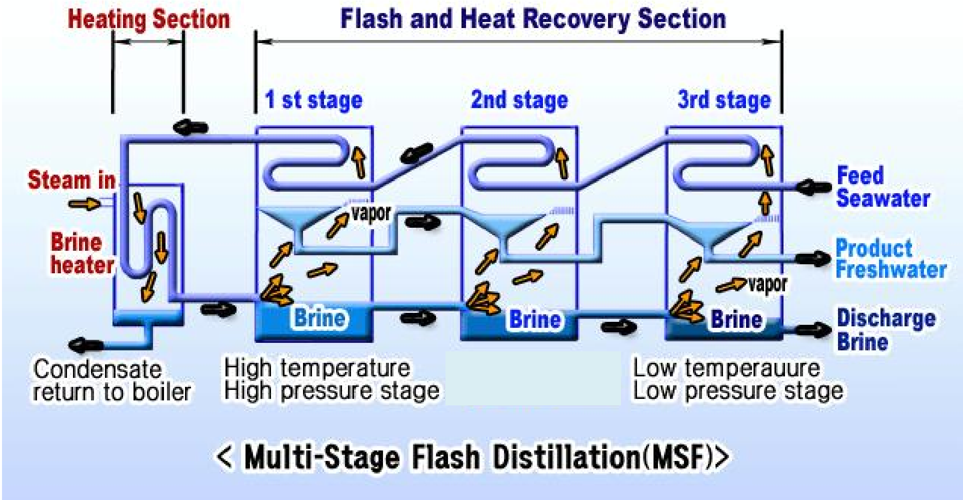

Figure 2.11 MSF process with brine circulation (Tayyebi and Alishiri, 2014)

The MED process is quite similar to the MSF process in terms of flash evaporation concept. In the MED process the feed seawater will flow through a number of evaporators in a series called effect. Then, the vapor from one series will subsequently use to evaporate the next series. MED uses the principle of evaporation and condensation at a various ambient pressure for every effect as shown in Figure 2.12. The membrane desalination process is a very popular and common method used for desalination because of the freshwater production. This is because the freshwater produced has high quality and economical viable due to low specific energy consumption.

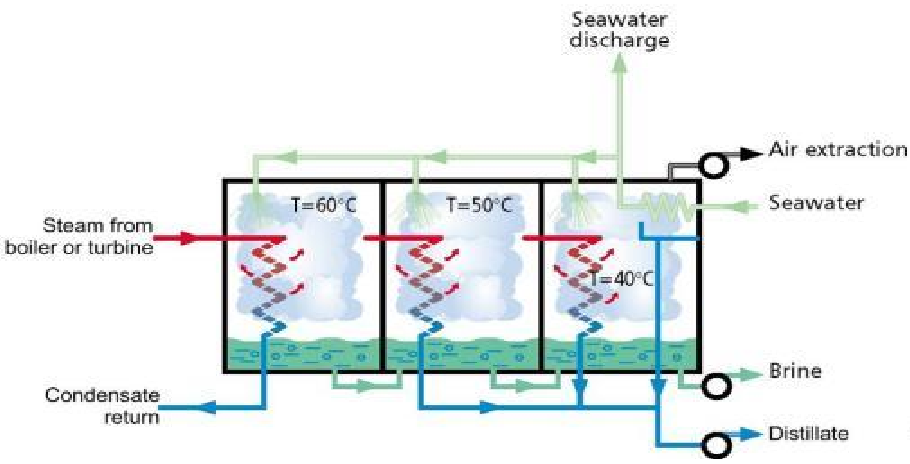

Figure 2.12 MED process (Palenzuela et al., 2014)

Reverse Osmosis (RO) and electrodialysis (ED) are desalination process which uses a membrane. The RO process involves high pressure to force freshwater to permeate through a semi-permeable membrane and leaving waste brine with high salinity behind. The feed seawater will pass the pre-treatment processed before passed the membrane to remove the unwanted particles that will plug the membrane. For the ED process, it needs electrical energy that caused salt ion electrically charged to move through the selective ion exchange membrane that leaving behind the low salinity of water production. The differences between this processes is that the RO process drive high force while the ED process uses electrical energy to operate. Both processes will leave the high concentration of brine to the other side. The schematic of RO process and ED process are shown as in Figure 2.13 and Figure 2.14 respectively.

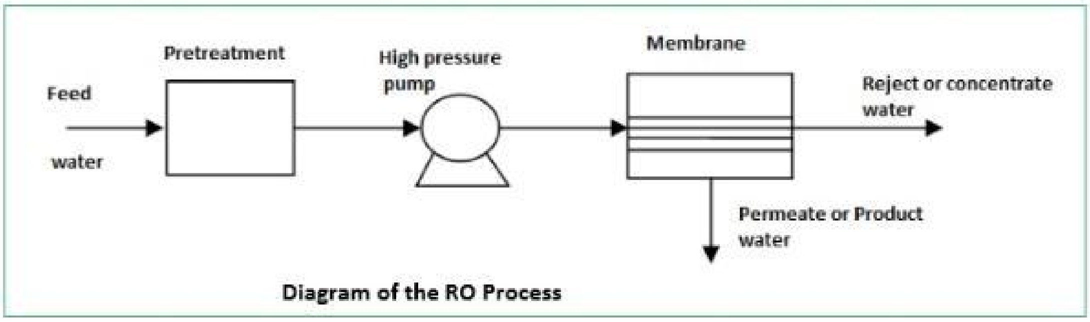

Figure 2.13 Schematic of Reverse Osmosis Process (Altaee et al., 2014)

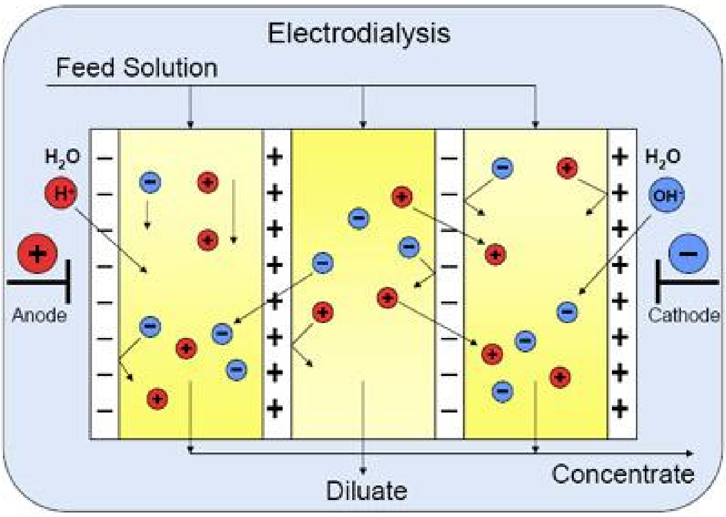

Figure 2.14 Schematic of ED process (Charcosset, 2009)

2.7 Desalination for Water Supply and Sustainability

As of 2013, the total number of desalination plants in the world is more than 17000 plants. Their global capacity is more than 80 million cubic meters per day coming from 150 different countries around the world and more than 300 million of people rely on desalinated water for their daily needs. The current production of freshwater nowadays has recorded an increase of twice compared to a decade ago. From Figure 2.15, RO process has takes the majority of the global installed capacity while the MSF and MED process are on the second and third place respectively. The projection of total capacity is increased up to 98 M m^3/d in 2015 when the case study conducted on 2013. The capacity of freshwater keeps increases is not only because of freshwater demand but also due to the significant advancement and cost reduction in producing freshwater. By mean, the current and future desalination method with technology advancement can support the water demand to meet the future needs.

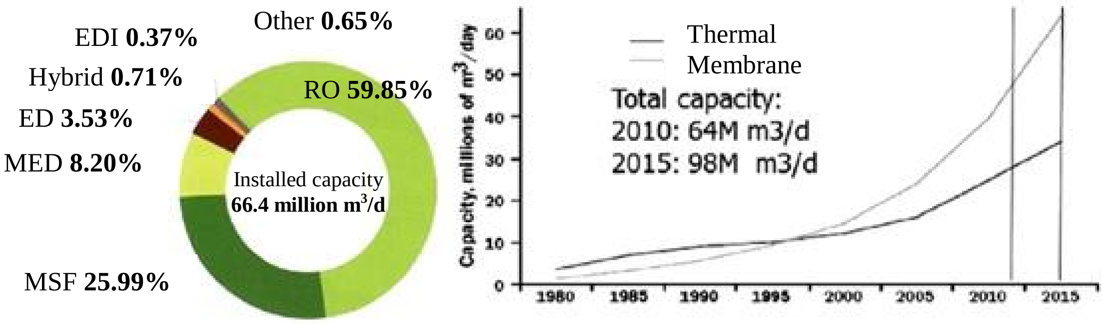

Figure 2.15 Installed (left) and forecast (right) desalination capacities by technology (as of first quarter of 2012) (Ghaffour et al., 2013)

2.8 Energy Consumption for Desalination

In desalination process, the heat whether from the boiler, waste heat, steam turbine heat or from the electricity is used as energy. Energy consumption of the desalination plant depends completely on the technique used to convert the saline water. The other main factor influenced the energy required for freshwater production are the plant capacity, the feed water treatment, salinity, temperature and the quality of the water. Figure 2.16 shows the comparison of the characteristics of the main desalination technologies.

	MSF	MED-TVC	MED	MVC	RO
Typical unit size m³ d⁻¹	50,000 - 70,000	10,000 - 35,000	5,000 - 15,000	100 - 2500	24,000
Electrical Energy Consumption kWh m⁻³	4 – 6	1.5 – 2.5	1.5 – 2.5	7 - 12	3 – 5.5
Thermal Energy Consumption kJ kg⁻¹	190 (GOR =12.2) – 390 (GOR =6)	145 (GOR =16) – 390 (GOR =6) #¹	230 (GOR =10) – 390 (GOR =6)	None	None
Electrical Equivalent #² for Thermal Energy kWh m⁻³	#³ 9.5 – 19.5	#⁴ 9.5 – 25.5	#⁵ 5 – 8.5	None	None
Total Equivalent Energy Consumption kWh m⁻³	13.5 - 25.5	11 - 28	6.5 - 11	7 - 12	3 - 3.5 (Up to 7 with Boron treatment)

Figure 2.16 Energy consumption for desalination (Dessne et al., 2015)

Figure 2.17 shows the parameters in MSF, MED and SWRO desalination process. This result has been presented by Sami Mutair (2013) during OTEC Africa Conference. For MED and MSF, the unavoidable disadvantage is the larger specific energy consumption required to heat the feed water. Alternatively, an integrated plant that makes use the energy extracted from the turbine will be an advantage in term of energy consumption. That is the reason why the RO process is more economical than another process. Besides, thermal plant integrated with the power generation plant is one of the solutions to overcome the high energy and power consumption needed for the desalination plant.

Main Technical Parameters	MED	MSF	SWRO
Raw water pre-treatment	Low requirement	Low requirement	Very high
Operating temperature (°C)	<70	<120	Ambient
Raw water utilization efficiency	15–40%	12–25%	35–40%
Product quality in TDS (mg/L)	5–10	5–10	300–500
Main energy source	Vapor, electricity	Vapor, electricity	Electricity

Figure 2.17 Comparison Parameters of Desalination. (Ghaffour et al., 2013)

2.9 LTTD Plant

The working principles of LTTD plant have been discussed in Section 2.2. In LTTD cycle the seawater need not be heated until it achieves the saturation temperature like in the conventional thermal desalination process. It applies the concept of flash boiling by lowering the pressure at the evaporator flash chamber and condenser. This process is cost effective rather than preheating the seawater. India has come out with the first floating 1 million liter per day (MLD) of LTTD plant as shown in Figure 2.18 (Kathiroli et al., 2008). Previously, NIOT has successfully commissioned a 0.1 MLD plant at Kavaratti Island in Lakshadweep, which has been operating since May 2005.

Figure 2.18 The First Floating LTTD Plant by NIOT, India.

2.10 OTEC Plant

There are several types of the OTEC cycle namely, an open cycle, close cycle and hybrid cycle. Figure 2.19 shows the location of completed, in development, planned and proposed OTEC projects around the world. During the 70's and 80's countries like the United States, Japan, and several other countries began experimenting with OTEC systems in an effort to bring this technology into reality. It has been established that Malaysia has the capacity to generate power from OTEC with the heat stored in the deep waters (over 700 meters in depth), covering a total area of 131,120 square kilometers, off the states of Sabah and Sarawak.

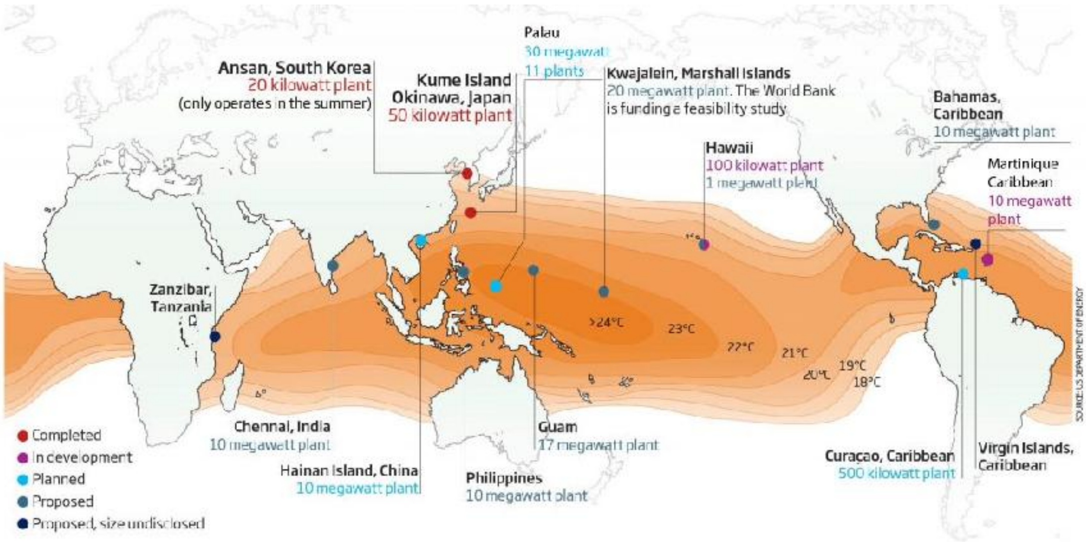

Figure 2.19 Completed, in development, planned and proposed OTEC plant around the world (Bkleute, 2016)

2.11 Integration Cycle of OTEC

The common working principle of OTEC is close-cycle (Organic Rankine Cycle) and its advantages are that it is more compact than an open-cycle system and can be intended to deliver the same amount of power. The closed-cycle can likewise be designed by utilizing effectively existing turbo machinery and heat exchanger design. However, the main technical limitation in OTEC cycle is a low thermodynamic efficiency, which lies between 3-5 % due to the small temperature difference between hot surface water and cold deep sea water. There are many researches that have been conducted in order to increase the efficiency of the OTEC cycle. Some of the researchers have made a modification towards a Closed Cycle OTEC to increase the efficiency. They have come out with the different cycle, which known as Uehara Cycle (Uehara et al., 1999) and Kalina Cycle (Sun et al., 2014).

2.12 Heat Exchanger

The heat exchanger is the main device used for the OTEC and desalination systems. The heat exchanger is targeted to the efficient transfer of heat from the hot fluid flow to the cold fluid flow. There are also special cases of heat exchanger like condenser and evaporator or boiler when the fluid flow changes from vapor to liquid and when the fluid change from liquid to vapor respectively. The heat exchanger is one of the major cost that covers about 25 – 50 percent of the plant cost (Uehara et al., 1988, Ikegami, 1990). As such, it will be one of the objective functions for the optimal design consideration. The value of the overall heat transfer coefficient will vary depending on the designer or constructor that is based on the acceptable designated value. The larger thermal conductance of the heat exchanger will give in advantage in terms of better surface heat transfer area. Currently, there are several types of heat exchanger used commercially. The shell and tube heat exchanger and plate heat exchanger are the basic types of heat exchanger design although many other design configurations have been developed. Classification of the heat exchanger can also be determined according to the type of fluids used, according to phase changes and according to the flow direction of the fluid. Figure 2.20 shows the types of the heat exchanger and the basic design of heat exchanger are presented below.

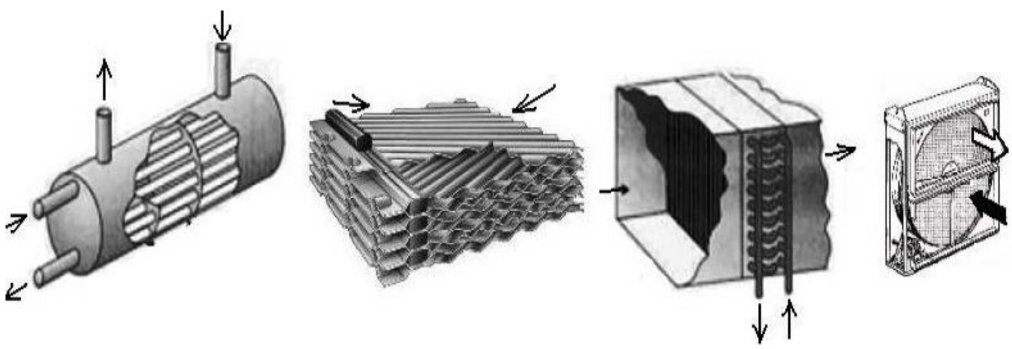

Figure 2.20 Types of heat exchanges: a) shell-and-tube b) plates c) open-flow d) rotating-wheel (Hesselgreaves et al., 2016)

2.12.1 Shell and Tube Heat Exchanger (STHE)

The STHE is the most common type of heat exchanger used in heavy industries as steam condenser, boilers and residential hot-water and heating systems. The principle working is that one of the flows goes along a bunch of the tubes and the other flows come within the outer shell. The configuration of the flows within the outer shell can be in cross flow or parallel to the tubes. Figure 2.21 shows the design configuration for the STHE. The baffle in STHE is used to support tube bundles and direct the flows to the fluids.

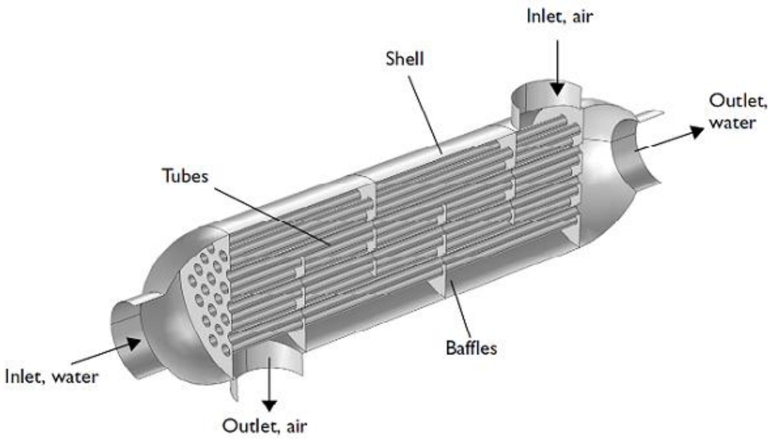

Figure 2.21 Shell and tube heat exchanger design

The Table 2.1 below shows the advantages and disadvantages of Shell and tube heat exchanger.

Table 2.1: Advantages and disadvantages of shell tube heat exchanger (Kakac et al., 2012)

Advantages	Disadvantages
• Can handle heavy duty and high temperature and pressures • Easy control and operate-able • Less expensive as compared to Plate type coolers • Can be used in systems with higher operating temperatures and pressures • Pressure drop across a tube cooler is less • Tube leaks are easily located and plugged since pressure test is comparatively easy • Tubular coolers in the refrigeration system can act as a receiver also. • Using sacrificial anodes protects the whole cooling system against corrosion • Tube coolers may be preferred for lubricating oil cooling because of the pressure differential	• Required large space • More Maintenance cost • Heat transfer efficiency is less compared to plate type cooler • Cleaning and maintenance are difficult since a tube cooler requires enough clearance at one end to remove the tube nest • The capacity of tube cooler cannot be increased. • Requires more space in comparison to plate coolers

2.12.2 Plate Heat Exchanger (PHE)

A plate heat exchanger is a compact heat exchanger where thin corrugated plates are stacked in contact with each other's. The two flow fluids are made to flow separately along the adjacent channel of the plates. Plate's assembly is shown in the Figure 2.22. PHE have a large conductance coefficient as for liquid-to-liquid use and ideally suitable for low viscosity fluids. The number of plates can be adjusted and configured depending on the need of the heat transfer amount by the process.

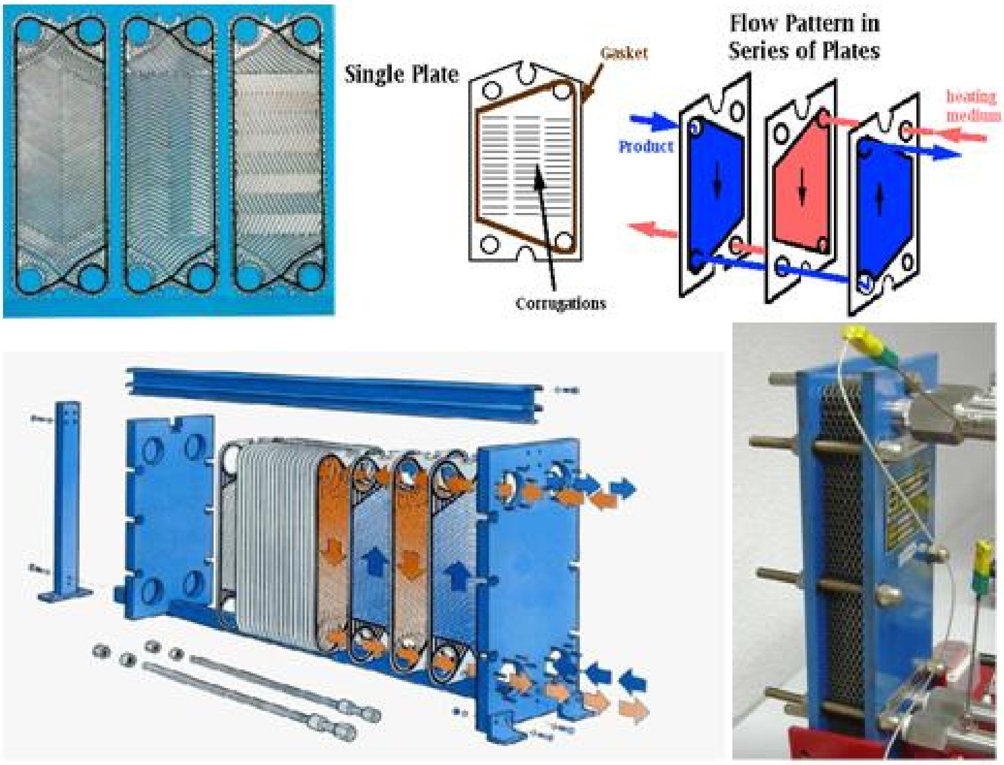

Figure 2.22 Plate heat exchanger (single plates, exploded assembly, assembled)

The advantages and disadvantages of the PHE are shown in Table 2.2.

Table 2.2: Advantages and disadvantages of PHE (Kakac et al., 2012)

Advantages	Disadvantages
• Negligible heat loss • Overall weight of set is less • Fits in less space • Less maintenance cost and overall heat transfer coefficient is more • Easy installation • Simple and Compact in size • Heat transfer efficiency is more • Can be easily cleaned • No extra space is required for dismantling • Capacity can be increased by introducing plates in pairs • Leaking plates can be removed in pairs, if necessary without replacement • Maintenance is simple • Turbulent flow helps to reduce deposits which would interfere with heat transfer	• Not compatible for higher temperature and pressure say above 200°C and 20 bars. • Initial cost is high since Titanium plates are expensive • Finding leakage is difficult since pressure test is not as easy as tube coolers • Bonding material between plates limits operating temperature of the cooler • Pressure drop caused by plate cooler is higher than tube cooler • Careful dismantling and assembling to be done • Joints may be deteriorated according to the operating conditions • Since Titanium is a noble metal, other parts of the cooling system are susceptible to corrosion

2.12.3 Heat Exchanger Selection

The heat exchanger used to transfer energy to one and another. In order to achieve optimum process operations, the proper type of heat exchanger needs to be selected based on some criteria’s and considerations. To make a better selection, the better to know how they operate and criteria of the different heat exchanger type.

Table 2.3 shows the details of the criteria of selection, types of the heat exchanger and cost.

Table 2.3: Heat exchanger criteria selection

Selection criteria	**Types of Heat exchanger**	**Cost criteria**
• Application • Operating pressures & temperatures • Fouling characteristics of the fluids • Available utilities Temperature driving force • Plot plan & layout constraints • Accessibility for cleaning and maintenance • Considerations for future expansions • Mechanical consideration	• Shell & tube heat exchangers 1) Baffle types -Segmental baffles -Double segmental baffles -No-tube-in-window baffles -Rod baffles -EM baffles -Helical baffles 2) Tube Enhancements -Twisted tubes -Low finned tubes -Tubes inserts • Compact type heat exchangers 1)Plate & frame heat exchangers (gasketed, semi-welded, welded) 2) Spiral 3)Blazed plate & frame 4) Plate-fin heat exchanger	• Purchase cost • Installation cost • Operating cost (pumping, fan) • Maintenance cost

2.13 Previous Research

The temperature difference between hot surface seawater and cold deep seawater even in the tropical area is only 26 - 30 °C. Although OTEC requires abundant of seawater flow rates, the best thermodynamic efficiency achieved lies in the range of 3-5% (Aydin et al., 2014). The net power efficiency can be defined as the net power divided by generated power. In a typical OTEC plant, the net power efficiency is between 50 - 80% of the system. Many considerable research efforts have been made to improve the performance of the OTEC system. Since the 80's, considerable research efforts have been made in two directions to improve the performance of the OTEC system (Yeh et al., 2005) . Thermodynamics optimization based on the process is one of the ways to get the optimum power generation. Besides, the specific power consumption of the systems also needs to be optimized. The net power output optimizations have been the main interests in research conducted to find the maximum power output of the OTEC system theoretically and practically. There are many input parameters that can be optimized to achieve the maximum output. The main parameters are the warm seawater and cold seawater temperature and the feed flow rate of seawater which influenced the performance of the OTEC system. Other than that, the pipe diameter, pipe length, pumping power, thermal conductance of heat exchanger, and working fluids can be optimized in order to figure out the maximum output of an OTEC system (Dincer et al., 2014). A study conducted by Yeh et.al (2005) found that the maximum output of an OTEC power plant with the effects of temperature and flow rate of cold seawater. The study considered the variable parameters based on a specific condition in Taiwan as the pipe length and diameter, seawater depth and flow rate. The optimization based on fixed pipe diameter and flow velocities condition. The results show that maximum power output can be achieved with larger pipe diameter for fixed inlet and outlet seawater temperature (Yeh et al., 2005). Sun, Ikegami et.al (2012) have conducted a research of 'Optimization design and exergy analysis of organic Rankine cycle in OTEC' and coming out with derivation and optimization of performance and exergy efficiency of (ORC) in OTEC system. The paper shows the optimization design with theoretically approached to find the maximum net power output of work turbine

A lot of researches have been done based on flash evaporation under vacuum process to figure out the performance and effectiveness by doing the simulation and pilot studies. Some studies on low-pressure evaporation have been developed by many researchers, such as Kumar et al. (2007) who conducted a pilot study and designed a desalination system utilizing ocean thermal gradient and system performance. The study was evaluated by varying the temperature in condenser and evaporator and pressure in the vacuum chamber. J. H. Tay et al. (1996) has investigated vacuum desalination application by using the waste heat from a steam turbine, received from the superheated vapor heater. The results showed that the desalination ratio of freshwater production is increased. As for Zhijiang and Wang (2015) modeling and an experiment on Ocean Thermal Energy for Desalination (OTED) were done. They have modeled the integrated device for evaporation and condensation using a Siphon process principle in order to get more freshwater with less energy consumption. From the results of the study, they found that the temperature difference has affected the yield production. Muthunayagam et al. (2005) have conducted both theoretical and experimental studies with through their flash evaporation model at the temperature between 26 ^{o}C to 32 ^{o}C. The results revealed, the height change in vaporizer does not give much influence the yield production. A simulation study also was carried out by Kudish et al. (2003) and the results obtained was validated with the experimental results. The result showed that a solar desalination system from their prototype is capable of producing 11 $kgm^{-2}d^{-1}$ of freshwater on a sunny day. Experimental study on spray flash desalination was demonstrated by Ikegami et al. (2006) by investigating the direction of injection and the result showed the spray flash desalination more efficient with using an upward jet method. A simulation model for the spray flash desalination system was studied by Satoru Goto et al. (2008) by using energy conservation and mass conservation law. The results obtained are compared with experimental study results. The constant condition and the properties of the fluid in this study were derived by PROPATH. In order to solve the energy and environmental problem for power generation and freshwater production, Nakamura et al. (2009) has developed a simulation model of integrated OTEC and construct a desalination plant. The salinity level also influenced the production of freshwater generated and quality of the freshwater from LTTD plant (Balaji et al., 2016). To propose the power generation and desalination system, previous research and study are highly recommended in order to achieve the proposed system performance and intended results. All the data and results from the previous research can be used as a reference and guideline to construct the future OTEC-LTTD plant.

2.14 Conclusion

The methods of generating electricity by using renewable energy have been discussed in this chapter. There are many researchers have been conducted and available plant that have been operated in order to use clean energy so as to protect our mother nature. This is essential as the current electricity generation is highly dependent on fuels, natural gas and coal which create a negative impact to the environment. Ocean is one of the sources used to extract the energy that contains in it to produce electricity. Several methods of generating electricity using the ocean as a medium are the wave, tidal and thermal energy as have discussed before. Thermal energy as OTEC is a clean and stable energy as the source of seawater is relatively abundant rather than other ocean energy method. The other input is the temperature gradient that can be extracted through the depth of the ocean. Many case studies have been conducted in order to improve the OTEC efficiency, performance and system design towards commercialization. The main input parameters are the temperature and seawater flow rate that give a huge impact of performance to the OTEC system. This interest to conduct the study is based on simulation of the input parameters to generate 1 MW of OTEC system. Beside electricity generation, OTEC also have by product such as freshwater and hydrogen which can be extracted from the OTEC plant. In order to produce freshwater, the desalination plant consume high electricity as have been discussed in Section 2.8. Furthermore, the other desalination system as MSF, MED, SEE-VC and RO have some disadvantages in terms of requirement of the plant to start operating as heating the seawater to the required temperature for MSF and MED and pre-treatment process for the RO plant. LTTD seems to be the effective technology needed to produce freshwater by creating vacuum condition to the system plant. It is also beneficial as well rather than the others concept. Thus, for this study, the simulation have been conducted to generate electricity and freshwater production by integrate the OTEC and LTTD plant. The freshwater produced can boost the OTEC plant rather than by drawing the seawater intake from surface and cold deep seawater from the OTEC system. The model of calculation and optimization is also presented in the methodology section.

CHAPTER 3

METHODOLOGY OF PRESENT STUDY

This chapter will cover on the flow and design parameters for the integrated OTEC-LTTD plant by conducting a simulation for this study. Numerous research studies have been done on the flash desalination process. In order to get the optimization of input parameters, it is essential to improve the component design in OTEC-LTTD plant so that it is able to generate freshwater production with less energy consumption. This chapter will discuss more on the problem-based design and mathematical modeling under specific parameters in order to achieve 1 MW turbine and produce more than 1000 t/d by using temperature of cold seawater at depth of 1000 m. The process flowchart is shown as in Appendix H.

3.1 Seawater Thermophysical Properties

The salinity in this study is assumed to be 35 g/kg same as in case study conducted at Sabah (Arsad and Akhir, 2013). The mathematical equations of seawater thermo physical properties are referred to Mostafa H.Sharqawy et al. (2010). All the properties of seawater results are presented in terms of regression equation as the functions of temperature and salinity.

3.2 Integrated OTEC Design (OTEC-LTTD)

The model design for OTEC system followed Sami Mutair Study (2013) and LTTD design is different with a Sami Mutair study which consist simple configuration of basic principles of LTTD model. The Sami Mutair design as shown in Figure 3.1 which consists of DCC, plate heat exchanger and cooling water pump.

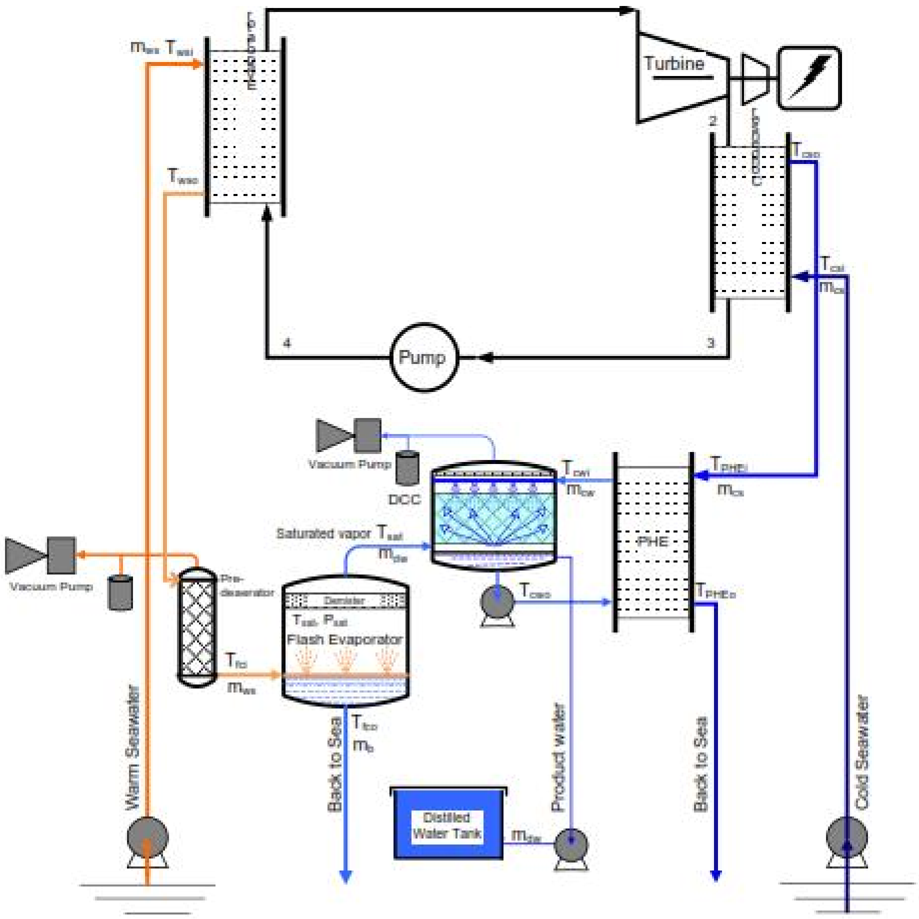

Figure 3.1 OTEC-LTTD plant simulation by Mutair

For the integrated OTEC desalination plant, the proposed system consists of the OTEC plant part and the desalination plant part as shown in Figure 3.2. The desalination plant receives the surface warm seawater from the outlet of the OTEC evaporator, and then it flows into the flash chamber. Otherwise, the outlet of the cold seawater from the OTEC condenser will flow into the condenser in the desalination plant. The vacuum pump 1 at pre-deaerator is used to evacuate half of the unwanted gases before entering the flash chamber. Vacuum pump 2 will create a vacuum condition by lowering the pressure in the flash evaporator and the desalination condenser then release the other unwanted gases contained in the system. The vapor from the flash chamber will flow to the desalination condenser by different pressure condition. It will condense through the desalination condenser when coming into contact with cold seawater drawn in OTEC condenser, thus the freshwater is generated.

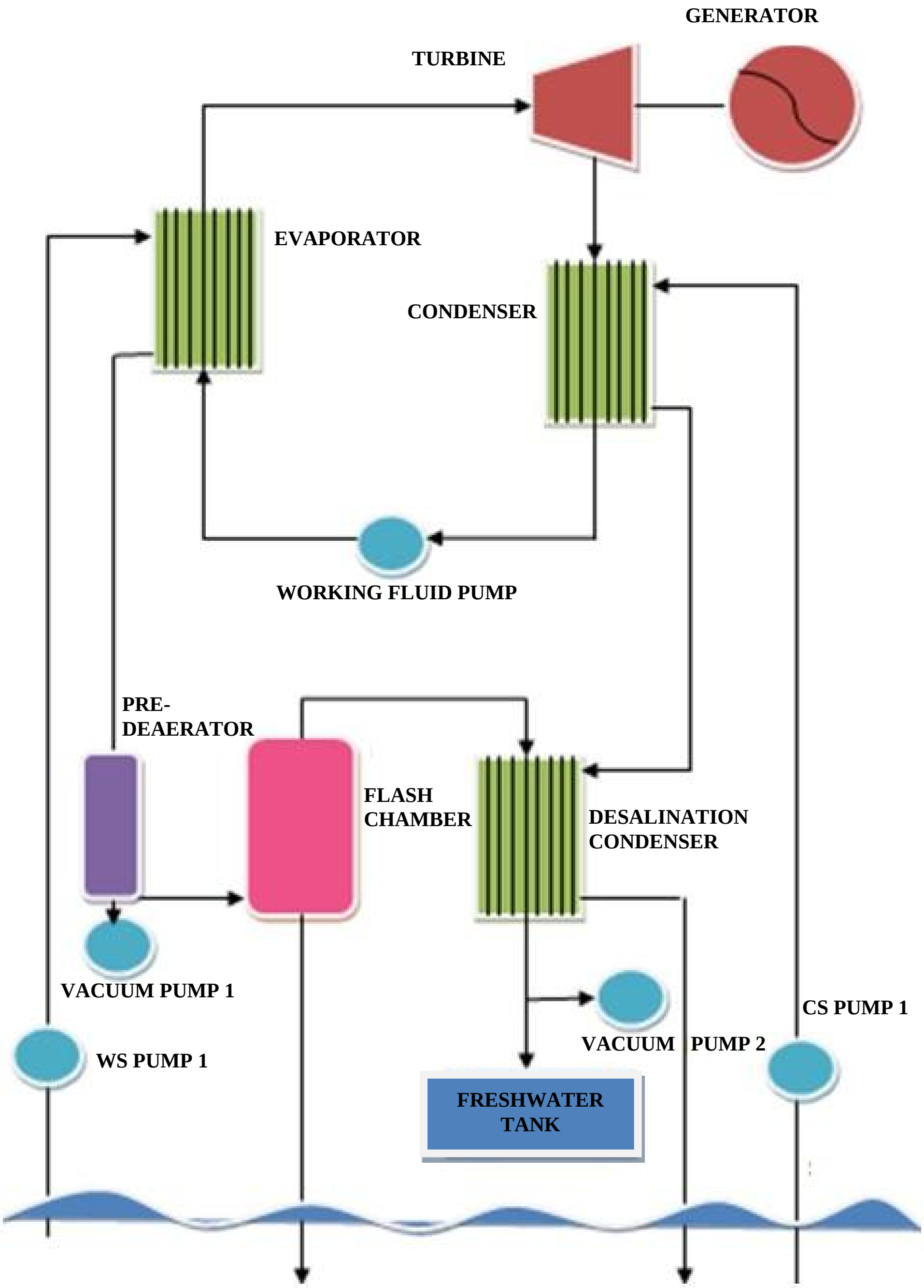

Figure 3.2 Schematic of OTEC-LTTD plant (This study)

3.3 Calculation Methods (Optimization Technique) by Simulation

The present study aims to optimize the performance of an existing flash desalination and integrated OTEC desalination system. The simulation input is shown in Table 3.1 where the thermal conductance value is found to be the optimum value to generate 1 MLD of freshwater for standalone LTTD plant. The cold seawater temperature taken is based on the lowest temperature taken for OTEC-LTTD plant in this study so to generate 1 MLD OTEC-LTTD plant at 30 ^oC of warm seawater temperature intake. Table 3.2 shows the thermal conductance of 11.0 MW/^oC to be the optimum value to achieve 1 MW turbine power. Based on fixed thermal conductance of all heat exchanger, the mass flow rate of warm and cold seawater intake varies from 26 ^oC to 30 ^oC with fixed cold seawater temperature at 4 ^oC. The design is made to achieve freshwater production of more than 1 MLD with 24 MWh/d electricity generations. The different depth of cold seawater intake also is taken into consideration to compare the net power output of the system. The highest cold seawater temperature is taken at 6 ^oC in order to maintain the temperature difference of 20 ^oC from the lowest temperature of warm seawater at 26 ^oC.

Table 3.1: Parameters for 1 MLD LTTD

Parameters	**Value**
Mass seawater flow rate, m_{ws}=m_{cs}	663 kg/s
Thermal conductance of heat exchanger	2.67 MW/ ^oC (OPT)
Inlet warm temperature	26 ^oC
Inlet cold seawater Temperature	4 ^oC
Depth of intake cold seawater	1000 m

The simulation of 1 MLD or the stand-alone desalination plant is to show the significance of input parameters of LTTD plant. The main input parameters are warm and cold seawater temperature and flow rate. These need to be configured in order to integrate with OTEC plant.

Table 3.2: Parameters for 1 MW OTEC-LTTD

Parameters	**Value**
Mass seawater flow rate, m_{ws}=m_{cs}	1796.8 kg/s – 1198.0 kg/s
Thermal conductance of all heat exchanger	11.0 MW/ ^{o}C (OPT)
Inlet warm temperature	26 ^{o}C-30 ^{o}C (Tropics data Temperature)
Inlet cold seawater Temperature	4 ^{o}C-6 ^{o}C
Diameter of pipe	1.2 m
Depth of intake cold seawater	760 m-1000 m (Idris; et al., 2014)

The integration of OTEC model follows the construction model of desalination plant (Goto et al., 2011) and integrated OTEC design (Nakamura et al., 2009). The initial condition applied in this study is shown in Table 3.3. Its design is based on 4 ^{o}C cold seawater temperature at 1000 m depth. The warm seawater temperature of 26 ^{o}C was taken as the lowest temperature intake for the tropics temperature condition. Based on this temperature intake, the value of required warm seawater and cold seawater intake, optimal thermal conductance of all heat exchanger, and mass flow rate of working fluid were selected in order to achieve 1000 kW turbine power. Based on the required mass flow rate of warm and cold seawater to achieve 1000 kW turbine, the optimal value of pipe diameter was selected based on the minimum losses where contribute to the higher net power output. Table 3.4 shows the average warm seawater temperature over the years data recorded in Kudat (Kryuchin, 2017), Sabah that will be taken into the simulation to generate data based throughout the year.

For OTEC-LTTD plant, the simulation of OTEC plant model flow chart is shown as in Appendix I. The input operating data is set as in Table 3.3. The system will guess the T_{cso} based on using iterative methods. With guessing the T_{cso} , the system will calculate the Q_E , Q_C, T_C and T_E of the system. Then, the Thermodynamics properties of the working fluids can be determined by using Propath which integrated with the Fortran simulation. The heat balance of the system is determined based on error 0.001. For the simulation, the flow rate of the working fluid is variable in order to achieve the maximum turbine power output. After getting the maximum power turbine output, the freshwater production is calculated based on equation in Section 3.6. The system performance is determined by produced the maximum power output based on proposed plant configuration.

Table 3.3: Initial condition of simulation

Parameters	**Value**
Turbine generator power, W_T Turbine efficiency, η_T Generator efficiency, η_G	1000 kW 0.90 0.95
Warm seawater intake pipe Cold seawater intake pipe	20 m 1000 m
Diameter of seawater pipe	1.2 m (OPT)
Warm seawater temperature	26 ^oC
Cold seawater temperature	4 ^oC
All pump efficiency, η_p	0.85
Plate heat exchanger length	2 m

Table 3.4: Warm seawater temperature data at Kudat, Sabah

Month	**Temperature (^{o}C)**
1	27.6
2	27.3
2	27.6
4	28.6
5	29.5
6	29.9
7	29.8
8	29.3
9	29.1
10	29.3
11	29.4
12	28.9

3.4 OTEC Cycle Equation

In the evaporator, the working fluid is vaporized in the evaporator by receiving heat from the warm seawater. The energy balance equation at each side of the evaporator can be written as Equation 3.1.

$$Q_E = m_{ws}Cp_{ws}(T_{wsi} - T_{so}) = m_{wf}(h_1 - h_4) \tag{3.1}$$

The seawater is assumed as an ideal incompressible fluid. The enthalpy and entropy of the working fluid, which is the function of pressure and vapor quality, were determined from PROPATH. Overall heat transfer coefficient and effective surface area of the evaporator correlates with the heat addition rate is shown in the following Equation 3.2.

$$Q_E = U_E A_E \Delta T_{lmE} \tag{3.2}$$

where ΔT_{lmE} is the Logarithmic Mean Temperature Difference across the evaporator, and the effective thermal conductance $U_E A_E$ can be approximated as in Equation 3.3.

$$\frac{1}{U_E A_E} = \frac{1}{h_W\ A_E} + \frac{1}{h_W\ A_E} \tag{3.3}$$

Basically the energy balance equation for the condenser is same like evaporator and written as in Equation 3.4.

$$Q_C = m_{cs}\, Cp_{cs}\, (T_{cso} - T_{csi}) = m_{wf}\, (h_2 - h_3) \tag{3.4}$$

The heat transfer area of the condenser can be defined as in Equation 3.5.

$$Q_C = U_C\, A_C\, \Delta T_{lmc} \tag{3.5}$$

Where the effective thermal conductance, $U_C A_C$ can be approximate as in Equation 3.6.

$$\frac{1}{U_C A_C} = \frac{1}{h_W\ A_C} + \frac{1}{h_W\ A_C} \tag{3.6}$$

The Logarithmic Mean Temperature Difference across the evaporator and condenser is correlated as below.

For condenser, it can be calculated as in Equation 3.7.

$$\Delta T_{lmC} = T_{C} - T_{C} \; / \ln \frac{T_{C} - T_{C}}{T_{C} - T_{C}} \tag{3.7}$$

For evaporator, it can be calculated as in Equation 3.8.

$$\Delta T_{lmE} = T_{W} - T_{W} \; / \ln \frac{T_{W} - T_{E}}{T_{W} - T_{E}} \tag{3.8}$$

3.5 Turbine Generator Power

The turbine generator power can be calculated from the product of mass working fluid flow rate, m_{wf} and the adiabatic heat loss across the turbine. The equation can be defined as in Equation 3.9.

$$W_{T\text{-}G} = m_{wf} \eta_T \eta_G (h_2 - h_1) \tag{3.9}$$

where, η_T and η_G are the turbine isentropic efficiency and generator mechanical efficiency which assume as 0.9 and 0.95 respectively (Nihous and Vega, 1993). By considering turbine power and pump powers, the obtained net power allows for the calculation of the net thermal efficiency as in Equation 3.10.

$$\eta_{th} = W_T / Q_E \tag{3.10}$$

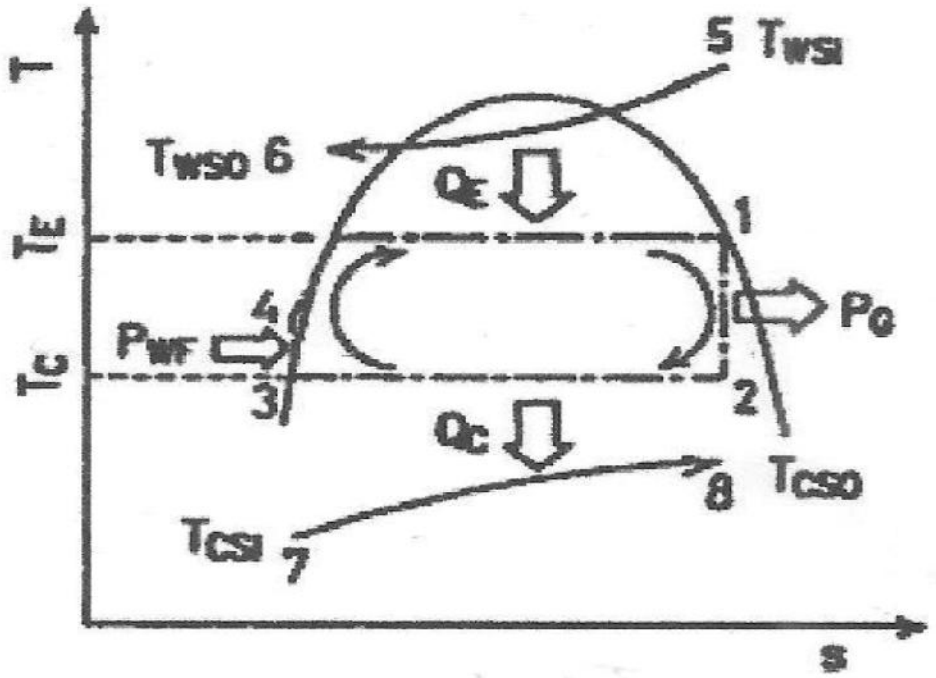

Figure 3.3 *T-s* diagram of the Closed Rankine cycle.

The calculation of the quantity states at each point (1-4) will be calculated by applying an iterative method with initial assumptions of the outlet of warm seawater and cold seawater temperature. The values of Q_E and Qc for seawater side were calculated by using Equation 3.1 and Equation 3.4 respectively. The evaporation and condensation temperature ($T_E;T_C$) were identified by Equation 3.6 and 3.7. Both their values will be used to find the quantity states at each point by linking to PROPATH to get the value of each state based on Organic Rankine Cycle. For the heat and mass balance of the system at the evaporator and condenser side, the Q_E for the working fluid side was determine for both of heat exchanger. Both of each side of evaporator and condenser for seawater and working fluid side heat balance was determine by using iterative method by applying absolute error of 0.001. After specifying the flow rate of warm and cold seawater, the pumping power of cold seawater and warm seawater will be determined by applying equation as discussed in pumping power section. The turbine power and net power generation was calculated by using Equation 3.8.

3.6 Optimization of LTTD Plant

For the standalone plant, the intake of warm seawater inlet temperature at flash chamber and cold seawater inlet temperature at desalination condenser is based on temperature data at surface warm seawater and deep cold seawater respectively. But, for the integrated OTEC-LTTD plant, the flash chamber inlet temperature and desalination condenser inlet temperature are dependent on the OTEC outlet temperature of evaporator and condenser respectively. For complete flash evaporation process, the flash chamber temperature exit, T_{fco} is greater than the generated steam condensation temperature, T_{sat} by the amount of boiling point rise, '*BPR*' associated to the salinity of the seawater, obtained from Mostafa H.Sharqawy et al.(2010). The flash chamber exit temperature, T_{fco} is evaluated as Equation 3.11.

$$T_{fco} = T_{sat} + BPR \tag{3.11}$$

The heat flow in the flash chamber Q_{fc} is calculated as Equation 3.12.

$$Q_{fc} = M_{ws} C_{pws} (T_{fci} - T_{fco}) \tag{3.12}$$

For equilibrium, the amount of heat released by the flash evaporation of warm seawater at the evaporator must be balanced with the amount of heat added to the desalination condenser, Q_{dc} defined as Equation 3.13.

$$Q_{dc} = M_{cs} C_{pcs} (T_{dco} - T_{dci}) \tag{3.13}$$

And the Logarithmic Mean Temperature Difference of PHE of desalination condenser, ΔT_{lmdc} is calculated as Equation 3.14

$$\Delta T_{lmdc} = Qdc/UA_{dc} \tag{3.14}$$

where the UA_{DC} is the thermal conductance of the desalination condenser. Once the thermal equilibrium between the two streams is established, the flow rate of distilled water m_{dw} is then calculated as Equation 3.15

$$m_d = \frac{m_w \ C_p \ (T_f \ - T_f \ )}{L} \tag{3.15}$$

Where L is the latent heat of vaporization.

3.7 Pumping Power

The total pumping power, WP_{tot} exerted in the various pumping lines of the OTEC-LTTD plant is written as Equation 3.16.

$$WP_{tot=} (WP_{ws} + WP_{cs} + WP_{wf+} WP_{vp}) / \eta_p \tag{3.16}$$

Where the parameters in the nominator refer, respectively, to the pumping power of warm seawater line, cold seawater line, working fluid line and the vacuum pump power exerted for eliminating the non-condensable gases contained in the feed seawater. η_p in the denominator is the pump efficiency.

3.7.1 Warm Seawater Pumping Power

The warm seawater pumping power can be defined as Equation 3.17 below.

$$WP_w = \frac{m_w \ \Delta H_w \ g}{\eta_w} \tag{3.17}$$

Where ΔH_w is the total head difference of the warm seawater piping, m_{ws} is mass warm seawater flow rate, g is gravitational acceleration, 9.18ms^{-2} and η_{wsp} is the efficiency of the warm seawater pump. ΔH_w can be evaluated as in Equation 3.18.

$$\Delta H_{ws} = \Delta H_{ws,Den} + \Delta H_{ws,fric} + \Delta H_{ws,PHE} \tag{3.18}$$

Where $\Delta H_{ws,Den}$ is the equivalent head imposed by the difference between the density of seawater at the intake depth and the average density of the seawater column located above the intake level where evaluated as Equation 3.19.

$$\Delta H_{ws,Den} = L_{ws} - \frac{1}{\rho_W}\left(\frac{1}{2}(\rho_W + \rho_{C})L_W\right) \tag{3.19}$$

Where L_{ws} is the warm seawater pipe length, and ρ_W and ρ_C is the density of warm and cold seawater respectively. The frictional head loss , $\Delta H_{ws,fric}$ is calculated by Darcy equation as Equation 3.20.

$$\Delta H_{W,f} = \frac{f\ V_W^2\ (\frac{L_W}{D_W})}{2g\mu_W} \tag{3.20}$$

where μ_W is the viscosity of the warm seawater. f is the friction factor obtained for turbulent flow by solving Colebrook equation as Equation 3.21 below.

$$\frac{1}{\sqrt{f}} = -2l\!\!\!\quad {}_1\left(\frac{\epsilon/D_W}{3.7} + \frac{2.5}{R\ \sqrt{f}}\right) \tag{3.21}$$

where $\in$ is the surface roughness of the used pipe taken as $0.03\text{x}10^{-3}$ m. D_{ws} is the pipe diameter of warm seawater. V_{ws} is the flow velocity of warm seawater evaluated as Equation 3.22.

$$V_W = \frac{m_W}{A_W\ \rho_W} \tag{3.22}$$

Reynold number in warm seawater diameter pipe can be calculated as in Equation 3.23.

$$R_W = \frac{\rho_W\ V_W\ D_W}{\mu_W} \tag{3.23}$$

The $\Delta H_{W,P}$ is the head loss in the cold seawater-side of the PHE, calculated by Darcy equation using the head loss coefficient obtained for the used plate from Taborek (Mutair and Ikegami, 2014) as Equation 3.24.

$$\Delta H_{w\ ,P} = \frac{f_w\ V_{w\ ,P}^2\ (\frac{L_w}{D_{e\ ,w}})}{2g} \tag{3.24}$$

Where f_{ws} the friction factor obtained from Taborek 1988 for 60 degrees chevron plate (heat exchanger design handbook) as defined in Equation 3.25.

$$f_w = (4)(0.678)R_{\ w}^{-0.2} \tag{3.25}$$

The Reynold number in the plate heat exchanger at the evaporator calculated as in Equation 3.26

$$R_{\ w} = \frac{\rho_w\ V_{w\ ,P}\ \ D_{e\ ,w}}{\mu_w} \tag{3.26}$$

where,$V_{ws,PHE}$ is the velocity of warm seawater at the plate heat exchanger,$Deq_{,ws}$ is the equivalent diameter evaluated as in Equation 3.27.

$$D_{e\ ,w} = 2\sigma \tag{3.27}$$

where σ is the clearance which assumed to be 0.005. For the stand alone LTTD plant, the warm seawater pumping power is set and assumed to be the same as OTEC seawater working pump. The head loss in evaporator is assumed to be the same as the head loss in the flash chamber. For the OTEC-LTTD plant, the working pump for seawater considered at OTEC plant follows the Sami Mutair (2013) study.

3.7.2 Cold Seawater Pumping Power

For the cold seawater pumping power, the equation and a calculation made for the warm seawater pumping power to be followed by using the input parameter for the cold seawater data from Equation 3.17 to Equation 3.27.

3.7.3 Working Fluid Pumping Power

The working fluid pumping power can be evaluated as Equation 3.28.

$$WP_{wf} = m_{wf}Wp\ \eta p \tag{3.28}$$

Where the *Wp* is the specific pumping power of the working fluid calculated based on ORC of the system.

3.7.4 Vacuum Pumping Power

The total vacuum pump power, *Pvp* is calculated as the sum of the powers necessary to evacuate the non-condensable gases released in the system in two stages. In the first stage, half of these gases is released in the pre-deaeration chamber at pressure of around 17 kPa and evacuated by compression to a pressure of 30 kPa and with re-injection into the warm seawater effluent. In the second stage, the non-condensable gases are released into the flash evaporator that are drawn with the generated steam to the desalination condenser and rejected by compression to the ambient atmospheric pressure. The total vacuum pump power is expressed by the following Equation 3.29.

$$P_{vp} = P_{vp1} + P_{vp2} \tag{3.29}$$

where P_{vp1} and P_{vp2} evaluated as Equation 3.30 and Equation 3.31 respectively.

$$P_{v\ 1} = \frac{nm_w\ k_a R_a}{2(k_a - 1)} \{ (T_w\ \ + 273.15)((\frac{3}{1})^{\frac{k_a-1}{k_a}} - 1) \text{ and} \tag{3.30}$$

$$P_{v\ 2} = \frac{nm_w\ k_a R_a}{2(k_a - 1)} \{ (T_s\ \ + 273.15)((\frac{P_{at}}{P_s})^{\frac{k_a-1}{k_a}} - 1) \tag{3.31}$$

K_a is the specific heat ratio of air taken as 1.4, R_a is the standard air constant value taken as 287 j/kgK and n is the mass concentration of air in feed seawater taken as 19.36 mg/kg based on the Hawaii experiment, Vega (Mutair and Ikegami, 2014).

3.8 Optimization of required Warm Seawater and Cold Seawater Mass Flow Rate, Optimal Piping Diameter and Thermal Conductance, *UA* of the system

Inlet and outlet intake temperature of warm and cold seawater and mass flow rate of warm and cold seawater are the main input parameters affecting the OTEC-LTTD system. The temperature will affect the output of turbine generator and influence the mass seawater flow rate of warm and cold seawater intake of the system. Thus, the optimization of the system will start with the required mass flow rate of the plant in order to generate 1 MW turbine power. The range of required warm seawater needed to produce required turbine power output can be determined by using the Equation 3.32.

$$W_m = \frac{(T_w{}^{1/2} - T_c{}^{1/2})^2}{C_w{}^{-1} - C_c{}^{-1}} \tag{3.32}$$

Where C_{ws} and C_{cs} evaluated as Equation 3.33 and Equation 3.34 respectively.

$$C_{ws} = m_{ws}C_{pws} \text{ and} \tag{3.33}$$

$$C_{cs} = m_{cs}C_{pcs} \tag{3.34}$$

Cp is the specific heat capacity of seawater. The value of required warm and cold seawater mass may not be accurate due to some assumptions that have been made before proceeding to use the equation. Warm and cold seawater flow rate is set to be the same. After getting the required seawater flow rate, the iterative method is used to find the exact mass seawater flow rate required by using method as discussed in Section 3.4.

The selection of pipe diameter is one of the most important parameter in determining the friction loss in warm and cold seawater pumping power. The mass flow rate will be the constant parameter in identifying the suitable pipe diameter. The velocity inside the pipe is related with the cross sectional area. As mentioned in Equation 3.21, the cross sectional area is inversely proportional to velocity inside the pipe. For example, if the pipe diameter increases, the velocity of the fluid will be slower and the friction loss reduced due to less friction occurs in the pipe diameter. The head loss due to friction will contribute to the total head loss in both piping system and affecting the calculation of pumping power in Equation 3.34. As such, the selection of the pipe diameter is based on the lowest reading of the total pumping power and highest value of net power output.

The thermal conductance value can be determined by fixing all the input parameter as in Table 3.2 for warm seawater temperature at 26 °C and cold seawater temperature at 4 °C. In order to generate 1 MW of turbine power output, the mass flow rate of warm and cold seawater and mass flow rate of working fluid will be variable. The program for the plant is set to find the required thermal conductance that can achieved net power output not less than 80 % of the power generated by the turbine. The system need to be set with the lower thermal conductance value that can achieve the required net power output. The thermal conductance value also can be set higher and have it finite value. That’s the important to set the required thermal conductance value based on net power output to achieve. The value of heat exchanger area can be calculated by using Equation 3.6 and Equation 3.3.

3.9 Assumptions and Limitation of the Research

The research has been conducted based on prediction for an observed phenomenon. There are some assumptions and prediction made for this simulation study based on some criteria by acknowledging the theoretical design and real plant design. The assumptions made in the simulation are as follows (Nakamura et al., 2009, Goto et al., 2008, Goto et al., 2010) :

i. The cycle of the OTEC system based on ORC cycle.

ii. The main devices for the OTEC systems and desalination systems are steady-state and steady-flow devices.

iii. The potential and kinetic energy of the ORC cycle can be neglected.

iv. There is no leakage for the systems (no time delay) and no pressure drop of the systems.

v. The saturated vapor enters the turbine at the ideal quality of the vapor.

vi. Ideal phase change at the saturated state occurs in the condenser and desalination condenser.

vii. Complete flash evaporation achieved in flash chamber.

viii. The errors in heat transfer rate of the system calculated as 0.001.

3.10 Validation Technique

`The validation is based on the software's used, fluid properties and comparison study of previous studies that was conducted by Sami Mutair (2013).

3.10.1 Software

In order to conduct the study, the main software program used is Visual Fortran. This program was chosen because it is easy to maintain and writing the program on windows. It is also possible to use graphical Integrated Development Environment (IDE) to compile, run, and debug with the previous Fortran software. Besides, the program features is easy to understand and use them to produce efficient, maintainable, and portable code which can collaborate and integrated with other software. The program is already been established and the first standard has been endorsed by American Standard Association, ANSI (Meek, 1990).

3.10.2 Thermodynamic Properties of the Fluids

There are many types of working fluids that can be used for the OTEC cycle. The criterion that the working fluids must have is a low boiling point so that the working fluids can evaporate with seawater as contact fluids in the evaporator. This study will compare the selection of the best three of working fluids which are ammonia, R134 and R22 types. The results will show why is the ammonia is selected to be the best working fluid based on some specific criteria.

The thermodynamic properties of the working fluid are derived by using PROPATH, a program package for thermo physical properties of the fluid. The Version 13.1 and released in 2008 was developed and distributed by PROPATH Group. There are several types of packages for users to find the thermo physical properties of fluids as by excel program known as (E-PROPATH), single shot program by referring this subroutine in internet package and computer program package as used in this study. PROPATH is a subroutine or a function type computer programming for thermo physical properties of fluids written by Fortran77. The properties can be extracted by writing a special function as stated in the user's manual. Figure 3.4 shows the data extracted by PROPATH and from the Thermodynamics: and engineering approach book written by Cengel et.al. referring to Dixon and Hall (2013). Based on both data value, the error calculated is 0.000164 and therefore the properties derived by PROPATH are acceptable.

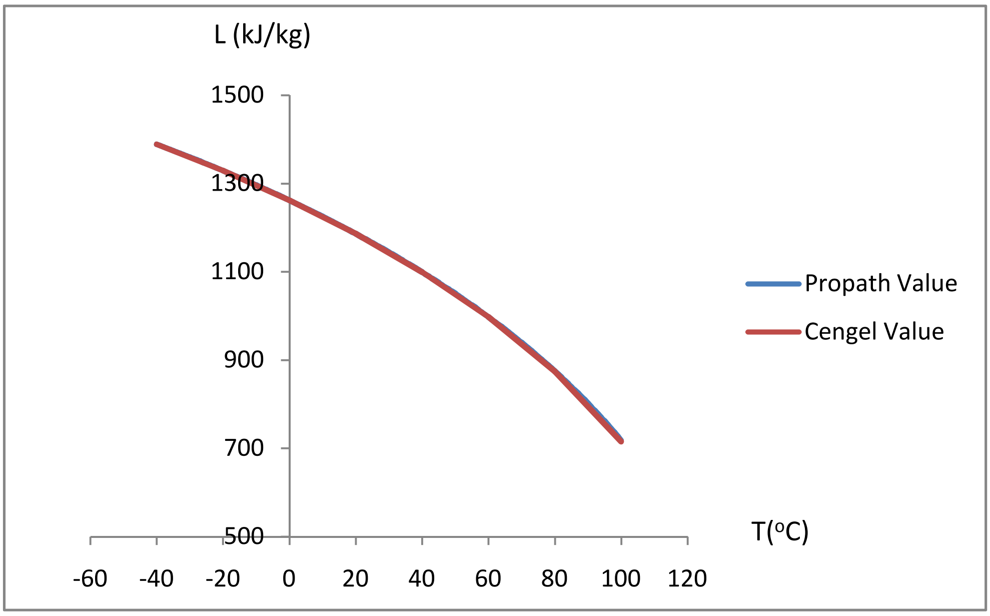

Figure 3.4 Enthalpy data obtained by PROPATH program and Thermodynamics by Cengel book (Dixon and Hall, 2013)

3.10.3 Seawater

Seawater is the main input parameter for the OTEC plant and the desalination plant and needed for designing both of the OTEC and the desalination plant. The details of the source, validity, and accuracy of each properties' function can be found in Matlab, EES, and Jacobians format which can be run on all computers that supports those software respectively (McDougall and Barker, 2011, Morgan, 2006). The full properties of seawater can be referred as Appendix A - G. In a Visual Fortran program, all the seawater function equations will be written as a subroutine of the program whereby the call function of the specific main program to call the results is based on specific temperature and salinity. Figure 3.5 shows the data generated by using a Matlab program by the GSW toolbox with a Csiro seawater library of EOS-80 that have been superseded by the GSW Oceanographic Toolbox with a salinity of 35 g/kg. The data of CSIRO refer to Mostafa H. Sharqawy (2010). A significant change is compared with past practice as GSW uses Absolute Salinity SA (mass fraction of salt in seawater) as opposed to Practical Salinity SP (which is essentially a measure of the conductivity of seawater) to describe the salt content of seawater. Ocean salinities have units of g/kg. The figure also shows the thermo physical properties of water by Roger and Mayhew, Engineering Thermodynamics book (Rogers and Mayhew, 1995). The data show the properties of seawater and water at 20 ˚C to 30 ˚C at atmospheric pressure. The data generated by this program is valid since it has been endorsed by SCOR and IAPSO. It is also parallel with Roger and Mayhew and the difference because of the different properties available of the fluids. The percentage difference of seawater and water is less than 5 %.

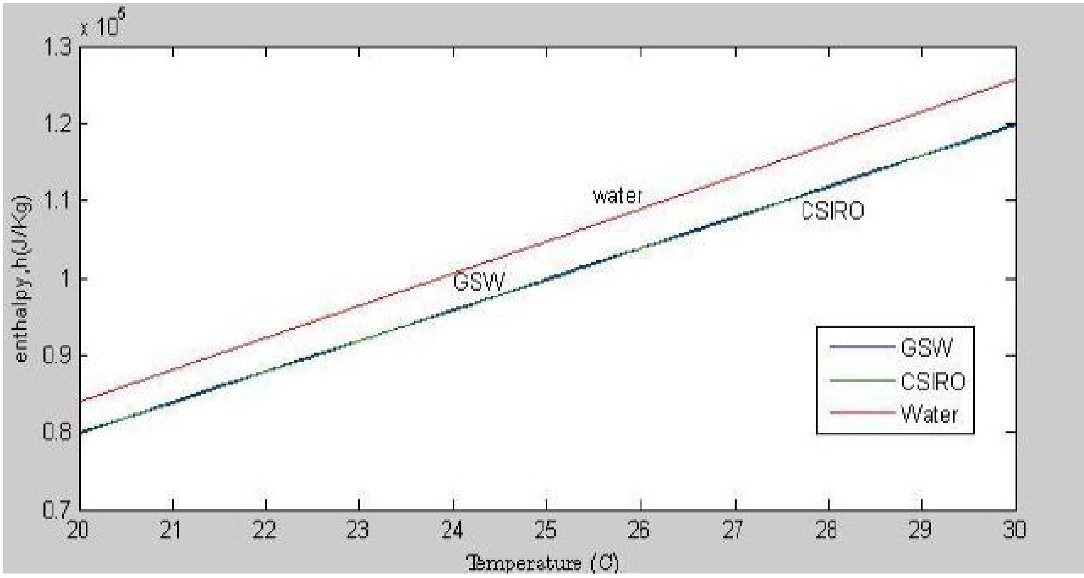

Figure 3.5 Data generate of enthalpy of seawater by GSW, CSIRO and water by Roger and Mayhew

3.10.4 Results Validation and Comparison

Table 3.5 shows the simulation validation results of OTEC plant by Sami Mutair (2013) with this study and freshwater production for this study. The salinity taken for validation is 40 g/kg. The results from this study are acceptable for a criterion-related validation with Sami Mutair results. The difference in all pumping power values is because of the lower intake of mass flow rate of warm and cold seawater. A slightly different result of warm and cold seawater intake is due to some parameters and value that is not stated in the study conducted by Sami Mutair (2013). To achieve 1000 kW of turbine power it would need 2036.72 kg/s of intake mass flow rate of warm and cold seawater. For the freshwater production, it is not much a difference between Mutair study and this study. The freshwater production for this study is calculated based on Equation 3.11 to Equation 3.15. Its difference is only in the freshwater production whereby due to some specific condition taken, based on simulation data optimization as the thermal conductance of condenser, an error assumption to calculate the heat balance and others is not stated in his study. But theoretically, it stated that the freshwater production is based on the effectiveness of the LTTD equation as discussed in Chapter 4. This shows that by using a simple configuration rather than Sami Mutair study, this study also can achieve the same amount of freshwater production. Configuration of LTTD plant in this study is more effective as it doesn't need to have DCC and a cooling water pump which requires a more complicated design and specific power consumption for LTTD plant. Table 3.6 and Table 3.7 are the data taken for comparison study. The comparison are based on the same temperature taken for both study but different input for salinity, and pipe water length which this study is based on off-shore based pipe length for the system. Table of heat and mass balance for validation study can be referred as in Appendix K.

Table 3.5: The validation and comparison study

Parameter	**Symbol**	**Unit**	**Mutair (OTEC-LTTD)**	**Validation**
Warm seawater				
Inlet temperature	T_{wsi}	°C	26.00	26.00
Outlet temperature	T_{wso}	°C	21.60	21.60
Cold seawater				
Inlet temperature	T_{csi}	°C	6.00	6.00
Outlet temperature	T_{cso}	°C	10.20	10.22
Flow rate				
Warm seawater	m_{ws}	kg/s	2040.00	2036.72
Cold seawater	m_{cs}	kg/s	2040.00	2036.72
Working fluid	m_{wf}	kg/s	29.0	29.0
Work Pump				
Warm seawater	WP_{ws}	kW	94.30	94.07
Cold seawater	WP_{cs}	kW	221.31	220.58
Working fluid	WP_{wf}	kW	9.58	9.57
Vacuum	WP_{vp}	kW	15.92	14.64
Condensation temperature	T_C	°C	10.99	10.99
Evaporation temperature	T_E	°C	20.8	20.78
Net power	W_{net}	kW	675.00	675.78
Freshwater production	m_{dw}	kg/s	15.00	15.07

Table 3.6: Data for Sami Mutair (2013) study

Type	**On-Shore Based plant**
T_{wsi}	26 °C
T_{csi}	6 °C
S	40 g/kg
$m_{ws} = m_{cs}$	2040 kg/s
L_{pcs}	3500 m
Intake depth	800 m
$UA_E = UA_C$	15 MW/°C

Table 3.7: Data used for comparison study

Type	**Off-Shore Based plant**
T_{wsi}	26 °C
T_{csi}	6 °C
St	35 g/kg
$m_{ws} = m_{cs}$	2023.9 kg/s
L_{pcs}	760 m
Intake depth	760 m
$UA_E = UA_C$	15 MW/°C

CHAPTER 4

RESULT AND DISCUSSION

4.1 Software Calibration Results

The results obtained by integrated the seawater simulation as a sub-routine in the main simulation program.

4.1.1 Seawater Properties

Seawater which contains salt can increase the boiling point elevation of pure water. Boiling point is the temperature when the liquid boils and turns into vapor. The particles gain energy and move faster when a liquid is being heated. As heat energy keeps on supplying to the liquid, the particles will eventually obtain enough energy to completely break the force between the molecules. Then the particles are now able to move freely and be far apart. The temperature remains constant during boiling because heat energy that is absorbed by the particles is used to break the forces holding them together. Due to the larger salt content, the energy needed for seawater to achieve its boiling point is increased. Therefore, it is very important to evaluate the main input parameter such as seawater physical properties for both OTEC and LTTD plant. To illustrate this, Figure 4.1, shows the relationship between temperature and boiling point for the various salinities of seawater. The boiling point increases when the salinity of seawater increases. In complete flash evaporation process, the exit temperature of the flash chamber is greater than generating steam condensation temperature. The amount of boiling point rises due to the increase of salinity and temperature of the seawater intake.

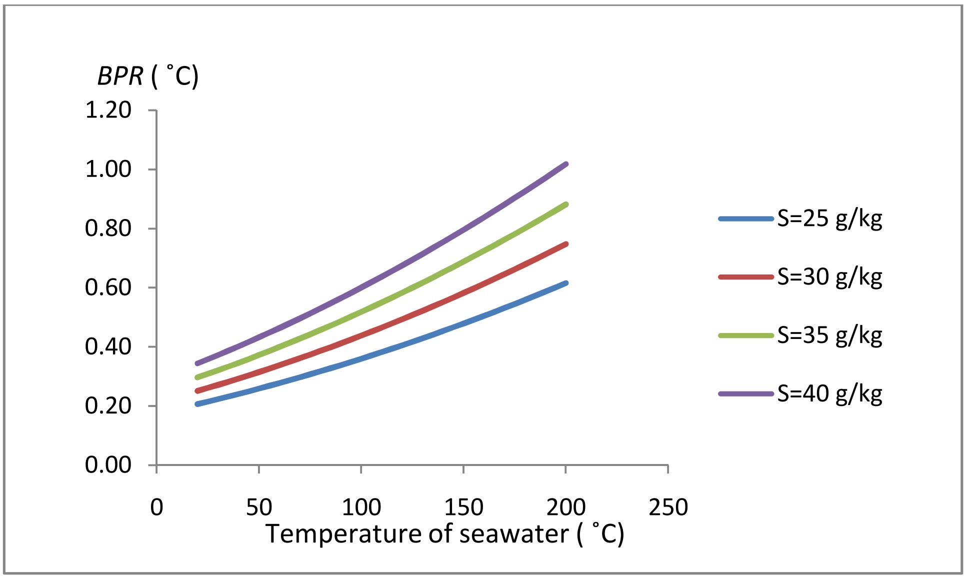

Figure 4.1 Boiling point rises with temperature with different salinity of seawater

Figure 4.2 indicates the graph of the specific heat capacity, C_p and boiling point versus temperature of seawater. The specific heat can be defined as the amount of heat per unit mass required to raise the temperature by one degree Celsius. As the temperature rises, the boiling point rise '*BPR*' and specific heat capacity would also increase. This is because in order to increase the temperature, greater heat is required to break the bond between the particles. The other properties of seawater can be referred to 'Thermophysical properties of seawater' by Mostafa H.Sharqawy .

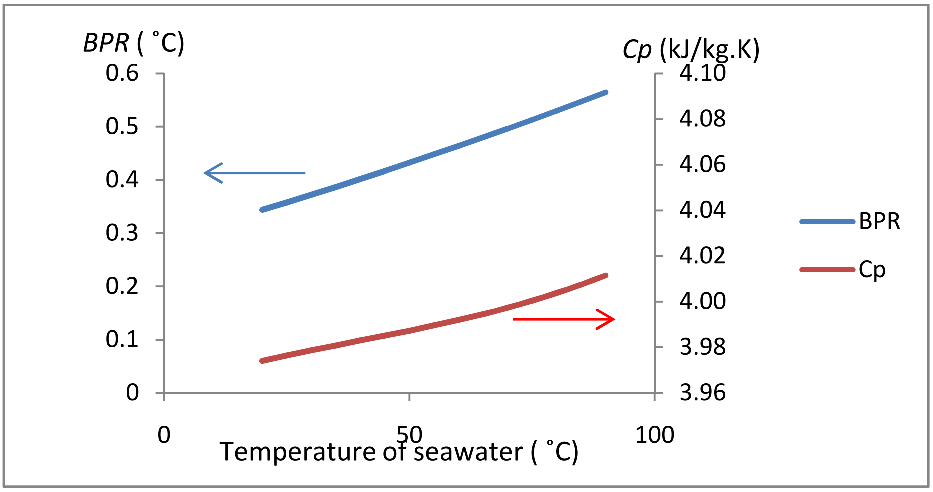

Figure 4.2 Variation of boiling point and specific heat capacity with the temperature of seawater of S = 40 g/kg

4.2 LTTD Plant

The optimization and results obtained from the simulation is to show the parameters that affect the LTTD plant and its configuration to integrate with OTEC plant.

4.2.1 Freshwater Production by Effect of the Thermal Conductance and Mass Flow Rate of Freshwater

Figure 4.3 shows the effects of thermal conductance and mass flow rate on freshwater production in the standalone LTTD plant. In this graph, it shows the thermal conductance of desalination condenser, UA_{dc} is the variable while the other parameters are kept constant . In order to produce 1000 t/d (around 11.57 kg/s) of freshwater, the required thermal conductance is 2.67 MW/°C. The graph shows that the freshwater is produced from 300 to 1000 tons per day when the thermal conductance increase to 2.7 MW/°C. However, at a certain point, the freshwater production cannot be increased any further even though the thermal conductance was raised again. This proved that the desalination condenser has its own finite value. In the real plant, various amount of m_{ws} and m_{cs} were investigated to achieve the freshwater production target.

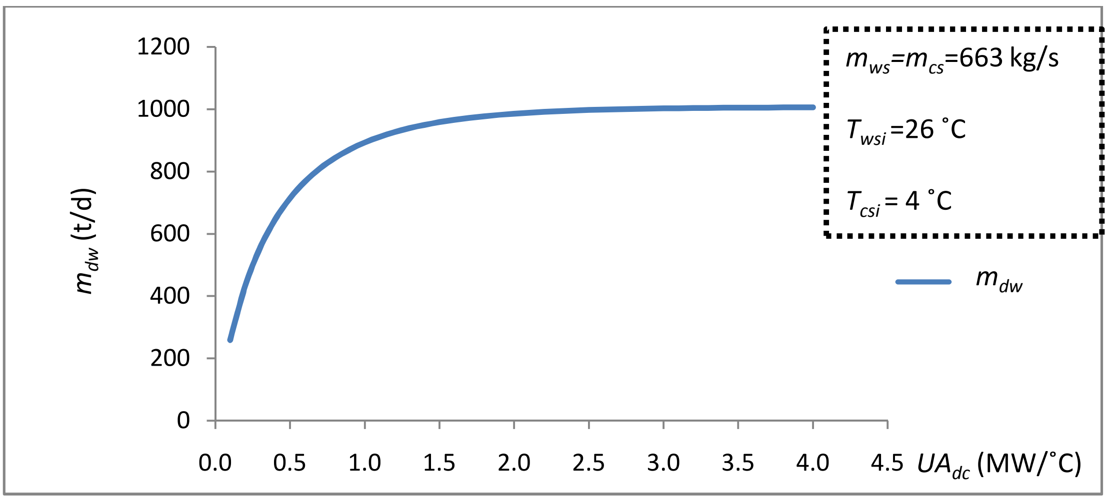

Figure 4.3 Desalinated water production in kg/s and t/d with different thermal conductance

As shown in Figure 4.4, with constant thermal conductance, the freshwater production will keep increasing with the increase of warm and cold seawater flow rate intake. In LTTD plant, the seawater flow rate is one of the main input parameters. By increasing the seawater flow rate, the freshwater production from the desalination plant is also increased. The freshwater production can be boosted either by increasing the temperature gradient or by taking a huge amount of seawater intake for both warm and cold seawater flow rate. This is due to the high amount of vapor produced from warm seawater where a huge amount of warm seawater flow rate intake will increase the heat added at the flash chamber to overcome the latent heat of vaporization to transfer the vapor to freshwater as in Equation 3.15.

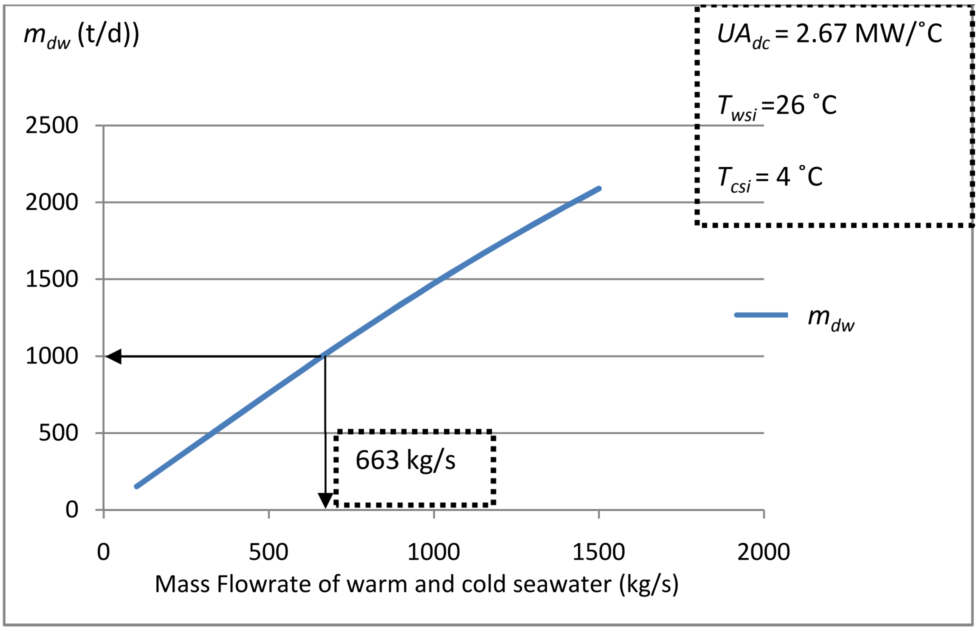

Figure 4.4 Desalinated water by different warm and cold seawater mass flow rate

4.2.2 Effects of Freshwater Production by Various Temperature of Warm Seawater

Figure 4.5 shows the relationship between the warm and cold seawater intake against warm seawater temperature to produce 1000 t/d of freshwater. The data can be obtained from a fixed thermal conductance area and cold seawater temperature at 4 ˚C. As seen from the figure, the resulting graph indicates a linear graph. With the larger temperature gradient between the warm and cold seawater, the warm and cold seawater flow rate intake decreased in order to achieve 1000 t/d. This is because based on the Equation 3.15, it provides proof that the freshwater production increased by having larger temperature difference. This means that the freshwater production will vary with the thermal conductance, flow rate of seawater, and temperature gradient of the warm and cold seawater. The warm and cold seawater is one of the main input parameters which affect the desalination ratio. However, in a real plant condition, the temperature has a limitation because it cannot be controlled. In order to get a larger temperature difference between warm seawater and cold seawater, the huge intake of depth is needed.

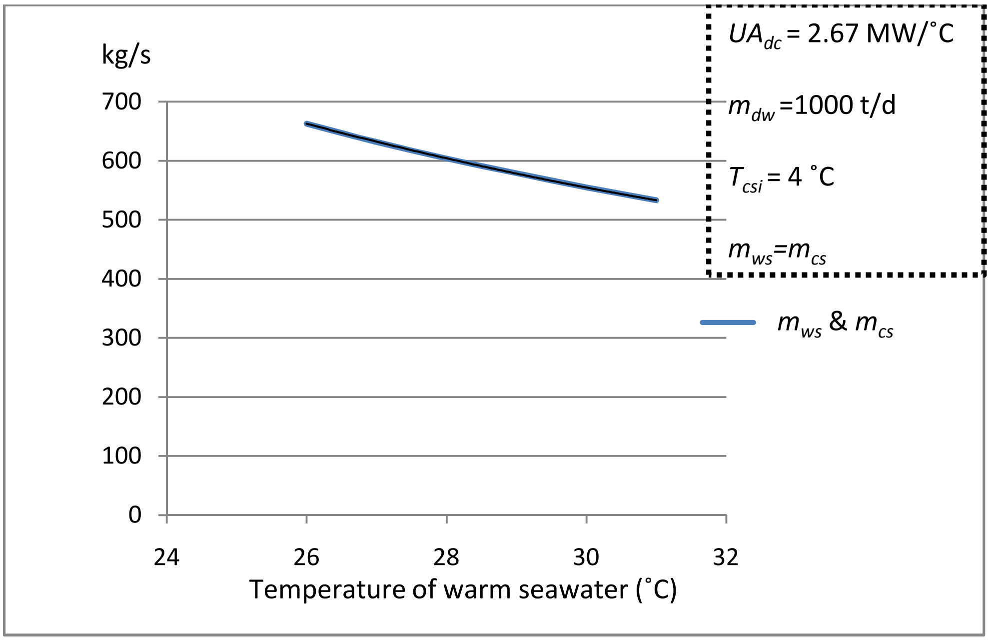

Figure 4.5 Desalinated water production by variable temperature of warm seawater

4.2.3 Desalination Ratio

In Figure 4.6, it shows that the freshwater desalination ratio increases as well as the thermal conductance, UA_{dc} increase. The mass flow rate of warm and cold seawater is kept constant with various thermal conductances, UA_{dc}. The temperature difference of the flash evaporation chamber (T_{wsi}-T_{fco}) and desalination condenser (T_{dco}-T_{dci}) increase with the increase of thermal conductance. This is because a larger thermal conductance has a larger heat transfer area which allows a better possible of fluid transfer.

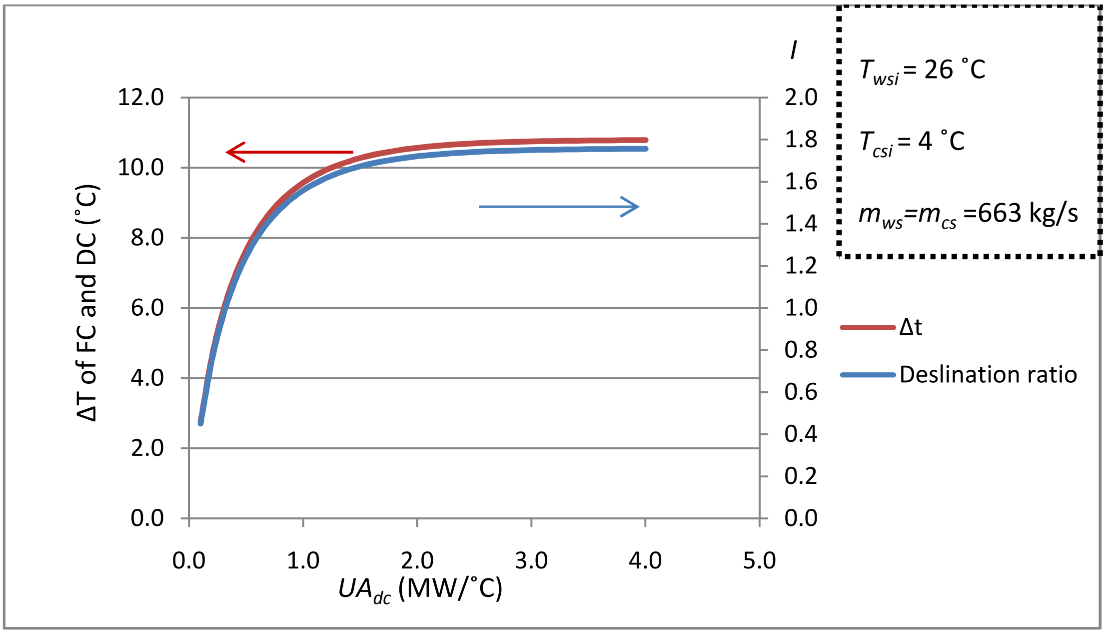

Figure 4.6 Desalinated water production and desalination ratio based on temperature differences in flash chamber and desalination condenser

In contrary, the desalination ratio will decrease with an increasing mass flow rate of warm and cold seawater with fixed the thermal conductance and temperature of warm and cold seawater. The large mass flow rate of seawater gives more freshwater production, but the desalination ratio decreased with increasing the mass flow rate of seawater as shown in Figure 4.7. The portion of seawater converts to freshwater is very small due to latent heat of warm seawater, L which is larger compared to the specific heat capacity, C_p of the warm seawater affecting by the salinity and temperature of seawater intake. As a solution, the LTTD needs seawater intake to increase the desalination ratio as there is an abundance of seawater available.

In a real plant, the desalination ratio does not have much intention as long as the plant can give more freshwater production with lower energy consumption. Although the larger thermal conductance lead to increase the desalination ratio and freshwater production, but it needs a large heat exchanger area to in order to increase the freshwater production.

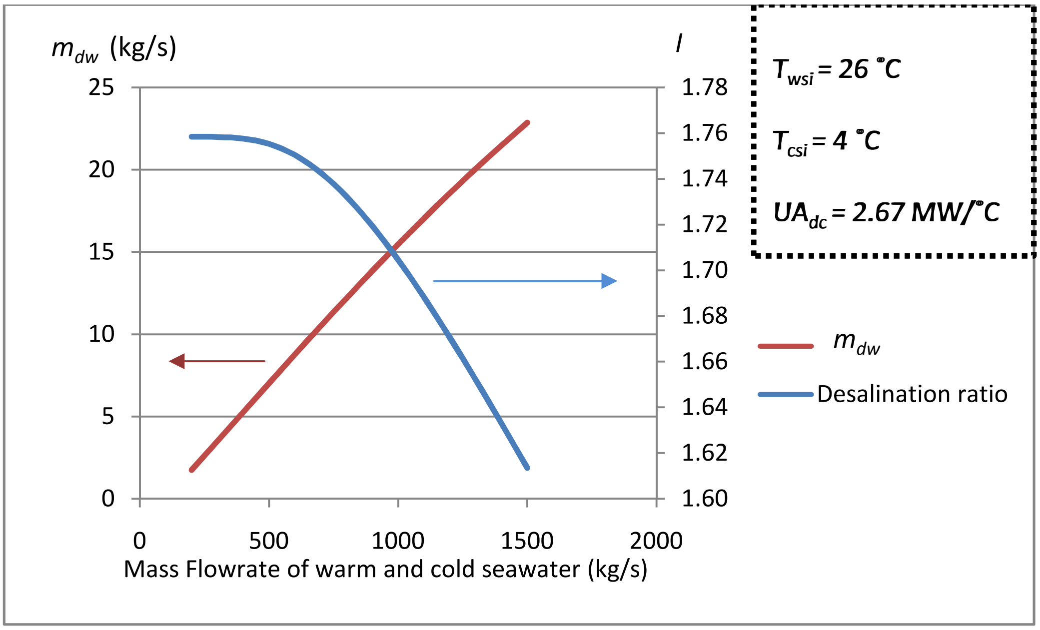

Figure 4.7 Desalinated water and desalination ratio with different seawater flow rate with constant thermal conductance

4.2.4 Significance of LTTD Plant Optimization

Figure 4.8 shows the relationship of thermal conductance, UA_{dc} with the mass of warm and cold seawater flow rate at a constant temperature difference of warm and cold seawater. In order to produce 1000 t/d of freshwater, a 0.5 MW/ ˚C of UA_{dc} needs 1321 kg/s and 1.0 MW/ ˚C of UA_{dc} needs 770 kg/s of warm and cold seawater mass flow rate intake capacity. From that comparison, larger UA_{dc} needs lower warm and cold seawater intake capacity to produce 1000 t/d. Figure 4.8 clearly shows that the graph is identical with each other for 2.67 MW/ ˚C and 3.0 MW/ ˚C of UA_{dc}. The mean for the input temperature of 26 ˚C and 4 ˚C of warm seawater and cold seawater respectively, it needs only 2.67 MW/ ˚C of UA_{dc} in order to produce 1000 t/d of freshwater. For the LTTD plant, the freshwater generated is dependent on the capacity of the plant and no limitation or capacity specification is needed to start operating. For different thermal desalination plants such as MSF and MED, as discussed in the literature review section, its limitation is the capacity of the plant. The capacity of the seawater must follow the requirement of the seawater capacity of the plant and typically 70% or more for input (seawater) in order to start operating. Besides that, the seawater temperature is also the main limitation for both plants which is needed in order to be heated at a certain degree. Of course, this consumes much energy rather than creating a vacuum to lower the boiling point of the seawater. For RO plant, the pre-treatment process of seawater is highly recommended as a requirement in order to prevent clogged the main membrane of the system.

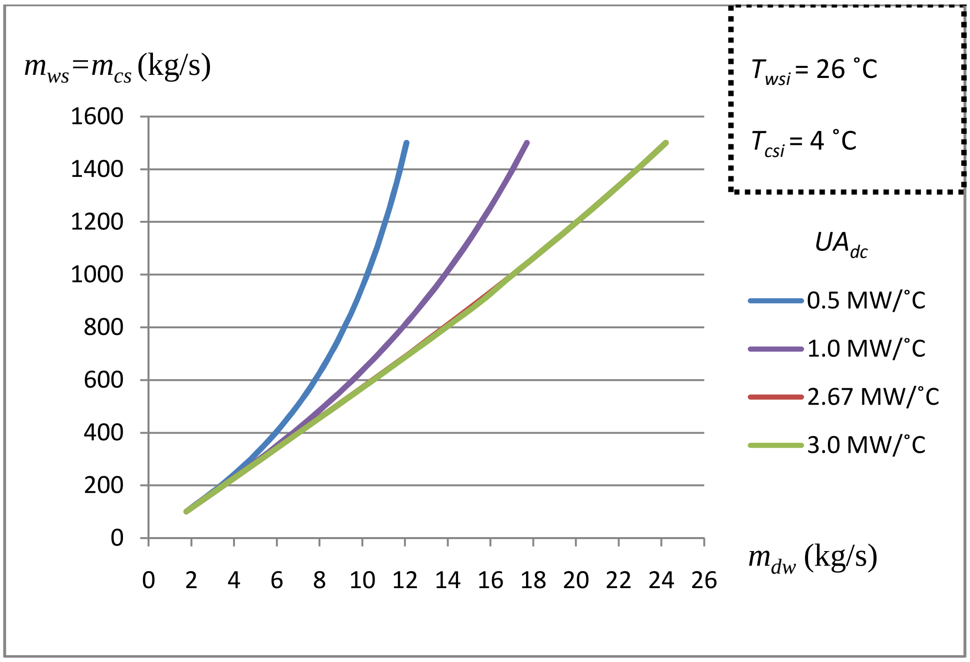

Figure 4.8 Warm and cold seawater mass flow rate by desalinated water production with different thermal conductance.

4.3 OTEC Plant

Simulation results for OTEC plant.

4.3.1 Working Fluid Optimization

The results obtained are based on the optimization process to produce 1 MW of turbine power for the OTEC plant. Figure 4.9 shows the efficiency of the OTEC cycle by using Ammonia, r22 and r134a as the working fluids of the cycle. From the graph provided, the efficiency of all the working fluids used would drop with a higher warm and cold seawater temperature difference at evaporator heat exchanger. Based on the 3 working fluids, ammonia gives a higher efficiency than the others and r22 and r134a where the graph line is slightly identical with each others. This is due to the higher heat transfer coefficients, the high latent heat of vaporization and better COP of the fluid. Ammonia fluid also has a low density at 1.013 bar of pressure at boiling point: 682 kg/m^3 (ammonia liquid), 1413 kg/m^3 (liquid R22) and 1376 kg/ m^3 (liquid R134a).

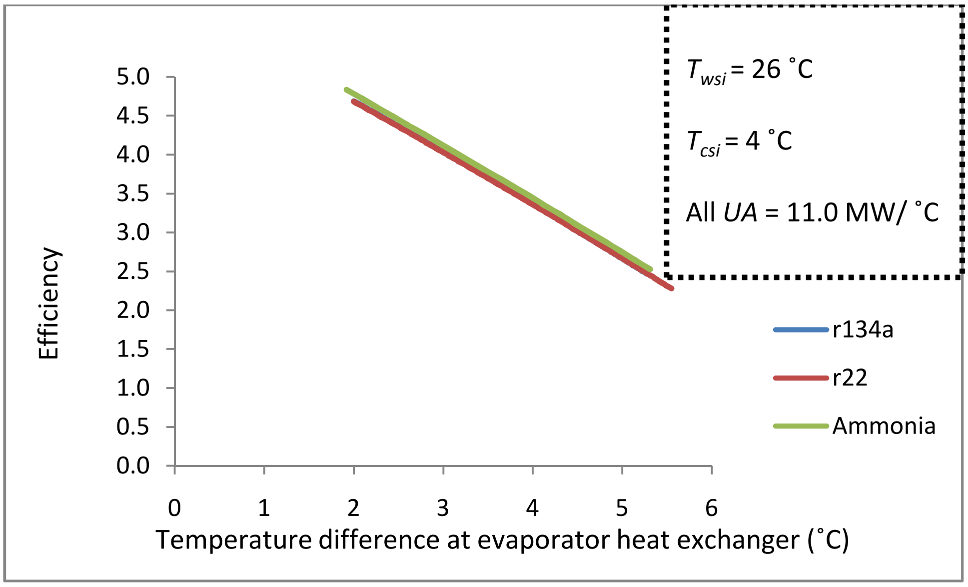

Figure 4.9 Efficiency of different working fluids with temperature difference of warm seawater in evaporator

As shown by the data found in Table 4.1, in order to achieve 1 MW of turbine power, the pumps would need more than 1700 kg/s of seawater drawn from the surface and deep of the ocean. To generate 1 MW, ammonia required a lower flow rate compared to others working fluids. The larger mass flow rate of working fluid consumed higher specific power consumption of the system. Apart from being cheaper in price, it is also another reason ammonia working fluid is regarded more favorable than other working fluids.

Table 4.1: Comparison of OTEC-LTTD cycle using Ammonia (jnh3), r134a and r22

Parameter	**Working fluid**		
	Ammonia	**r134a**	**r22**
m_{ws}=m_{cs} **(kg/s)**	1797	1850	1785
m_{wf} **(kg/s)**	26	153	161
WP_{ws} **(kW)**	58.63	60.39	58.24
WP_{cs} **(kW)**	113.65	118.46	112.6
WP_{wf} **(kW)**	9.24	18.81	27.01
$WPvp$ **(kW)**	14.38	14.77	14.28
W_{net} **(kW)**	804.1	787.57	787.87
m_{dw} **(kg/s)**	16.49	17.66	16.29

4.3.2 OTEC *T-s* Diagram

The working principle of OTEC is based on Organic Rankine Cycle. In a closed-cycle OTEC, ammonia is selected as a working fluid due to its low boiling point. Figure 4.10 shows the *T-s* diagram of ammonia working fluid to produce 1 MW of electricity for simulation input as in Table 3.1. In order to achieve 1 MW of turbine power, the simulation study used the same mass flow rate of warm and cold seawater of 1796.8 kg/s with 11 MW/˚C of thermal conductance value, while the other parameters are kept constant. The evaporation temperature is 20.3 ^{o}C and the condensation temperature is 9.43 ^{o}C which is being calculated by using log mean temperature difference. Point 1 is the saturated vapor state at inlet of the turbine. Point 2 is the mixture state at the outlet of the turbine and the inlet of the condenser which the turbine is assumed to be isentropically (s_1=s_2). Point 3 is the outlet of the condenser which is the saturated liquid condition. The ammonia working fluid goes through the evaporator by the working fluid pump and is being heated by warm seawater to generate saturated vapor.

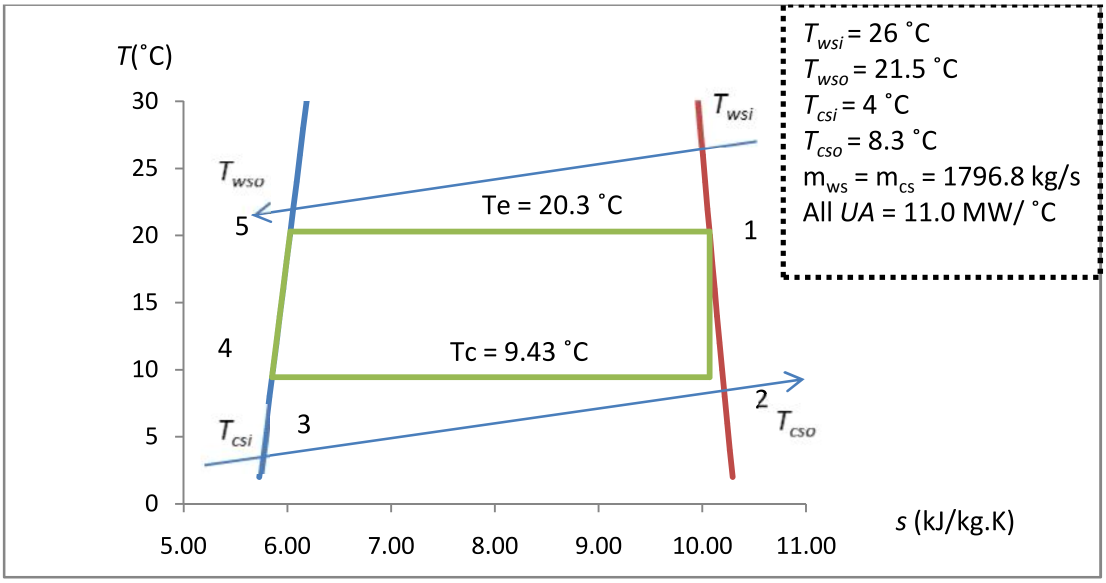

Figure 4.10 *T-s* diagram for ammonia working fluid to produce a 1 MW turbine power generation (emphasized)

Table 4.2 shows the data for the quantity state for the OTEC cycle proposed for this study based on point for *T-s* diagram as in Figure 4.10. The table for heat and mass balance for each point temperature can be referred as in Appendix L.

Table 4.2: Value for the quantity state for the OTEC cycle

T_{wsi} (°C)	26.0	27.0	28.0	29.0	30.0
T_{csi} (°C)	4.0	4.0	4.0	4.0	4.0
T_1 (°C)	20.3	20.8	21.3	21.8	22.6
s_1 (kJ/kg.K)	10.1	10.1	10.1	10.1	10.0
P_1 (Kpa)	863.1	877.3	891.7	906.1	927.9
h_1 (kJ/kg)	517.4	517.8	518.1	518.5	519.0
T_2 (°C)	9.4	9.9	10.4	10.9	11.1
s_2 (kJ/kg.K)	10.1	10.1	10.1	10.1	10.0
P_2 (Kpa)	601.4	611.4	621.6	631.8	637.0
h_2 (kJ/kg)	472.2	472.5	472.9	473.2	471.8
T_3 (°C)	9.4	9.9	10.4	10.9	11.1
s_3 (kJ/kg.K)	5.9	5.9	5.9	5.9	5.9
P_3 (Kpa)	601.4	611.4	621.6	631.8	637.0
h_3 (kJ/kg)	-718.8	-716.5	-714.3	-712.1	-710.9
T_4 (°C)	9.5	10.0	10.5	10.9	11.2
s_4 (kJ/kg.K)	5.9	5.9	5.9	5.9	5.9
P_4 (Kpa)	863.1	877.3	891.7	906.1	927.9
h_4 (kJ/kg)	-718.4	-716.1	-713.9	-711.6	-710.5

4.3.3 Variation of Work Turbine with Various Thermal Conductance

Figure 4.11 shows the relationship of mass seawater flow rate and the net power output on the various thermal conductance ($UA_E = UA_C$). The figure shows the variation of the warm seawater flow rate in order to produce turbine power of 1 MW and the net output gained by variation of mass seawater and thermal conductance of the system. Based on the graph, W_{net} of 1 MW turbine power will increase with decreasing cold and warm seawater mass flow rate. Thus, by increasing the thermal conductance value, the mass flow rate of cold and warm seawater also decreased while the W_{net} increase. By an observation, certain value of thermal conductance gives much effect to the mass flow rate of seawater intake and W_{net} as well. But at a certain point, the value of thermal conductance will become finite which means the value of seawater mass flow rate and W_{net} will remain constant. The larger mass flow rate will affect the net output power because the pumping power of warm seawater and cold seawater will increase with increasing mass flow rate of seawater intake.

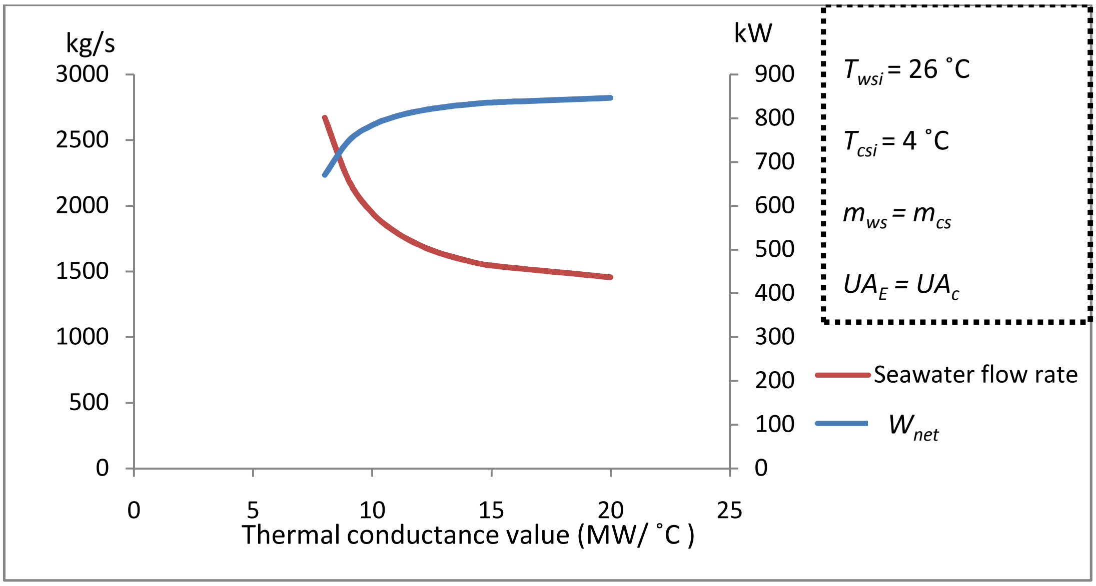

Figure 4.11 Seawater mass flow rate and net output power generation with a variation of thermal conductance

4.3.4 Variation of Work Turbine with Temperature Difference of Warm and Cold Seawater at OTEC Heat Exchanger

The temperature difference at inlet and outlet of seawater in the plate heat exchanger for evaporator and condenser need to be optimized because it can affect the system performance. Figure 4.12 shows the variation of turbine power generation with temperature difference in the warm and cold sources of evaporator and condenser. The graph shows that the turbine power keeps increasing until it reaches a certain peak, then it starts to decline along with a larger temperature difference. The inlet and outlet temperature difference of the evaporator and condenser is slightly identical to each other. The Q_E is increased linearly as the temperature difference at evaporator and condenser is increased. As can be seen in Table 3.2, by varying the mass working fluids of the cycle, the working turbine of the system definitely will be affected. Based on the effectiveness equation of the OTEC cycle as discussed in section 4.5, the higher efficiency does not mean the turbine generator is at the optimum power output. From the graph presented in Figure 4.9 and 4.12, the maximum output power of the turbine generator lies between 4 ˚C to 5 ˚C of temperature differences. The optimization results will be the guideline for determining the optimum work turbine produced. For the different intake of warm seawater temperature optimal temperature difference will be discussed in Section 4.4 for the OTEC-LTTD plant.

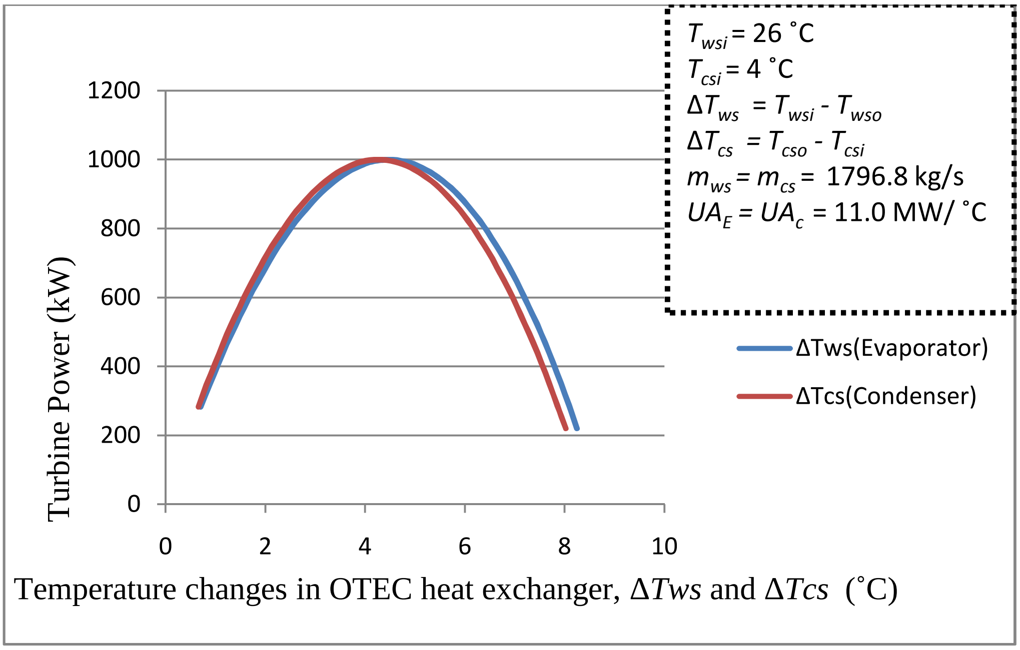

Figure 4.12 Turbine power output with a temperature difference of seawater in OTEC heat exchanger

4.3.5 Pipe Diameter Effects on Net Work Turbine

The selection of the pipe diameter is based on the seawater mass flow rate to achieve 1 MW turbine power at constant condition as depicted in Figure 4.13 which create the minimum losses on the system. The net power output kept increasing with increasing diameter of seawater pipe until the net power output remains constant by a further increase of the seawater pipe diameter. By increasing the pipe diameter it causes the flow velocity of the seawater in pipes to decrease which affects the head loss of seawater pipe of warm and cold seawater pipe. The pipe diameter size is dependent on how much flow rate of the seawater needed for the plant. It needs to be optimized in order to find the optimal pipe diameter for the specific conditions of the OTEC plant. This is because if the pipe diameter is too small for the required seawater flow rate for specific OTEC plant generation, it will affect the net power output of the plant. As for the 1 MW OTEC plant, it needs at least 1.2 m or larger size of pipe diameter in order to produce optimum power generation. In the same condition, the net work output remains the same although with further increase of the pipe diameter after at optimal pipe diameter. The optimization of required pipe diameter and optimal pipe diameter is important due to cost analysis. In offshore piping condition, the pipe design and configuration need to be analyzed in order to prevent higher capital investment. In the OTEC system, the installation cost of the cold seawater pipe is higher due to the length of the pipe and a challenge to submerge the pipe into the ocean with high depth.

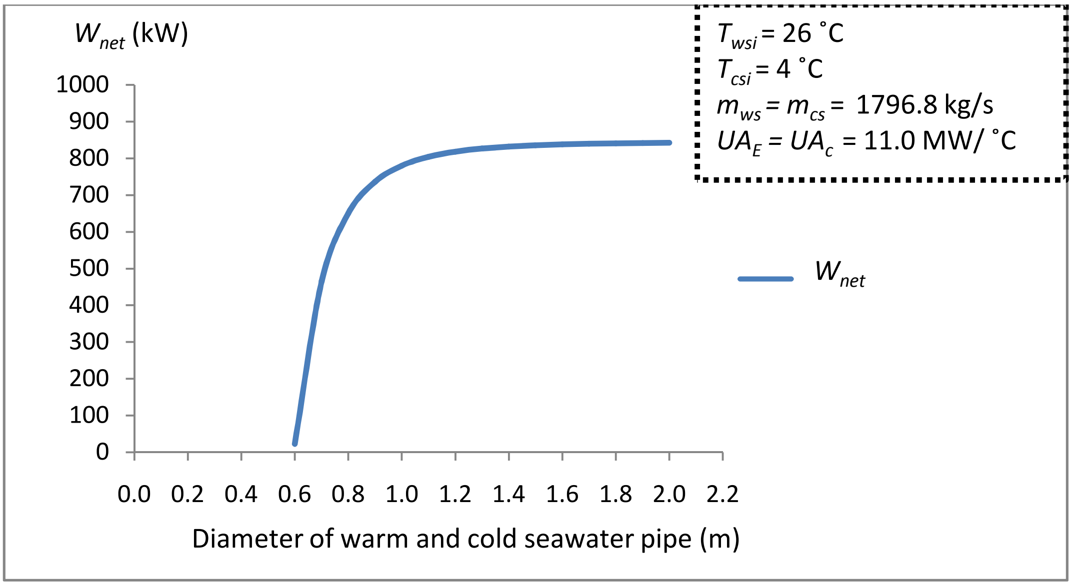

Figure 4.13 Variation of W_{net} power by different diameter of seawater pipe diameter

4.3.6 Work Pump Effect with Variation of Thermal Conductance

The net power output can be described as the total turbine power output minus all the pumping power (warm seawater, cold seawater and working fluid) of the system. Figure 4.14 shows the 1 MW OTEC plant output with the net power output and all pumping works with different thermal conductance. The pumping power for cold seawater and warm seawater decreases in a logarithmic-like relationship with increasing the thermal conductance of the evaporator and condenser. This is due to the seawater intake for cold seawater and warm seawater decreases with the increase of thermal conductance to produce a maximum work turbine. The different density and friction factors also give much effect to the pumping power of cold seawater which consumes much energy due to the depth of cold seawater rather than depth of warm seawater intake. The pumping power for ammonia is constant for a 1 MW power output which is 9.24 kW (26 kg/s) for all values of thermal conductance. The value of temperature difference in heat exchanger of evaporator (T_{wsi} - T_{wso}) and condenser (T_{cso} - T_{csi}) is shown in the Figure 4.14. In order to achieve heat and mass balance in an evaporator and condenser, a larger thermal conductance needs larger temperature difference. The calculation is made based on the Equation 3.1, 3.2 and Equation 3.4, 4.5 for evaporator and condenser side respectively based on 0.001 error.

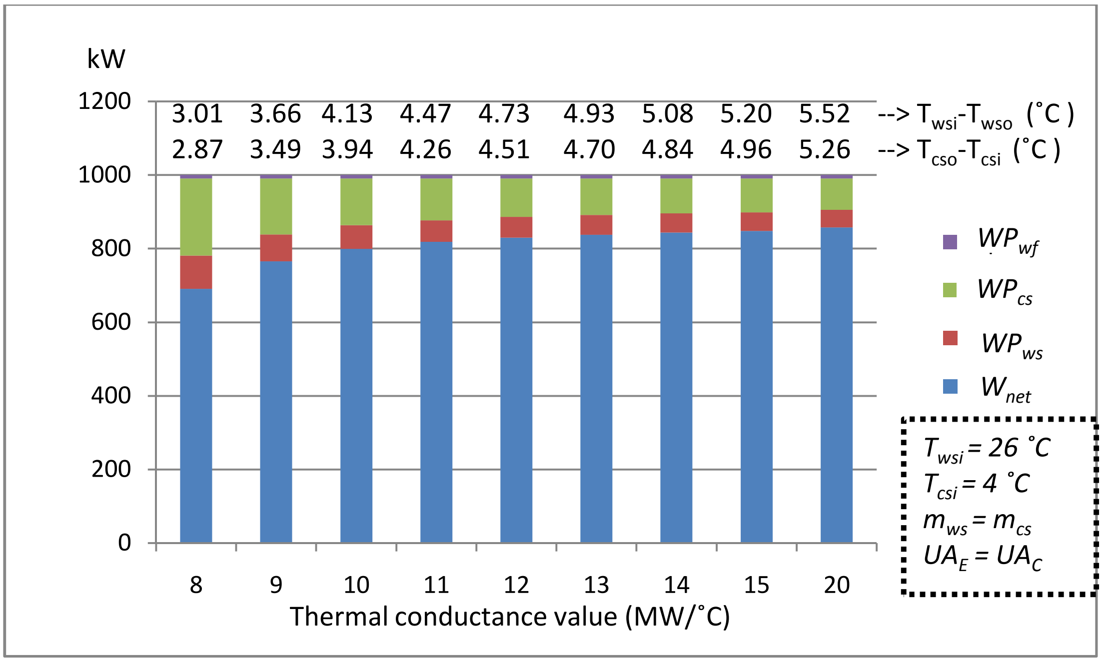

Figure 4.14 Work turbine, work net and work pump for warm seawater, cold seawater and working fluid with variable thermal conductance

.

4.3.7 OTEC Optimization Application

The simulation results show that there are many important parameters that can be taken into the calculation in order to design or propose the OTEC plant. It is very useful to make a consideration in terms of performance, cost analysis, electricity and net electricity generation production. The data from the previous studies can be used a reference in order to select the best condition design to achieve the performance and efficiency to produce a desired or intended result. The OTEC single purpose is to generate electricity based on the green method which extracts the temperature difference of the warm and the cold source of seawater. For commercial purposes, there are many advantages that can be gained from an OTEC plant namely that it extract hydrogen production, lithium, freshwater, marine culture and others.

4.4 OTEC-LTTD Plant

The proposed hybrid power generation and freshwater plant for the study.

4.4.1 Integration of OTEC-LTTD Plant

The main objective of the desalination plant is to design a plant which can give an energy-cost-effective to produce freshwater. The simulation condition used in this study is similar to the previous CC-OTEC plant. In this study, the OTEC plant is integrated with the LTTD plant to construct OTEC-LTTD plant for the generation of electricity and freshwater. The freshwater production will be configured at the optimum turbine power output. As in OTEC-LTTD plant, the freshwater production will be configured and optimized after the optimum turbine power output is achieved. The simulation study has to be conducted before the real plant builds. From the previous research, the error of simulation study and experimental study is counted less than 10 % and can be adopted.

4.4.2 Variation of Work Turbine and Freshwater Production

Figure 4.15 shows the effect of temperature difference at the evaporator and condenser of the OTEC cycle for 1 MW turbine power with net power output and freshwater production for proposed 1 MW OTEC-LTTD plant. The result shows that at turbine power generation of 1 MW, the freshwater production is 16.49 kg /s with a net power output of 804.1 kW. The freshwater production is declining linearly by further increasing the warm and cold seawater temperature difference at the inlet and outlet of the evaporator and condenser. In order to generate more electricity generation and freshwater production, a larger OTEC-LTTD plant capacity is needed.

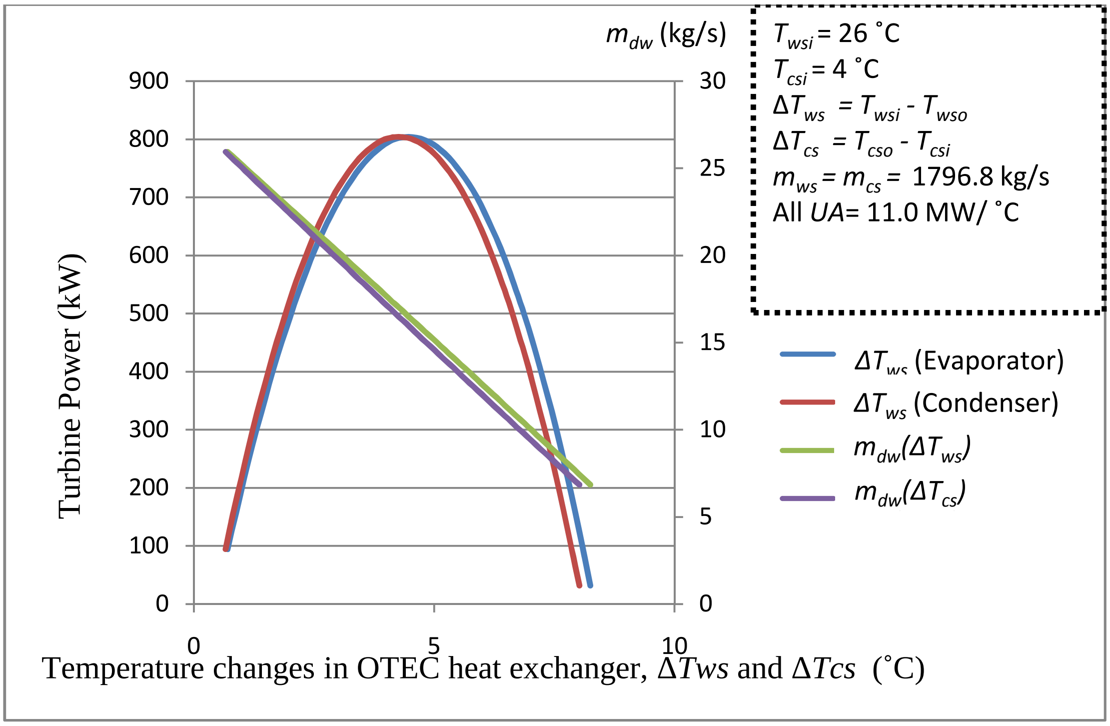

Figure 4.15 Turbine power and net power output with freshwater production by temperature change in the OTEC heat exchanger

4.5 Simulation Data Based on Tropical Warm Seawater Temperature

The proposed OTEC-LTTD plant is to generate 24 MWh/d of electricity and more than 1000 t/d of freshwater. From Table 4.3 at the highest temperature data to generate 1 MWh of electricity at 30 ^{o}C, the freshwater production is 11.5 kg/s corresponding to 1000 t/d. An increase in temperature would result in a higher net power output due to lower needs of intake capacity of warm and cold seawater. The difference in pumping power for the working fluid is affected by the increasing of T_E and T_C of the system. Increasing of T_E and T_C will increased the pressure of the evaporator and condenser respectively and increased the specifc volume of saturated liquid at condenser exit for the working fluid side.

Table 4.3: Simulation results corresponding to generate 1 MW at various warm seawater temperature

T_{wsi} (°C)	26.0	27.0	28.0	29.0	30.0
T_{csi} (°C)	4.0	4.0	4.0	4.0	4.0
$m_{ws}= m_{cs}$ (kg/s)	1796.8	1563.9	1390.3	1255.2	1198.7
m_{wf} (kg/s)	26.0	26.0	26.0	26.0	26.0
WP_{ws} (kW)	58.6	50.7	44.8	40.3	38.5
WP_{cs} (kW)	113.7	94.0	80.6	70.9	66.8
WP_{wf} (kW)	9.2	9.4	9.6	9.7	10.3
WP_{vp} (kW)	14.4	12.4	11.0	9.8	9.3
W_{net} (kW)	804.1	833.5	854.1	869.3	875.2
m_{dw} (kg/s)	16.5	14.5	12.9	11.6	11.5
$P1$ (kPa)	863.1	877.3	891.7	906.1	927.9
T_E (°C)	20.3	20.8	21.3	21.8	22.6
T_{wso} (°C)	21.5	21.9	22.2	22.6	23.3
T_C (°C)	9.4	9.9	10.4	10.9	11.1
T_{cso} (°C)	8.3	8.9	9.5	10.1	10.4
$(T_c)_{dc}$ (°C)	15.5	15.8	16.2	16.5	17.0
T_{dco} (°C)	13.9	14.6	15.2	15.8	16.3
T_1 (°C)	20.3	20.8	21.3	21.8	22.6
T_2 (°C)	9.4	9.9	10.4	10.9	11.1
T_3 (°C)	9.4	9.9	10.4	10.9	11.1
T_4 (°C)	9.5	10.0	10.5	10.9	11.2
ΔTws	4.5	5.1	5.8	6.4	6.7
ΔTcs	4.3	4.9	5.5	6.1	6.4
WP_{tot}	195.8	166.5	146.0	130.7	124.8

4.6 Simulation Data Based on Variation of Warm Seawater Temperature and Cold Seawater Temperature at Different Depth

The temperature of warm seawater is fluctuating over the years. In Table 4.3, it shows that the corresponding data based on various warm seawater temperature and cold seawater temperature intake to generate 1 MW of turbine power. The table shows the results for warm seawater temperature at 26 °C and 27 °C with different cold seawater temperature taken at several depths at 4 °C, 5 °C and 6 °C. The other table generated is based on proposal to generate 1 MW turbine power at various warm and cold seawater temperatures as in Appendix J. The simulation input for depth can be seen in Table 3.2. The minimum lower temperature is taken to maintain the performance of OTEC cycle performance which is the temperature gradient must be at least or more than 20 ^oC at 6 ^oC of cold seawater temperature. From the results, the net power output is decrease and the freshwater production is increased when the temperature of cold seawater increased. This is due to the intake capacity of mass flow rate of warm and cold seawater which is the higher capacity of mass flow rate of seawater needs high power consumption for pumping power. On the contrary, higher intake capacity of warm and cold seawater will boost more freshwater production as discussed in Section 4.2.3.

Table 4.4: Simulation results corresponding to generate 1 MW turbine power at various cold seawater temperature

T_{wsi} (°C)	26.0	26.0	26.0	27.0	27.0	27.0
T_{csi} (°C)	4.0	5.0	6.0	4.0	5.0	6.0
$m_{ws=}$ m_{cs} (kg/s)	1796.8	2147.4	2634.5	1563.9	1837	2158.2
m_{wf} (kg/s)	26.0	29.0	29.0	26.0	29.0	29.0
WP_{ws} (kW)	58.6	71.5	88.8	50.7	60.4	71.5
WP_{cs} (kW)	113.7	139.1	190.8	94.0	111.0	134.5
WP_{wf} (kW)	9.2	9.4	9.6	9.4	9.6	9.7
WP_{vp} (kW)	14.4	16.9	20.4	12.4	14.4	16.6
Wnet (kW)	804.1	763.2	690.4	833.5	804.6	767.7
m_{dw} (kg/s)	16.5	18.3	21.9	14.5	15.8	18.4
P1 (kPa)	863.1	861.8	876.5	877.3	875.7	890.6
T_E (°C)	20.3	20.3	20.8	20.8	20.8	21.3
T_{wso} (°C)	21.5	21.9	22.6	21.9	22.2	22.9
T_C (°C)	9.4	10.5	11.0	9.9	11.0	11.5
T_{cso} (°C)	8.3	9.0	9.2	8.9	9.6	9.9
$(T_c)_{dc}$ (°C)	15.5	16.2	17.1	15.8	16.5	17.2
T_{dco} (°C)	13.9	14.2	14.4	14.6	15.0	15.2
T_1 (°C)	20.3	20.3	20.8	20.8	20.8	21.3
T_2 (°C)	9.4	10.5	11.0	9.9	11.0	11.5
T_3 (°C)	9.4	10.5	11.0	9.9	11.0	11.5
T_4 (°C)	9.5	10.6	11.1	10.0	11.0	11.5
ΔTws	4.5	4.2	3.4	5.1	4.9	4.1
ΔTcs	4.3	4.0	3.2	4.9	4.6	3.9
WP_{tot}	195.9	236.8	309.6	166.5	195.4	232.3

The net power output is mainly dependent on the temperature of warm and cold seawater which is one of the main input parameter. Figure 4.16 shows the results of net power output at various warm and cold seawater intake temperatures in form of graph based on Table 4.4 and Appendix J. The higher temperature gradient is a benefit to get more power output from OTEC plant.

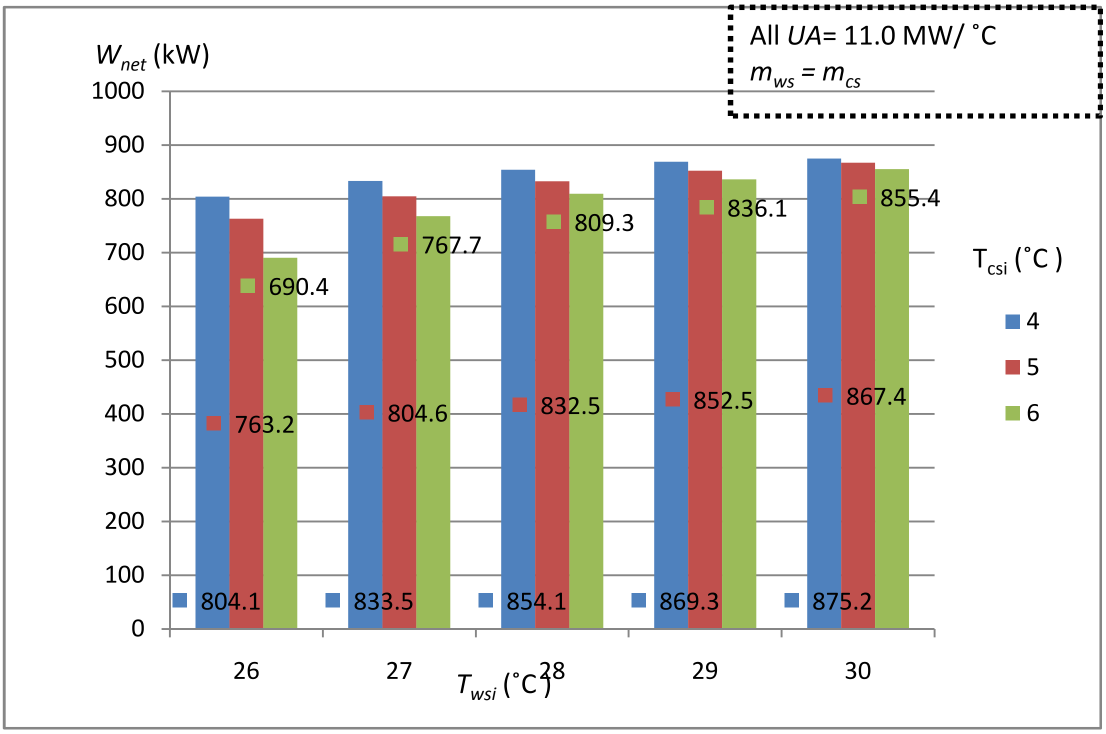

Figure 4.16 Work net at various warm and cold seawater temperature.

4.7 Simulation Study Based on Warm Seawater Surface Temperature Data at Kudat, Sabah

Figure 4.17 shows the simulation results based on warm seawater surface temperature data in Kudat, Sabah. The temperatures data were taken from Table 3.4. The highest electricity production was recorded on June while the lowest is on January. However, if we look on the freshwater production, at the higher electricity production, the amount of freshwater produced is low. This is due to the lower mass seawater flow rate intake to generate 1 MW gross power output.

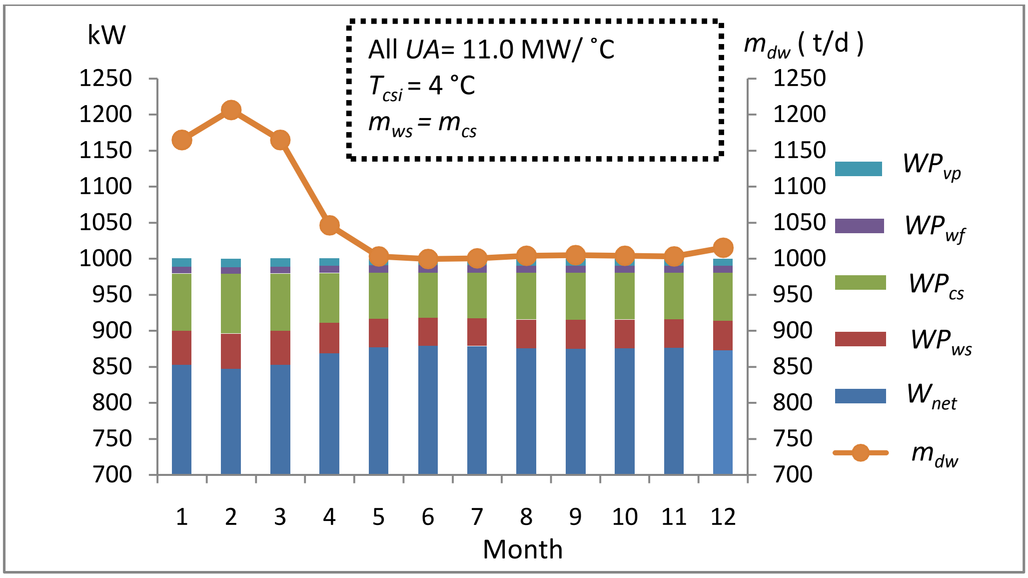

Figure 4.17 Simulation Data based on Variation of Warm Seawater Temperature data at Kudat,Sabah.

4.8 Comparison Study

Validation studies have been made as in Section 3.10. The comparison have been made based on several different input based on Table 3.6 and 3.7. For standalone LTTD plant, the mass flow rate of seawater intake to achieve 16.53 kg/s as same as OTEC-LTTD plant need slightly half of the mass flow rate for the OTEC-LTTD plant as shown in Table 4.5. This is because the temperature difference of the desalination plant received from the OTEC plant is lowered than standalone LTTD plant. But, for the standalone desalination and LTTD plant, it needs specific energy consumption to operate which is 105.2 kW. For the OTEC-LTTD plant, the specific energy consumption needed for both OTEC and LTTD plant can be recycled from energy generated by OTEC. This is the reason why there are many desalination plants combined with the power generation plant to minimize the energy consumption. According to Sami Mutair (2013), the 1 MW power generation plant can gives more than 1000 t/d of freshwater when integrated with the LTTD plant. Interestingly, the result obtained in this study also generated more than 1000 tons per day of freshwater. The pumping power is only required for the OTEC plant in the OTEC-LTTD plant. The results of pumping powers of all pumps for OTEC-LTTD in this study is different with Sami (OTEC-LTTD) were because of the geographical and tropical condition to deliver a warm seawater and cold seawater from the several depths and length. For the output power generation and freshwater production, tropical data gives the different output which the main parameters in utilizing the performance of OTEC-LTTD plant is the temperature of the warm and cold seawater. Even with 1 °C increase and decrease in the temperature will give much effect on the output and performance of the system. In this study, the Plate Heat Exchanger (PHE) type was selected for desalination condenser because it is easier to set up for the real plant compact compared to other types available in the market.

Table 4.5: Comparison study

Parameter	Symbol	Unit	Mutair (OTEC-LTTD)	This Study (OTEC-LTTD)	This Study LTTD
Salinity	St	g/kg	40.0	35.0	35.0
Warm seawater					
Inlet temperature	T_{wsi}	°C	26.0	26.0	26.0
Outlet temperature	T_{wso}	°C	21.6	21.6	16.2
Cold seawater					
Inlet temperature	T_{csi}	°C	6.0	6.0	6.0
Outlet temperature	T_{cso}	°C	10.2	10.2	15.8
Flow rate					
Warm seawater	m_{ws}	kg/s	2040.0	2023.9	1040.0
Cold seawater	m_{cs}	kg/s	2040.0	2023.9	1040.0
Working fluid	m_{wf}	kg/s	29.0	29.0	-
Work Pump					
Warm seawater	WP_{ws}	kW	94.3	67.2	33.9
Cold seawater	WP_{cs}	kW	221.3	133.8	56.0
Working fluid	WP_{wf}	kW	9.6	9.6	-
Vacuum	WP_{vp}	kW	15.9	16.0	15.2
Condensation temperature	T_C	°C	11.0	11.0	15.8
Evaporation temperature	T_E	°C	20.8	20.8	16.2
Net power	W_{net}	kW	658.9	773.5	-
Freshwater production	m_{dw}	kg/s	15.0	16.5	16.5
Total Pumping Power	WP_{tot}	kW	341.1	226.5	105.2

4.9 Optimization Effectiveness Equation

From the study, the output power for the OTEC system is evaluated based on Equation 4.1.

$$W_N = W_{T\text{-}G} - W_{Pwf} - W_{Pws} - W_{Pcs} \tag{4.1}$$

where the net power is equal to the turbine power minus all the pumping power of the system. From Equation 3.9 and Equation 4.1, the turbine generator output is influenced by the input parameters, which are the temperature of warm and cold seawater and mass flow rate of warm and cold seawater. The system depends on how much flow rate of seawater is needed for the OTEC plant. Besides, the thermal conductance also influenced the specific power consumption for the pumping power. All the parameters need to be optimized in order to achieve an optimal power of a turbine generator. The other factor of the pumping power includes the calculation of the length, roughness, and diameter of the pipe. For the desalination plant, the amount of freshwater produced can be evaluated as in Equation 3.15

$$m_d = \frac{m_w \; C_i \quad (T_f \; - T_f \;)}{L} \tag{3.15}$$

.

The C_{pws} of seawater is almost constant due to the small change for different temperature and salinity of the seawater. Based on the equation, the portion of seawater converts into freshwater is very small due to latent heat or sensible heat of seawater which is relatively larger than C_{pws}. For the LTTD system, the temperature difference is relatively small. Thus, in order to increase desalination ratio and production of freshwater, high amount of seawater is needed. In an OTEC-LTTD plant, the temperature difference between warm seawater and cold seawater sources for LTTD system can be ignored because the plant receives the warm seawater and cold seawater from the outlet temperature of seawater at the evaporator and condenser of the OTEC system. In order to achieve the optimal design parameters, the design simulation and configuration should be optimized since the output of OTEC-LTTD plant depending on several parameters.

CHAPTER 5

CONCLUSION

The OTEC-LTTD plant consists of power generation and desalination system. In general, all types of desalination plant consumed higher specific energy consumption in order to produce freshwater. In this study, its main objective is to construct an energy-effective desalination plan. An OTEC-LTTD plant is proposed as it makes use of the temperature gradient of the warm and the cold seawater to generate electricity and freshwater. As for this study, the freshwater power consumption that's required is lower because the power generated from OTEC part is being used to generate freshwater. For the proposed OTEC-LTTD plant, the optimum diameter required in order to pump mass flow rate of warm and cold seawater of 1796.8 kg/s is 1.2 m and the value of optimum thermal conductance is 11.0 MW/°C. The optimum temperature difference found in the evaporator and condenser of heat exchanger of OTEC have been determined and presented in Table 4.3, 4.4 and Appendix J. The saturation temperature of evaporator, T_E and condensation temperature, T_C also presented on the table that need to be set to find the heat balance and optimum turbine power. From the results, the 1 MW OTEC-LTTD plant can produce 1425 t/d of freshwater and can be used to supply residential areas which is generated through the use of 24 MWh/d of electricity generated on OTEC plant with 804 kW of net power produced. RO as an energy efficient desalination system, of which about 208 kW (3.5 kWh/t) is needed for specific energy consumption to produce 59.36 t/h (16.49 kg/s) of freshwater. Therefore, it can be concluded that an OTEC plant can be more beneficial and advantages with the LTTD plant. With the presence of LTTD plant in the OTEC cycle, the freshwater can be produced as a byproduct without consuming much energy. From optimization, the best performance can be selected based on some criteria as the maximum plant output, the control system of the input parameters, and the optimum design. The plant can generate more than 1000 t/d of freshwater at the higest temperature based on tropical area at 30 °C. The cold seawater intake at 1000 m depth that reaching 4 °C temperature is seen to give more net power due to larger temperature differential. For this proposed plant,the optimum design can be seen as in diagram in Figure 5.1. Interestingly, Malaysia has a better potential to build an integrated OTEC-LTTD plant. This is due to the location of the site around the Sabah Trough, which has more than 20˚C temperature gradient and close to the populated island with insufficient electricity and freshwater supply.

In this study, a simulation approach has been proposed based on a mathematically based problem design to compute the optimal results for the OTEC-LTTD plant. From the foregoing results, it can be concluded as follows:

i. Feasibility of using Ocean Thermal Energy for Power Generation and Desalination.

ii. The obtained results indicate that using the ocean thermal energy in driving the desalination process is promising, and at the right location and design, it can be effective and reliable.

iii. Conventional methods consume more energy and give an impact to the environments.

iv. The integrated plant gives several advantages on pumping work and vacuum system of the plant.

v. The production of freshwater also boosted the OTEC plant (Energy efficient for desalination).

vi. Under present conditions, freshwater can be produced lower than specific energy consumption than others desalination plant.

Figure 5.1 Proposed 1 MW OTEC-LTTD plant optimization results

REFERENCES

Altaee, A., Zaragoza, G. and Van Tonningen, H. R. 2014. Comparison Between Forward Osmosis-Reverse Osmosis and Reverse Osmosis Processes for Seawater Desalination. *Desalination,* 336**,** 50-57.

Ani 2016. India's First Ocean Power Generation Project Coming Up in Kavaratti, Lakshadweep.

Arsad, S. and Akhir, M. F. 2013. The Characteristics and Origin of Water Masses Along the Sabah Coast. *International Journal,* 1.

Aydin, H., Lee, H.-S., Kim, H.-J., Shin, S. K. and Park, K. 2014. Off-Design Performance Analysis of a Closed-Cycle Ocean Thermal Energy Conversion System With Solar Thermal Preheating and Superheating. *Renewable Energy,* 72**,** 154-163.

Balaji, D., Jayaraj, K., Phani Kumar, S.V.S. and Ramana Murthy, M.V., 2016. Water Quality Improvement Studies in Lttd Plant. *Desalination and Water Treatment*, *57*(52), Pp.24705-24715.

Banat, F. Economic and Technical Assessment of Desalination Technologies. Iwa Conference-New Technologies for Water and Wastewater Treatment in the 21st Century, Geneva, Switzerland, June, 2007. 6-8.

Bkleute 2016. Nederlands: OTEC Map. Retrieved from Nederlands: OTEC Map website: http://www.otecsymposium.org/

Bregman, R., Knapp, R. and Takahashi, P. Design Considerations for Ocean Energy Resource Systems. Oceans'95. Mts/Ieee. Challenges of Our Changing Global Environment. *Conference Proceedings*., 1995. Ieee, 1084-1091.

Charcosset, C. 2009. A Review of Membrane Processes and Renewable Energies for Desalination. *Desalination,* 245**,** 214-231.

Cho, B.-O. and Park, C.-W. 2014. Development of Start· Stop Control System at Water Turbine Generator for Tidal Power Plant. *Journal of the Korean Institute of Illuminating and Electrical Installation Engineers,* 28**,** 106-112.

Chung, H., Wibowo, S., Fajar, B., Shin, Y. and Jeong, H. 2012. Study on Low Pressure Evaporation of Fresh Water Generation System Model. *Journal of Mechanical Science and Technology,* 26**,** 421-426.

Cosgrove, W. J. and Rijsberman, F. R. 2014. *World Water Vision: Making Water Everybody's Business,* Routledge.

Dalton, G. J., Alcorn, R. and Lewis, T. 2010. Case Study Feasibility Analysis of the Pelamis Wave Energy Convertor in Ireland, Portugal and North America. *Renewable Energy,* 35**,** 443-455.

Darus, Z. M., Hashim, N. A., Manan, S. N. A., Rahman, M. A. A., Maulud, K. N. A. and Karim, O. A. Potential of Wind Energy in Sustainable Development of Resort Island in Malaysia: A Case Study of Pulau Perhentian (Perhentian Island). Proceedings of the 10th Wseas International Conference on Mathematical Methods, Computational Techniques and Intelligent Systems, 2008. *World Scientific and Engineering Academy and Society (Wseas),* 431-435.

Dessne, P., Fachina, V., Golmen, L. G., Miller, A. K., Panchal, C., Hammar, L., Jamaluei, Z. Y., Duckers, L., Blanchard, R. and Banerjee, S. 2015. *OTEC Matters 2015,* Högskolan I Borås.

Dincer, I., Midilli, A. and Kucuk, H. 2014. *Progress in Exergy, Energy, and the Environment*, Springer.

Dixon, S. L. and Hall, C. 2013. *Fluid Mechanics and Thermodynamics of Turbomachinery*, Butterworth-Heinemann.

Drew, B., Plummer, A. R. and Sahinkaya, M. N. 2009. A Review of Wave Energy Converter Technology. *Sage Publications,* Sage Uk: London, England.

Elimelech, M. and Phillip, W. A. 2011. The Future of Seawater Desalination: Energy, Technology, and the Environment. *Science,* 333**,** 712-717.

Ellabban, O., Abu-Rub, H. and Blaabjerg, F. 2014. Renewable Energy Resources: Current Status, Future Prospects and Their Enabling Technology. *Renewable and Sustainable Energy Reviews,* 39**,** 748-764.

Ghaffour, N., Lattemann, S., Missimer, T., Ng, K. C., Sinha, S. and Amy, G. 2014. Renewable Energy-Driven Innovative Energy-Efficient Desalination Technologies. *Applied Energy,* 136**,** 1155-1165.

Ghaffour, N., Missimer, T. M. and Amy, G. L. 2013. Technical Review and Evaluation of the Economics of Water Desalination: Current and Future Challenges for Better Water Supply Sustainability. *Desalination,* 309**,** 197-207.

Goto, S., Motoshima, Y., Sugi, T., Yasunaga, T., Ikegami, Y. and Nakamura, M. 2011. Construction of Simulation Model for OTEC Plant Using Uehara Cycle. *Electrical Engineering in Japan,* 176**,** 1-13.

Goto, S., Yamamoto, Y., Sugi, T., Yasunaga, T., Ikegami, Y. and Nakamura, M. 2008. A Simulation Model of Spray Flash Desalination System. *Ifac Proceedings Volumes,* 41**,** 15909-15914.

Goto, S., Yamamoto, Y., Sugi, T., Yasunaga, T., Ikegami, Y. and Nakamura, M. 2010. Construction of Simulation Model for Spray Flash Desalination System. *Electrical Engineering in Japan,* 170**,** 9-17.

Gude, V. G. 2015. Energy Storage for Desalination Processes Powered by Renewable Energy and Waste Heat Sources. *Applied Energy,* 137**,** 877-898.

Hesselgreaves, J. E., Law, R. and Reay, D. 2016. *Compact Heat Exchangers: Selection, Design and Operation*, Butterworth-Heinemann.

Hoekstra, A. Y. 2014. Water Scarcity Challenges to Business. *Nature Climate Change,* 4**,** 318-320.

Hosseini, S. E. and Abdul Wahid, M. 2014. The Role of Renewable and Sustainable Energy in the Energy Mix of Malaysia: A Review. *International Journal of Energy Research,* 38**,** 1769-1792.

Huang, J. C., Krock, H. J. and Oney, S. K. 2003. Revisit Ocean Thermal Energy Conversion System. *Mitigation and Adaptation Strategies for Global Change,* 8**,** 157-175.

Idris, W. O., Sulaiman, N., Ibrahim1, M. Z. B., Nik, W. B. W., Ahmad, F. M. and Ayob, F. A. M. 2014. Modeling Net Power of Sabah Trough and its Effectiveness. *Journal of Energy Technologies and Policy* 4.

Ikegami, Y. 1990. Optimization of a Closed-Cycle OTEC System. *Journal of Solar Energy Engineering,* 112**,** 247.

Ikegami, Y., Sasaki, H., Gouda, T. and Uehara, H. 2006. Experimental Study on a Spray Flash Desalination (Influence of the Direction of Injection). *Desalination,* 194**,** 81-89.

Jaafar, A. B. 2013. Ocean Thermal Potential in Malaysia and the Energy-Water-Foof Nexus for Sustainability.

Jin, Z. and Wang, H. 2015. Modelling and Experiments on Ocean Thermal Energy for Desalination. *International Journal of Sustainable Energy,* 34**,** 103-112.

Kakac, S., Liu, H. and Pramuanjaroenkij, A. 2012. *Heat Exchangers: Selection, Rating, and Thermal Design,* Crc Press.

Kathiroli, S., Jalihal, P. and Sistla, P. V. Barge Mounted Low Temperature Thermal Desalination Plant. The Eighteenth International Offshore and Polar Engineering Conference, 2008. International Society of Offshore and Polar Engineers.

Khan, N., Kalair, A., Abas, N. and Haider, A. 2017. Review of Ocean Tidal, Wave and Thermal Energy Technologies. *Renewable and Sustainable Energy Reviews,* 72**,** 590-604.

Kim, S. J., Ko, S. H., Kang, K. H. and Han, J. 2013. Direct Seawater Desalination by Ion Concentration Polarization. *Nature Nanotechnology,* 8**,** 609-609.

Kryuchin, S. 2017. Kudat Sea Temperature Average, Malaysia | Sea Temperatures.

Kudish, A. I., Evseev, E. G., Walter, G. and Priebe, T. 2003. Simulation Study on a Solar Desalination System Utilizing an Evaporator/Condenser Chamber. *Energy Conversion and Management,* 44**,** 1653-1670.

Kulkarni, G. and Joshi, S. 2016. Performance of Working Fluids in Ocean Thermal Energy Conversion Technology and Different Applications.

Kumar, R. S., Mani, A. and Kumaraswamy, S. 2007. Experimental Studies on Desalination System for Ocean Thermal Energy Utilisation. *Desalination,* 207**,** 1-8.

Lee, J.-M., Lee, H.-W., Kim, Y.-J., Park, H.-G., Hong, S.-P. and Koo, J.-Y. 2013. Improving Fouling Resistance of Seawater Desalination Membranes Via Surface Modification. *Journal of Water Reuse and Desalination,* 3**,** 217-223.

López, I., Andreu, J., Ceballos, S., De Alegría, I. M. and Kortabarria, I. 2013. Review of Wave Energy Technologies and the Necessary Power-Equipment. *Renewable and Sustainable Energy Reviews,* 27**,** 413-434.

Mahdzir and A. B. J. A. M. 2016. Proceedings: 2nd National Workshop on Ocean Energy 2016.Ocean Energy.

Mcdougall, T. J. and Barker, P. M. 2011. Getting Started with Teos-10 and the Gibbs Seawater (Gsw) Oceanographic Toolbox. *Scor/Iapso Wg,* 127**,** 1-28.

Meek, B. The Fortran (Not The Foresight) Saga: The Light and the Dark. Acm Sigplan Fortran Forum, 1990. Acm, 23-32.

Miller, S., Shemer, H. and Semiat, R. 2015. Energy and Environmental Issues in Desalination. *Desalination,* 366**,** 2-8.

Mistry, K. H., Antar, M. A. and Lienhard V, J. H. 2013. An Improved Model for Multiple Effect Distillation. *Desalination and Water Treatment,* 51**,** 807-821.

Morgan, P. 2006. A Library of Matlab Computational Routines for the Properties of Sea Water.

Mutair, S. and Ikegami, Y. 2014. Design Optimization of Shore-Based Low Temperature Thermal Desalination System Utilizing the Ocean Thermal Energy. *Journal of Solar Energy Engineering,* 136**,** 041005.

Muthunayagam, A., Ramamurthi, K. and Paden, J. R. 2005. Modelling and Experiments on Vaporization of Saline Water at Low Temperatures and Reduced Pressures. *Applied Thermal Engineering,* 25**,** 941-952.

Nair, S., George, B., Malano, H. M., Arora, M. and Nawarathna, B. 2014. Water–Energy–Greenhouse Gas Nexus of Urban Water Systems: Review of Concepts, State-of-Art and Methods. *Resources, Conservation and Recycling,* 89**,** 1-10.

Nakamura, S., Goto, S., Sugi, T., Ikegami, Y. and Nakamura, M. Simulation Model of Integrated OTEC and Desalination Plant and its Application. Iccas-Sice, 2009, 2009. Ieee, 5078-5083.

Nihous, G. and Vega, L. 1993. Design of a 100 MW OTEC-Hydrogen Plantship. *Marine Structures,* 6**,** 207-221.

Noordin, A. I. M. 2012. Malaysian National News Agency :: Bernama.

Owens, W. and Trimble, L. 1981. Mini-OTEC Operational Results. *Asme Journal of Solar Energy Engineering,* 103**,** 233-240.

Palenzuela, P., Hassan, A. S., Zaragoza, G. and Alarcón-Padilla, D.-C. 2014. Steady State Model for Multi-Effect Distillation Case Study: Plataforma Solar De Almería Med Pilot Plant. *Desalination,* 337**,** 31-42.

Panchal, C. and Bell, K. 1987. Simultaneous Production of Desalinated Water and Power Using a Hybrid-Cycle OTEC Plant. *Transaction of the Asme,* 109**,** 156-160.

Ravindran, M. and Abraham, R. The Indian 1 MW Demonstration OTEC Plant and the Development Activities. Oceans'02 Mts/Ieee, 2002. Ieee, 1622-1628.

Rogers, G. F. C. and Mayhew, Y. R. 1995. *Thermodynamic and Transport Properties of Fluids*, Blackwell.

Saboori, B. and Sulaiman, J. 2013. Environmental Degradation, Economic Growth and Energy Consumption: Evidence of the Environmental Kuznets Curve in Malaysia. *Energy Policy,* 60**,** 892-905.

Sami Mutair, Y. I. 2013. Simultaneous Power Generation and Desalinated Water Production Using the Renewable Thermal Energy of the Ocean. *Ocean Engineering* , *57*,.89-97.

Sharqawy, M. H., Lienhard, J. H. and Zubair, S. M. 2010. Thermophysical Properties of Seawater: A Review of Existing Correlations and Data. *Desalination and Water Treatment,* 16**,** 354-380.

Sun, F., Ikegami, Y., Jia, B. and Arima, H. 2012. Optimization Design and Exergy Analysis of Organic Rankine Cycle in Ocean Thermal Energy Conversion. *Applied Ocean Research,* 35**,** 38-46.

Sun, F., Zhou, W., Ikegami, Y., Nakagami, K. and Su, X. 2014. Energy–Exergy Analysis and Optimization of the Solar-Boosted Kalina Cycle System 11 (Kcs-11). *Renewable Energy,* 66**,** 268-279.

Tay, J., Low, S. and Jeyaseelan, S. 1996. Vacuum Desalination for Water Purification Using Waste Heat. *Desalination,* 106**,** 131-135.

Tayyebi, S. and Alishiri, M. 2014. The Control of Msf Desalination Plants Based on Inverse Model Control by Neural Network. *Desalination,* 333**,** 92-100.

Tierney, J. E., Abram, N. J., Anchukaitis, K. J., Evans, M. N., Giry, C., Kilbourne, K. H., Saenger, C. P., Wu, H. C. and Zinke, J. 2015. Tropical Sea Surface Temperatures for the Past Four Centuries Reconstructed From Coral Archives. *Paleoceanography,* 30**,** 226-252.

Uehara, H., Dilao, C. O. and Nakaoka, T. 1988. Conceptual Design of Ocean Thermal Energy Conversion (OTEC) Power Plants in the Philippines. *Solar Energy,* 41**,** 431-441.

Uehara, H., Ikegami, Y., Mitsumori, T., Sasaki, K. and Nogami, R. The Experimental Research on Ocean Thermal Energy Conversion Using the Uehara Cycle. Procedings of International OTEC/Dowa Conference, Imari, Japan, 1999. 132-141.

Upadhyay, S. and Sharma, M. 2014. A Review on Configurations, Control and Sizing Methodologies of Hybrid Energy Systems. *Renewable and Sustainable Energy Reviews,* 38**,** 47-63.

Vega, L. A. 2013. Ocean Ocean/Oceanic Thermal Energy Conversion Ocean/Oceanic Thermal Energy Conversion (OTEC). *Renewable Energy Systems.* Springer.

Vosough, A. 2011. Wave Energy. *International Journal of Multidisciplinary Sciences and Engineering,* 2**,** 60-63.

Yamada, N., Hoshi, A. and Ikegami, Y. 2009. Performance Simulation of Solar-Boosted Ocean Thermal Energy Conversion Plant. *Renewable Energy,* 34**,** 1752-1758.

Yeh, R.-H., Su, T.-Z. and Yang, M.-S. 2005. Maximum Output of an OTEC Power Plant. *Ocean Engineering,* 32**,** 685-700.

Zhou, Q., Bai, Y., Li, Y., Wang, X., Wang, H., Du, M., Zhang, S., Meng, J., Duan, L. and Shi, Y. Reviews of Development and Utilization of Tidal Energy Over Chinese Offshore. Oceans 2016-Shanghai, 2016. IEEE, 1-5.

APPENDIX A

Vapor Pressure and Boiling Point Elevation of Seawater

Vapor (saturation) pressure, kPa

Boiling point elevation, K

Temp, °C	Salinity, g/kg												
	0	**10**	**20**	**30**	**40**	**50**	**60**	**70**	**80**	**90**	**100**	**110**	**120**
0	0.611	0.608	0.604	0.601	0.597	0.593	0.590	0.586	0.582	0.578	0.575	0.571	0.567
10	1.228	1.221	1.214	1.207	1.199	1.192	1.185	1.177	1.170	1.162	1.154	1.147	1.139
20	2.339	2.325	2.312	2.298	2.284	2.270	2.256	2.242	2.228	2.213	2.199	2.184	2.169
30	4.247	4.222	4.197	4.172	4.147	4.122	4.096	4.070	4.044	4.018	3.992	3.965	3.938
40	7.384	7.341	7.298	7.255	7.211	7.167	7.123	7.078	7.033	6.987	6.941	6.895	6.848
50	12.351	12.279	12.207	12.135	12.062	11.988	11.914	11.839	11.763	11.687	11.610	11.532	11.454
60	19.946	19.829	19.713	19.596	19.478	19.359	19.239	19.118	18.996	18.873	18.749	18.624	18.497
70	31.201	31.018	30.837	30.654	30.470	30.284	30.096	29.907	29.716	29.523	29.329	29.133	28.935
80	47.415	47.139	46.863	46.585	46.305	46.022	45.737	45.449	45.159	44.866	44.571	44.273	43.972
90	70.182	69.776	69.368	68.957	68.542	68.124	67.701	67.276	66.846	66.413	65.975	65.534	65.089
100	101.418	100.835	100.245	99.651	99.052	98.447	97.837	97.221	96.601	95.974	95.343	94.705	94.062
110	143.376	142.558	141.725	140.884	140.037	139.182	138.320	137.450	136.572	135.687	134.793	133.892	132.982
120	198.665	197.541	196.386	195.222	194.048	192.863	191.668	190.463	189.246	188.019	186.782	185.533	184.272

Temp, °C	Salinity, g/kg												
	0	**10**	**20**	**30**	**40**	**50**	**60**	**70**	**80**	**90**	**100**	**110**	**120**
0	0.000	0.067	0.138	0.213	0.291	0.373	0.458	0.547	0.640	0.736	0.836	0.939	1.046
10	0.000	0.073	0.150	0.232	0.317	0.407	0.501	0.599	0.701	0.807	0.917	1.032	1.151
20	0.000	0.079	0.163	0.251	0.344	0.442	0.545	0.652	0.764	0.880	1.002	1.128	1.258
30	0.000	0.085	0.176	0.272	0.373	0.479	0.590	0.707	0.829	0.956	1.088	1.225	1.368
40	0.000	0.092	0.190	0.293	0.402	0.517	0.637	0.764	0.895	1.033	1.176	1.325	1.480
50	0.000	0.099	0.204	0.315	0.433	0.556	0.686	0.822	0.964	1.112	1.267	1.428	1.595
60	0.000	0.106	0.219	0.338	0.464	0.597	0.736	0.882	1.035	1.194	1.360	1.532	1.711
70	0.000	0.114	0.234	0.362	0.497	0.639	0.788	0.944	1.107	1.277	1.455	1.639	1.831
80	0.000	0.121	0.250	0.387	0.530	0.682	0.841	1.007	1.181	1.363	1.552	1.748	1.952
90	0.000	0.129	0.267	0.412	0.565	0.726	0.895	1.072	1.257	1.450	1.651	1.860	2.076
100	0.000	0.138	0.284	0.438	0.601	0.772	0.952	1.139	1.335	1.540	1.752	1.973	2.203
110	0.000	0.146	0.302	0.465	0.638	0.819	1.009	1.208	1.415	1.631	1.856	2.089	2.331
120	0.000	0.155	0.320	0.493	0.676	0.868	1.068	1.278	1.497	1.725	1.962	2.207	2.462

APPENDIX B

Density and Specific Volume of Seawater

Density, kg/m

Temp, °C	Salinity, g/kg												
	0	10	20	30	40	50	60	70	80	90	100	110	120
0	999.8	1007.9	1016.0	1024.0	1032.0	1040.0	1048.0	1056.1	1064.1	1072.1	1080.1	1088.1	1096.2
10	999.7	1007.4	1015.2	1023.0	1030.9	1038.7	1046.6	1054.4	1062.2	1070.1	1077.9	1085.7	1093.6
20	998.2	1005.7	1013.4	1021.1	1028.8	1036.5	1044.1	1051.8	1059.5	1067.2	1074.9	1082.6	1090.3
30	995.7	1003.1	1010.7	1018.2	1025.8	1033.4	1040.9	1048.5	1056.1	1063.6	1071.2	1078.7	1086.3
40	992.2	999.7	1007.1	1014.6	1022.1	1029.5	1037.0	1044.5	1052.0	1059.4	1066.9	1074.4	1081.8
50	988.0	995.5	1002.9	1010.3	1017.7	1025.1	1032.5	1039.9	1047.3	1054.7	1062.1	1069.5	1076.9
60	983.2	990.6	998.0	1005.3	1012.7	1020.0	1027.4	1034.7	1042.1	1049.5	1056.8	1064.2	1071.5
70	977.8	985.1	992.5	999.8	1007.1	1014.5	1021.8	1029.1	1036.5	1043.8	1051.2	1058.5	1065.8
80	971.8	979.1	986.5	993.8	1001.1	1008.5	1015.8	1023.1	1030.5	1037.8	1045.1	1052.5	1059.8
90	965.3	972.6	980.0	987.3	994.7	1002.0	1009.4	1016.8	1024.1	1031.5	1038.8	1046.2	1053.5
100	958.4	965.7	973.1	980.5	987.9	995.2	1002.6	1010.0	1017.4	1024.8	1032.2	1039.6	1047.0
110	950.9	958.3	965.8	973.2	980.6	988.1	995.5	1003.0	1010.4	1017.8	1025.3	1032.7	1040.2
120	943.1	950.6	958.1	965.6	973.1	980.6	988.1	995.6	1003.1	1010.6	1018.1	1025.6	1033.1

Specific volume, m³/kg

Temp, °C	Salinity, g/kg												
	0	10	20	30	40	50	60	70	80	90	100	110	120
0	0.00100	0.00099	0.00098	0.00098	0.00097	0.00096	0.00095	0.00095	0.00094	0.00093	0.00093	0.00092	0.00091
10	0.00100	0.00099	0.00099	0.00098	0.00097	0.00096	0.00096	0.00095	0.00094	0.00093	0.00093	0.00092	0.00091
20	0.00100	0.00099	0.00099	0.00098	0.00097	0.00096	0.00096	0.00095	0.00094	0.00094	0.00093	0.00092	0.00092
30	0.00100	0.00100	0.00099	0.00098	0.00097	0.00097	0.00096	0.00095	0.00095	0.00094	0.00093	0.00093	0.00092
40	0.00101	0.00100	0.00099	0.00099	0.00098	0.00097	0.00096	0.00096	0.00095	0.00094	0.00094	0.00093	0.00092
50	0.00101	0.00100	0.00100	0.00099	0.00098	0.00098	0.00097	0.00096	0.00095	0.00095	0.00094	0.00094	0.00093
60	0.00102	0.00101	0.00100	0.00099	0.00099	0.00098	0.00097	0.00097	0.00096	0.00095	0.00095	0.00094	0.00093
70	0.00102	0.00102	0.00101	0.00100	0.00099	0.00099	0.00098	0.00097	0.00096	0.00096	0.00095	0.00094	0.00094
80	0.00103	0.00102	0.00101	0.00101	0.00100	0.00099	0.00098	0.00098	0.00097	0.00096	0.00096	0.00095	0.00094
90	0.00104	0.00103	0.00102	0.00101	0.00101	0.00100	0.00099	0.00098	0.00098	0.00097	0.00096	0.00096	0.00095
100	0.00104	0.00104	0.00103	0.00102	0.00101	0.00100	0.00100	0.00099	0.00098	0.00098	0.00097	0.00096	0.00096
110	0.00105	0.00104	0.00104	0.00103	0.00102	0.00101	0.00100	0.00100	0.00099	0.00098	0.00098	0.00097	0.00096
120	0.00106	0.00105	0.00104	0.00104	0.00103	0.00102	0.00101	0.00100	0.00100	0.00099	0.00098	0.00098	0.00097

APPENDIX C

Specific Internal Energy and Enthalpy of Seawater

Specific internal energy, kJ/kg

	Salinity, g/kg												
Temp, °C	**0**	**10**	**20**	**30**	**40**	**50**	**60**	**70**	**80**	**90**	**100**	**110**	**120**
10	42.0	41.2	40.5	39.7	39.0	38.2	37.5	36.7	36.0	35.2	34.5	33.7	33.0
20	83.9	82.7	81.4	80.2	78.9	77.7	76.5	75.2	74.0	72.8	71.5	70.3	69.1
30	125.7	124.0	122.3	120.6	118.8	117.1	115.4	113.7	112.0	110.2	108.5	106.8	105.1
40	167.5	165.3	163.1	160.9	158.7	156.5	154.3	152.1	149.9	147.7	145.5	143.3	141.1
50	209.3	206.6	203.9	201.3	198.6	195.9	193.2	190.5	187.8	185.1	182.4	179.8	177.1
60	251.1	248.0	244.8	241.6	238.4	235.3	232.1	228.9	225.8	222.6	219.4	216.2	213.1
70	293.0	289.3	285.7	282.0	278.4	274.7	271.0	267.4	263.7	260.1	256.4	252.8	249.1
80	334.9	330.7	326.6	322.5	318.3	314.2	310.0	305.9	301.8	297.6	293.5	289.4	285.2
90	376.9	372.3	367.6	363.0	358.4	353.8	349.1	344.5	339.9	335.3	330.7	326.0	321.4
100	419.0	413.9	408.8	403.7	398.6	393.5	388.4	383.3	378.2	373.0	367.9	362.8	357.7
110	461.2	455.6	450.0	444.4	438.9	433.3	427.7	422.1	416.5	410.9	405.3	399.7	394.2
120	503.6	497.5	491.4	485.4	479.3	473.2	467.2	461.1	455.0	448.9	442.9	436.8	430.7

Specific enthalpy, kJ/kg

	Salinity, g/kg												
Temp, °C	**0**	**10**	**20**	**30**	**40**	**50**	**60**	**70**	**80**	**90**	**100**	**110**	**120**
10	42.1	41.4	40.6	39.8	39.1	38.3	37.6	36.8	36.1	35.3	34.6	33.8	33.1
20	84.0	82.8	81.5	80.3	79.0	77.8	76.6	75.3	74.1	72.9	71.6	70.4	69.1
30	125.8	124.1	122.4	120.7	118.9	117.2	115.5	113.8	112.1	110.3	108.6	106.9	105.2
40	167.6	165.4	163.2	161.0	158.8	156.6	154.4	152.2	150.0	147.8	145.6	143.4	141.2
50	209.4	206.7	204.0	201.4	198.7	196.0	193.3	190.6	187.9	185.2	182.5	179.8	177.2
60	251.2	248.1	244.9	241.7	238.5	235.4	232.2	229.0	225.9	222.7	219.5	216.3	213.2
70	293.1	289.4	285.8	282.1	278.5	274.8	271.1	267.5	263.8	260.2	256.5	252.9	249.2
80	335.0	330.8	326.7	322.6	318.4	314.3	310.1	306.0	301.9	297.7	293.6	289.5	285.3
90	377.0	372.4	367.7	363.1	358.5	353.9	349.2	344.6	340.0	335.4	330.8	326.1	321.5
100	419.1	414.0	408.9	403.8	398.7	393.6	388.5	383.4	378.3	373.1	368.0	362.9	357.8
110	461.4	455.8	450.2	444.6	439.0	433.4	427.8	422.2	416.6	411.1	405.5	399.9	394.3
120	503.8	497.7	491.6	485.6	479.5	473.4	467.3	461.3	455.2	449.1	443.1	437.0	430.9

APPENDIX D

Latent Heat of Vaporization and Specific Entropy of Seawater

Latent heat of vaporization, kJ/kg

	Salinity, g/kg												
Temp, °C	**0**	**10**	**20**	**30**	**40**	**50**	**60**	**70**	**80**	**90**	**100**	**110**	**120**
0	2500.9	2475.9	2450.9	2425.9	2400.9	2375.9	2350.8	2325.8	2300.8	2275.8	2250.8	2225.8	2200.8
10	2477.2	2452.5	2427.7	2402.9	2378.1	2353.4	2328.6	2303.8	2279.0	2254.3	2229.5	2204.7	2180.0
20	2453.6	2429.0	2404.5	2379.9	2355.4	2330.9	2306.3	2281.8	2257.3	2232.7	2208.2	2183.7	2159.1
30	2429.8	2405.5	2381.2	2356.9	2332.6	2308.3	2284.0	2259.7	2235.4	2211.1	2186.8	2162.5	2138.2
40	2406.0	2381.9	2357.9	2333.8	2309.7	2285.7	2261.6	2237.6	2213.5	2189.4	2165.4	2141.3	2117.3
50	2382.0	2358.1	2334.3	2310.5	2286.7	2262.9	2239.0	2215.2	2191.4	2167.6	2143.8	2120.0	2096.1
60	2357.7	2334.1	2310.5	2287.0	2263.4	2239.8	2216.2	2192.7	2169.1	2145.5	2121.9	2098.3	2074.8
70	2333.1	2309.8	2286.4	2263.1	2239.8	2216.4	2193.1	2169.8	2146.4	2123.1	2099.8	2076.5	2053.1
80	2308.1	2285.0	2261.9	2238.8	2215.8	2192.7	2169.6	2146.5	2123.4	2100.4	2077.3	2054.2	2031.1
90	2282.6	2259.7	2236.9	2214.1	2191.3	2168.4	2145.6	2122.8	2100.0	2077.1	2054.3	2031.5	2008.7
100	2256.5	2233.9	2211.3	2188.8	2166.2	2143.7	2121.1	2098.5	2076.0	2053.4	2030.8	2008.3	1985.7
110	2229.7	2207.4	2185.1	2162.8	2140.5	2118.2	2095.9	2073.6	2051.3	2029.0	2006.7	1984.4	1962.1
120	2202.1	2180.1	2158.1	2136.1	2114.1	2092.0	2070.0	2048.0	2026.0	2003.9	1981.9	1959.9	1937.9

Specific entropy, kJ/kg K

	Salinity, g/kg												
Temp, °C	**0**	**10**	**20**	**30**	**40**	**50**	**60**	**70**	**80**	**90**	**100**	**110**	**120**
10	0.151	0.152	0.150	0.146	0.141	0.135	0.128	0.121	0.113	0.105	0.096	0.086	0.076
20	0.296	0.295	0.291	0.286	0.279	0.271	0.263	0.254	0.244	0.234	0.224	0.213	0.201
30	0.437	0.433	0.428	0.420	0.412	0.403	0.393	0.382	0.371	0.360	0.348	0.336	0.323
40	0.572	0.567	0.560	0.551	0.541	0.530	0.519	0.507	0.495	0.482	0.469	0.456	0.442
50	0.704	0.697	0.688	0.678	0.666	0.654	0.642	0.628	0.615	0.601	0.587	0.573	0.557
60	0.831	0.823	0.813	0.801	0.788	0.775	0.761	0.746	0.732	0.717	0.701	0.686	0.669
70	0.955	0.945	0.934	0.921	0.907	0.892	0.877	0.861	0.845	0.829	0.812	0.795	0.777
80	1.075	1.064	1.051	1.037	1.022	1.006	0.989	0.972	0.955	0.937	0.919	0.901	0.882
90	1.193	1.180	1.166	1.150	1.133	1.116	1.098	1.080	1.061	1.042	1.023	1.003	0.983
100	1.307	1.293	1.277	1.260	1.242	1.223	1.204	1.184	1.164	1.144	1.123	1.101	1.079
110	1.419	1.403	1.386	1.367	1.348	1.327	1.307	1.285	1.263	1.241	1.219	1.195	1.171
120	1.528	1.511	1.492	1.472	1.450	1.428	1.406	1.382	1.359	1.335	1.310	1.285	1.259

APPENDIX E

Specific Heat and Thermal Conductivity of Seawater

Specific heat at constant pressure, J/kg K

	Salinity, g/kg												
Temp, °C	**0**	**10**	**20**	**30**	**40**	**50**	**60**	**70**	**80**	**90**	**100**	**110**	**120**
0	4206.8	4142.1	4079.9	4020.1	3962.7	3907.8	3855.3	3805.2	3757.6	3712.4	3669.7	3629.3	3591.5
10	4196.7	4136.7	4078.8	4022.8	3968.9	3916.9	3867.1	3819.2	3773.3	3729.5	3687.7	3647.9	3610.1
20	4189.1	4132.8	4078.2	4025.3	3974.1	3924.5	3876.6	3830.4	3785.9	3743.0	3701.8	3662.3	3624.5
30	4183.9	4130.5	4078.5	4027.8	3978.6	3930.8	3884.4	3839.4	3795.8	3753.6	3712.7	3673.3	3635.3
40	4181.0	4129.7	4079.6	4030.7	3982.9	3936.4	3891.0	3846.7	3803.7	3761.8	3721.1	3681.6	3643.2
50	4180.6	4130.8	4081.9	4034.1	3987.3	3941.5	3896.6	3852.9	3810.1	3768.3	3727.5	3687.8	3649.0
60	4182.7	4133.7	4085.5	4038.3	3992.0	3946.5	3902.0	3858.3	3815.5	3773.7	3732.7	3692.6	3653.4
70	4187.1	4138.5	4090.6	4043.6	3997.3	3951.9	3907.4	3863.6	3820.6	3778.5	3737.2	3696.7	3657.0
80	4194.0	4145.3	4097.3	4050.1	4003.7	3958.1	3913.3	3869.2	3825.9	3783.5	3741.7	3700.8	3660.7
90	4203.4	4154.2	4105.9	4058.3	4011.5	3965.4	3920.2	3875.7	3832.0	3789.1	3746.9	3705.6	3665.0
100	4215.2	4165.4	4116.4	4068.2	4020.9	3974.3	3928.5	3883.6	3839.4	3796.0	3753.5	3711.7	3670.8
110	4229.4	4178.8	4129.1	4080.2	4032.2	3985.1	3938.7	3893.3	3848.6	3804.9	3761.9	3719.9	3678.6
120	4246.1	4194.7	4144.2	4094.6	4045.9	3998.2	3951.3	3905.4	3860.3	3816.2	3773.0	3730.7	3689.4

Thermal conductivity, W/m K

	Salinity, g/kg												
Temp, °C	**0**	**10**	**20**	**30**	**40**	**50**	**60**	**70**	**80**	**90**	**100**	**110**	**120**
0	0.572	0.571	0.570	0.570	0.569	0.569	0.568	0.568	0.567	0.566	0.566	0.565	0.565
10	0.588	0.588	0.587	0.587	0.586	0.585	0.585	0.584	0.584	0.583	0.583	0.582	0.582
20	0.604	0.603	0.602	0.602	0.601	0.601	0.600	0.600	0.599	0.599	0.598	0.598	0.597
30	0.617	0.617	0.616	0.616	0.615	0.615	0.614	0.614	0.613	0.613	0.612	0.612	0.611
40	0.630	0.629	0.629	0.628	0.628	0.627	0.627	0.626	0.626	0.625	0.625	0.624	0.624
50	0.641	0.640	0.640	0.639	0.639	0.638	0.638	0.637	0.637	0.636	0.636	0.635	0.635
60	0.650	0.650	0.649	0.649	0.648	0.648	0.647	0.647	0.647	0.646	0.646	0.645	0.645
70	0.658	0.658	0.658	0.657	0.657	0.656	0.656	0.655	0.655	0.655	0.654	0.654	0.653
80	0.665	0.665	0.665	0.664	0.664	0.663	0.663	0.663	0.662	0.662	0.661	0.661	0.661
90	0.671	0.671	0.670	0.670	0.670	0.669	0.669	0.669	0.668	0.668	0.667	0.667	0.667
100	0.676	0.675	0.675	0.675	0.674	0.674	0.674	0.673	0.673	0.673	0.672	0.672	0.672
110	0.679	0.679	0.679	0.678	0.678	0.678	0.677	0.677	0.677	0.676	0.676	0.676	0.675
120	0.682	0.681	0.681	0.681	0.680	0.680	0.680	0.679	0.679	0.679	0.679	0.678	0.678

APPENDIX F

Dynamic Viscosity and Kinematic Viscosity of Seawater

Dynamic viscosity x 10^3, kg/m s

	Salinity, g/kg												
Temp, °C	**0**	**10**	**20**	**30**	**40**	**50**	**60**	**70**	**80**	**90**	**100**	**110**	**120**
0	1.791	1.820	1.852	1.887	1.925	1.965	2.008	2.055	2.104	2.156	2.210	2.268	2.328
10	1.306	1.330	1.355	1.382	1.412	1.443	1.476	1.511	1.548	1.586	1.627	1.669	1.714
20	1.002	1.021	1.043	1.065	1.089	1.114	1.140	1.168	1.197	1.227	1.259	1.292	1.326
30	0.797	0.814	0.832	0.851	0.871	0.891	0.913	0.936	0.960	0.984	1.010	1.037	1.064
40	0.653	0.667	0.683	0.699	0.716	0.734	0.752	0.771	0.791	0.812	0.833	0.855	0.878
50	0.547	0.560	0.573	0.587	0.602	0.617	0.633	0.649	0.666	0.684	0.702	0.721	0.740
60	0.466	0.478	0.490	0.502	0.515	0.528	0.542	0.556	0.571	0.586	0.602	0.618	0.635
70	0.404	0.414	0.425	0.436	0.447	0.459	0.471	0.484	0.497	0.510	0.524	0.538	0.553
80	0.354	0.364	0.373	0.383	0.393	0.404	0.415	0.426	0.437	0.449	0.462	0.474	0.487
90	0.315	0.323	0.331	0.340	0.349	0.359	0.369	0.379	0.389	0.400	0.411	0.422	0.434
100	0.282	0.289	0.297	0.305	0.313	0.322	0.331	0.340	0.350	0.359	0.369	0.380	0.390
110	0.255	0.262	0.269	0.276	0.283	0.291	0.299	0.308	0.316	0.325	0.334	0.344	0.354
120	0.232	0.238	0.245	0.251	0.258	0.265	0.273	0.280	0.288	0.297	0.305	0.314	0.323

Kinematic viscosity x 10^7, m^2/s

	Salinity, g/kg												
Temp, °C	**0**	**10**	**20**	**30**	**40**	**50**	**60**	**70**	**80**	**90**	**100**	**110**	**120**
0	17.92	18.06	18.23	18.43	18.65	18.90	19.16	19.46	19.77	20.11	20.46	20.84	21.24
10	13.07	13.20	13.35	13.51	13.69	13.89	14.10	14.33	14.57	14.82	15.09	15.38	15.67
20	10.04	10.16	10.29	10.43	10.58	10.75	10.92	11.10	11.30	11.50	11.71	11.93	12.17
30	8.01	8.12	8.23	8.36	8.49	8.63	8.77	8.93	9.09	9.26	9.43	9.61	9.80
40	6.58	6.68	6.78	6.89	7.00	7.13	7.25	7.38	7.52	7.66	7.81	7.96	8.11
50	5.53	5.62	5.71	5.81	5.91	6.02	6.13	6.24	6.36	6.48	6.61	6.74	6.87
60	4.74	4.82	4.91	4.99	5.08	5.18	5.28	5.38	5.48	5.59	5.70	5.81	5.93
70	4.13	4.20	4.28	4.36	4.44	4.52	4.61	4.70	4.79	4.89	4.98	5.08	5.19
80	3.65	3.71	3.78	3.85	3.93	4.00	4.08	4.16	4.25	4.33	4.42	4.51	4.60
90	3.26	3.32	3.38	3.45	3.51	3.58	3.65	3.73	3.80	3.88	3.96	4.04	4.12
100	2.94	3.00	3.05	3.11	3.17	3.24	3.30	3.37	3.44	3.51	3.58	3.65	3.73
110	2.68	2.73	2.78	2.84	2.89	2.95	3.01	3.07	3.13	3.20	3.26	3.33	3.40
120	2.46	2.51	2.55	2.60	2.65	2.71	2.76	2.82	2.88	2.93	3.00	3.06	3.12

APPENDIX G

Surface Tension and Prandtl Number of Seawater

Surface tension x 10^3, N/m

Temp, °C	Salinity, g/kg												
	0	10	20	30	40	50	60	70	80	90	100	110	120
0	75.65	75.85	76.01	76.14	76.25	76.35	76.43	76.51	76.57	76.64	76.69	76.75	76.80
10	74.22	74.47	74.66	74.82	74.96	75.07	75.17	75.26	75.35	75.42	75.49	75.56	75.62
20	72.74	73.03	73.25	73.44	73.59	73.73	73.85	73.96	74.05	74.14	74.22	74.30	74.37
30	71.19	71.53	71.78	71.99	72.17	72.32	72.46	72.58	72.69	72.79	72.88	72.97	73.05
40	69.60	69.97	70.25	70.49	70.68	70.86	71.01	71.14	71.26	71.38	71.48	71.57	71.66
50	67.94	68.35	68.66	68.92	69.13	69.32	69.49	69.64	69.77	69.89	70.01	70.11	70.21
60	66.24	66.68	67.01	67.29	67.53	67.73	67.91	68.07	68.21	68.35	68.47	68.58	68.69
70	64.48	64.95	65.31	65.61	65.86	66.07	66.27	66.44	66.59	66.73	66.87	66.99	67.10
80	62.67	63.17	63.55	63.87	64.13	64.36	64.56	64.75	64.91	65.06	65.20	65.33	65.44
90	60.82	61.34	61.74	62.07	62.35	62.59	62.80	62.99	63.16	63.32	63.47	63.60	63.73
100	58.91	59.45	59.87	60.22	60.51	60.76	60.98	61.18	61.36	61.52	61.67	61.81	61.95
110	56.96	57.52	57.96	58.31	58.61	58.87	59.10	59.31	59.50	59.67	59.82	59.97	60.10
120	54.97	55.54	55.99	56.36	56.67	56.93	57.17	57.38	57.57	57.75	57.91	58.06	58.20

Extrapolated data

Prandtl number

Temp, °C	Salinity, g/kg												
	0	10	20	30	40	50	60	70	80	90	100	110	120
0	13.18	13.21	13.25	13.31	13.40	13.50	13.63	13.78	13.94	14.13	14.34	14.56	14.81
10	9.32	9.36	9.41	9.48	9.56	9.65	9.76	9.87	10.00	10.14	10.30	10.46	10.64
20	6.95	7.00	7.06	7.12	7.19	7.27	7.36	7.46	7.56	7.67	7.79	7.92	8.05
30	5.40	5.45	5.51	5.57	5.63	5.70	5.78	5.86	5.94	6.03	6.13	6.23	6.33
40	4.34	4.38	4.43	4.49	4.54	4.60	4.67	4.74	4.81	4.88	4.96	5.04	5.13
50	3.57	3.61	3.66	3.71	3.76	3.81	3.87	3.93	3.99	4.05	4.12	4.18	4.25
60	3.00	3.04	3.08	3.12	3.17	3.22	3.27	3.32	3.37	3.42	3.48	3.54	3.60
70	2.57	2.60	2.64	2.68	2.72	2.76	2.81	2.85	2.90	2.94	2.99	3.04	3.09
80	2.23	2.27	2.30	2.33	2.37	2.41	2.45	2.49	2.53	2.57	2.61	2.66	2.70
90	1.97	2.00	2.03	2.06	2.09	2.13	2.16	2.20	2.23	2.27	2.31	2.35	2.39
100	1.76	1.78	1.81	1.84	1.87	1.90	1.93	1.96	1.99	2.03	2.06	2.10	2.13
110	1.59	1.61	1.63	1.66	1.69	1.71	1.74	1.77	1.80	1.83	1.86	1.89	1.93
120	1.45	1.47	1.49	1.51	1.54	1.56	1.59	1.61	1.64	1.67	1.70	1.73	1.76

APPENDIX H

Process Flow chart

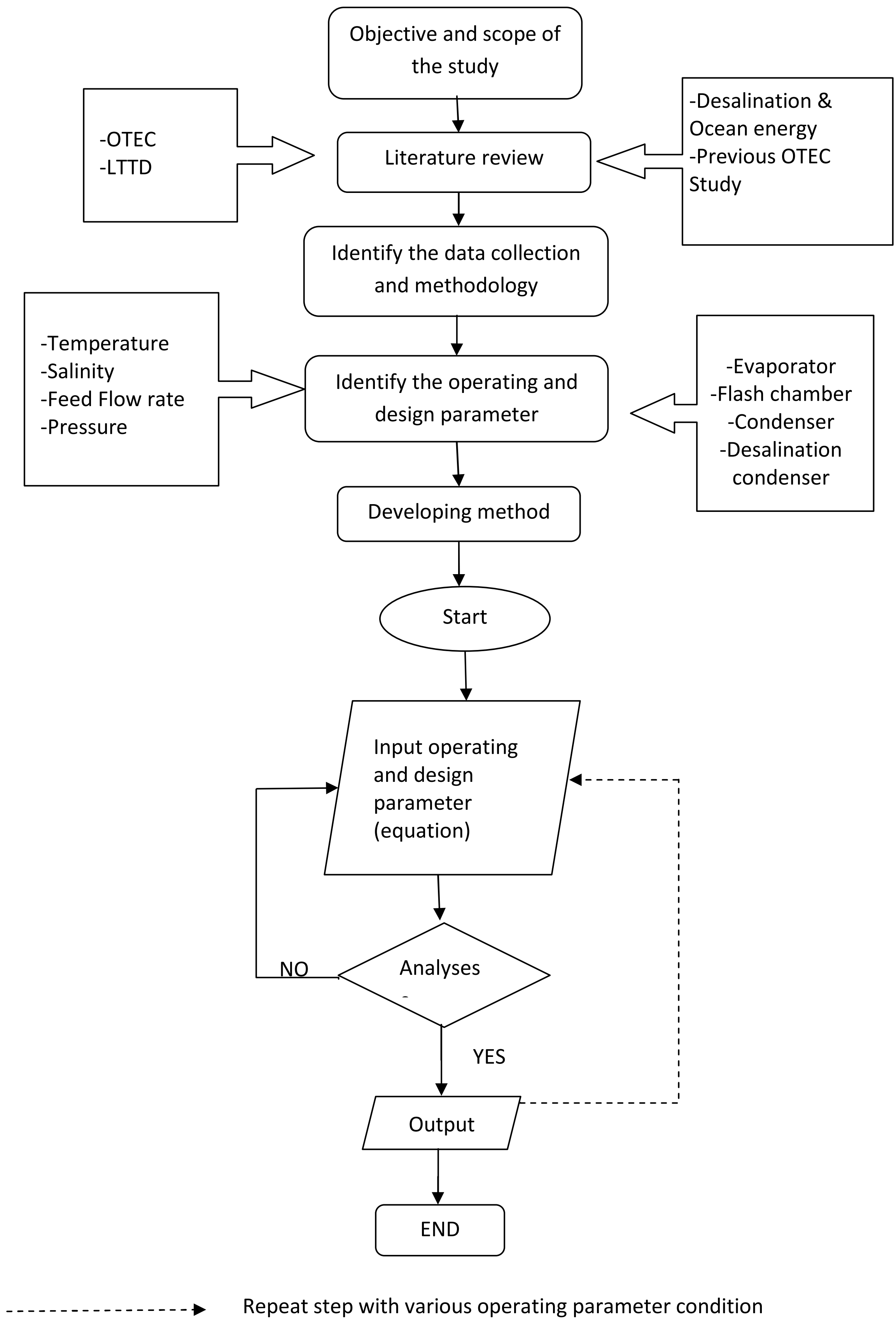

Objective and scope of the study
-OTEC
-LTTD
Literature review
-Desalination & Ocean energy
-Previous OTEC Study
Identify the data collection and methodology
-Temperature
-Salinity
-Feed Flow rate
-Pressure
Identify the operating and design parameter
-Evaporator
-Flash chamber
-Condenser
-Desalination condenser
Developing method
Start
Input operating and design parameter (equation)
Analyses
NO
YES
Output
END
Repeat step with various operating parameter condition

APPENDIX I

OTEC Simulation Process Flow Chart

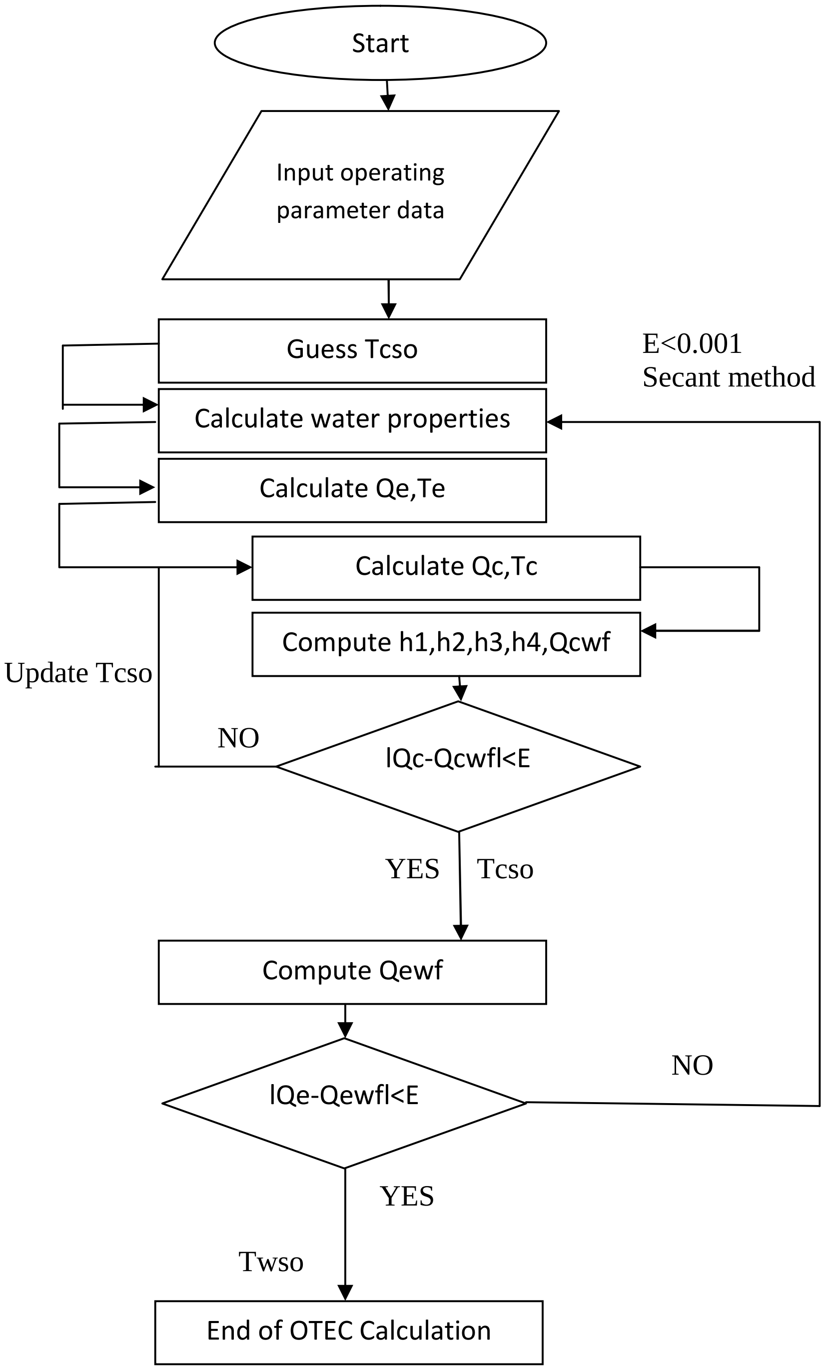
Start
Input operating parameter data
Guess Tcso
E<0.001
Secant method
Calculate water properties
Calculate Qe,Te
Calculate Qc,Tc
Compute h1,h2,h3,h4,Qcwf
Update Tcso
NO
lQc-Qcwfl<E
YES
Tcso
Compute Qewf
NO
lQe-Qewfl<E
YES
Twso
End of OTEC Calculation

APPENDIX J

Simulation Data based on Variation of Warm Seawater Temperature and Cold Seawater Temperature at Different Depth

Simulation results corresponding to generate 1MW turbine power at various cold seawater temperature.

T_{wsi} (^oC)	28.0	28.0	28.0	29.0	29.0	29.0
T_{csi} (^oC)	4.0	5.0	6.0	4.0	5.0	6.0
$m_{ws=}$ m_{cs} (kg/s)	1390.3	1609.0	1843.0	1255.2	1436.0	1614.0
m_{wf} (kg/s)	26.0	29.0	29.0	26.0	29.0	29.0
WP_{ws} (kW)	44.8	52.5	60.4	40.3	46.5	52.4
WP_{cs} (kW)	80.6	92.8	106.3	70.9	80.1	89.2
WP_{wf} (kW)	9.6	9.7	9.9	9.7	9.9	10.1
WP_{vp} (kW)	11.0	12.5	14.1	9.8	11.1	12.3
$Wnet$ (kW)	854.1	832.5	809.3	869.3	852.5	836.1
m_{dw} (kg/s)	12.9	13.9	15.9	11.6	12.4	14.0
$P1$ (kPa)	891.7	889.7	904.8	906.1	903.9	919.2
Te (^oC)	21.3	21.3	21.8	21.8	21.8	22.3
T_{wso} (^oC)	22.2	22.5	23.2	22.6	22.8	23.5
T_c (^oC)	10.4	11.4	11.9	10.9	11.9	12.4
T_{cso} (^oC)	9.5	10.3	10.6	10.1	10.9	11.2
$(T_c)_{dc}$ (^oC)	16.2	16.8	17.5	16.5	17.1	17.8
T_{dco} (^oC)	15.2	15.6	15.9	15.8	16.2	16.6
$T1$ (^oC)	21.3	21.3	21.8	21.8	21.8	22.3
$T2$ (^oC)	10.4	11.4	11.9	10.9	11.9	12.4
$T3$ (^oC)	10.4	11.4	11.9	10.9	11.9	12.4
$T4$ (^oC)	10.5	11.5	12.0	10.9	12.0	12.5
ΔTws	5.8	5.5	4.8	6.4	6.2	5.5
ΔTcs	5.5	5.3	4.6	6.1	5.9	5.2
WP_{tot}	146.0	167.5	190.7	130.7	147.5	163.9

Simulation results corresponding to generate 1MW turbine power at various cold seawater temperature.

T_{wsi} (^oC)	30.0	30.0	30.0
T_{csi} (^oC)	4.0	5.0	6.0
$m_{ws=}$ m_{cs} (kg/s)	1198.0	1301.0	1439.0
m_{wf} (kg/s)	26.0	29.0	29.0
WP_{ws} (kW)	38.5	41.8	46.4
WP_{cs} (kW)	66.8	70.8	77.1
WP_{wf} (kW)	10.3	10.0	10.2
WP_{vp} (kW)	9.3	10.0	10.9
$Wnet$ (kW)	875.2	867.4	855.4
m_{dw} (kg/s)	11.6	11.2	12.5
$P1$ (kPa)	927.9	918.2	933.7
Te (^oC)	22.6	22.3	22.8
T_{wso} (^oC)	23.3	23.2	23.9
T_c (^oC)	11.1	12.4	12.9
T_{cso} (^oC)	10.4	11.5	11.9
$(T_c)_{dc}$ (^oC)	17.0	17.5	18.1
T_{dco} (^oC)	16.3	16.8	17.2
$T1$ (^oC)	22.6	22.3	22.8
$T2$ (^oC)	11.1	12.4	12.9
$T3$ (^oC)	11.1	12.4	12.9
$T4$ (^oC)	11.2	12.4	12.9
ΔTws	6.7	6.8	6.2
ΔTcs	6.4	6.5	5.9
WP_{tot}	124.8	132.6	144.6

APPENDIX K

Heat and Mass Balance for Validation Study

Heat and mass balance for validation study

Validation Heat and Mass Balance of the System								
T_{wsi}=26 °C ,T_{csi}=6 °C								
m_{cs}=m_{ws}=2036.7 kg/s								
		Evaporator		*Condenser*		*FC**	*DC***	
m_{wf}(kg/s)	m_{dw}(kg/s)	Q_{ews} (J)	Q_{ewf} (J)	Q_{ccs} (J)	Q_{cwf} (J)	Q_{fc} (J)	Q_{dc} (J)	W_T(kW)
2	26.05	2506929	2506836	2354200	2350597	64068580	64067724	134.1
5	24.83	6252101	6253530	5878309	5883955	61073432	61015128	317.2
6	24.42	7498495	7498798	7054087	7063731	60057316	60010936	373.41
7	24.01	8739579	8742259	8228050	8244487	59046836	59007852	427.23
8	23.59	9983735	9983923	9397697	9426258	58038824	58003924	478.63
9	23.18	11222766	11223706	10578746	10608997	57028392	56997268	527.59
10	22.77	12458448	12461712	11752124	11792721	56022744	55995092	574.17
11	22.36	13689143	13697914	12923252	12977421	55017500	54997820	618.37
12	21.96	14931987	14932311	14090688	14163184	54012044	53994716	660.11
13	21.54	16163825	16164734	15276444	15349869	53001716	52989868	699.36
14	21.14	17393286	17395430	16449730	16537545	51999896	51989588	736.28
15	20.73	18619812	18624308	17622128	17726198	51001272	50989788	770.8
16	20.32	19842804	19851372	18793226	18915824	50000672	49994872	802.93
17	19.92	21061692	21076626	19962438	20106416	49007480	48998968	832.67
18	19.51	22299688	22300046	21129180	21298164	48003296	47999072	859.85
19	19.1	23520658	23521376	22317880	22490734	46999184	46995608	884.53
20	18.7	24739714	24741062	23490446	23684312	46002152	46000012	906.94
21	18.29	25956594	25958910	24662598	24878868	45007256	45004764	926.92
22	17.89	27171112	27174928	25834204	26074394	44013544	44010776	944.51
23	17.48	28383114	28389110	27005146	27270888	43019856	43019056	959.69
24	17.08	29592352	29601466	28175252	28468348	42028760	42028092	972.47
25	16.68	30798596	30811992	29344342	29666776	41039500	41038696	982.85
26	16.27	32001738	32020700	30512222	30866152	40051872	40051236	990.85
27	15.87	33201328	33227594	31678558	32066484	39066296	39065968	996.48
28	15.47	34432068	34432580	32843186	33268226	38083020	38058112	999.26
29	15.07	35635056	35635836	34005736	34470616	37091700	37077264	1000
30	14.66	36835232	36836400	35209292	35673868	36092240	36074976	997.7
31	14.26	38034068	38035764	36379720	36878168	35103672	35089536	993.46
32	13.86	39230848	39233280	37549824	38083440	34114320	34106388	986.8
33	13.46	40425560	40428940	38719552	39289672	33128682	33122352	977.72
34	13.06	41618096	41622752	39888864	40496868	32142760	32140394	966.23
35	12.66	42808472	42814708	41057692	41705008	31161138	31157266	952.34
36	12.26	43996624	44004816	42225968	42914136	30178354	30176972	936.02
37	11.86	45182368	45193072	43393708	44124200	29197894	29197144	917.3
38	11.46	46365784	46379488	44560784	45335220	28219370	28218080	896.18

*Flash Chamber **Desalination Condenser

APPENDIX L

Heat Balance of OTEC-LTTD Based on Different Warm Seawater Temperature

Heat balance of OTEC-LTTD based on different warm seawater temperature

Validation Heat and Mass Balance of the System								
T_{csi} = 4 , All UA=11 MW/ °C , W_T=1000 kW								
			Evaporator		Condenser		FC*	DC**
T_{wsi} (°C)	m_{ws} (kg/s)	m_{dw} (kg/s)	Q_{ews} (J)	Q_{ewf} (J)	Q_{ccs} (J)	Q_{cwf} (J)	Q_{fc} (J)	Q_{dc} (J)
26	1796.8	16.49	32129214	32130060	30542008	30964462	40631032	40628892
27	1563.94	14.46	32058008	32080966	30548428	30915552	35626224	35624220
28	1390.33	12.89	32011218	32031934	30545048	30866676	31740114	31738332
29	1255.22	11.63	31981778	31982906	30533142	30817872	28636250	28634698
30	1198	11.56	31960012	31966398	30528542	30751296	28437154	28434734

*Flash Chamber

**Desalination Condenser

APPENDIX M

Proposed OTEC-LTTD Plant Configuration

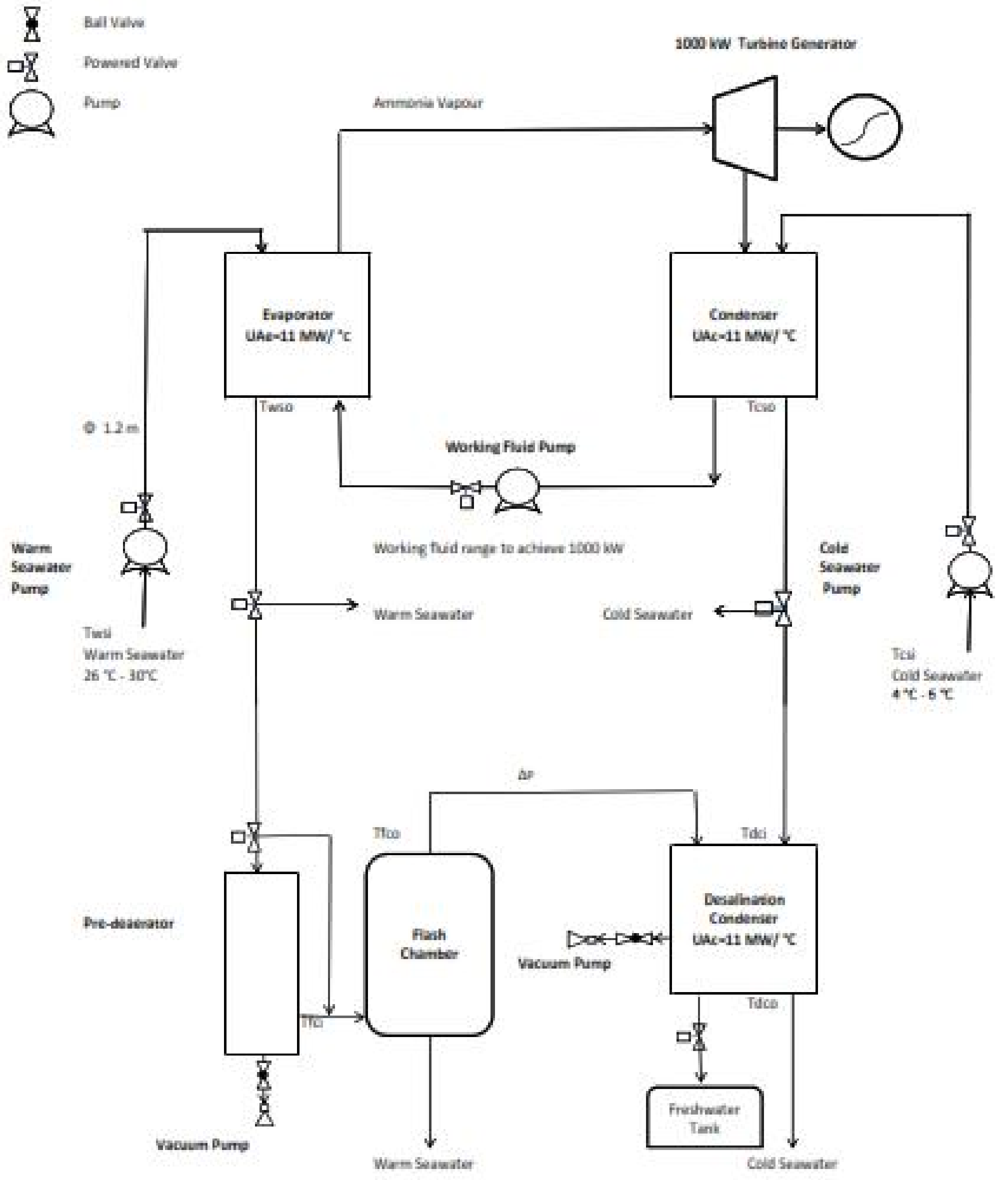
Ball Valve
Powered Valve
Pump
1000 kW Turbine Generator
Ammonia Vapour
Evaporator
UAe=11 MW/ °c
Condenser
UAc=11 MW/ °C
Twso
Tcso
@ 1.2 m
Working Fluid Pump
Working fluid range to achieve 1000 kW
Warm
Seawater
Pump
Cold
Seawater
Pump
Warm Seawater
Cold Seawater
Twsi
Warm Seawater
26 °C - 30°C
Tcsi
Cold Seawater
4 °C - 6 °C
ΔP
Tfco
Tdci
Pre-deaerator
Flash
Chamber
Desalination
Condenser
UAc=11 MW/ °C
Vacuum Pump
Tfci
Tdco
Freshwater
Tank
Vacuum Pump
Warm Seawater
Cold Seawater

APPENDIX N

Published Paper , Conference and Symposium

1. Chik, M.A.T., Othman, N.A., Sarip, S., Ikegami, Y., My, A., Othman, N., Yacob, R., Hara, H., Zakaria, Z. and Izzuan, H., 2015. Design optimization of power generation and desalination application in Malaysia utilizing ocean thermal energy. *Jurnal Teknologi*, *77*(1), pp.177-185.

2. MY, A., Othman, N.A., Sarip, S., Ikegami, Y., Chik, M.A.T., Othman, N., Yacob, R., Hara, H. and Zakaria, Z., 2015. Simulation study on enhancing hydrogen production in an ocean thermal energy (OTEC) system utilizing a solar collector. *optimization*, *2*, p.3.

3. International Platform in Ocean Energy for Young Researcher 2015 (Presenter),Japan

4. 3 rd International OTEC symposium Malaysia 2015 (Presenter),Malaysia